

CARINTHIA UNIVERSITY OF APPLIED SCIENCES
School of Engineering and IT
Department of Geoinformation & Environmental Technologies
Graduate Program of Spatial Information Management

Master's Thesis

Environmental Monitoring and Change Detection of Dynamic River Environments regarding Vegetation and Geomorphology

Submitted in partial fulfillment of the requirements of the academic degree
Master of Science in Engineering

Author: Lina-Luzie ZANDER, B.Eng.

Registration No.: 1310362002

Supervisors: FH-Prof. Mag. Dr. Gernot Paulus MSc, MAS
Department of Geoinformation & Environmental Technologies
Carinthia University of Applied Sciences, Villach, Austria

FH-Prof. Dr.-Ing. Karl-Heinrich Anders
Department of Geoinformation & Environmental Technologies
Carinthia University of Applied Sciences, Villach, Austria

Villach, September 2015

STATUTORY DECLARATION

I hereby declare that

- this master's thesis has been written by myself without any external unauthorized help and that it has not been submitted to any other institution to achieve an academic grading.
- I have not used sources or means without citing them in the text; any thoughts from others or literal quotations are clearly marked.
- the enclosed master's thesis is the same version as the version evaluated by the supervisors.
- one copy of the master's thesis is deposited and made available in the CUAS library (§ 8 Austrian Copyright Law).

I fully understand that I am responsible myself for the application for a patent, trademark or ornamental design and that I have to prosecute any resultant claims by myself.

Place, Date

Signature

ABSTRACT

After significant river regulations, especially in the first half of the 20th century, in recent decades the field of river restoration and management has evolved enormously. As a response to increased recognition of river ecological values, river functions and ecosystem services, the European Union has integrated riverine environmental monitoring into legal obligations for all member states. Although the environmental policy framework is now clearly defined, one problem that persists still lies with the ability to reliably acquire environmental data in dynamic river environments. Whereas field sampling and measurement methods are very time-consuming and therefore costly, Earth-observation satellites are able to cover large areas within a short period of time, but such sensors are typically of moderate or coarse spatial resolution. In order to rectify this situation, the suitability of a remotely piloted aircraft system (RPAS) as well as recent satellite technologies are evaluated and tested for riverine environmental monitoring purposes according to the European legal situation. Two different areas in Carinthia have been selected as study sites. Having been declared as NATURA 2000 protected sites, both river reaches are of high ecologic value, and river restoration has been conducted for these reaches in recent years. During multi-temporal missions of the RPAS platform, RGB and NIR images with a spatial resolution of up to 3 cm are collected, analyzed and compared with very high-resolution satellite-derived products. Representing recent satellite data acquired in four or eight multispectral bands by GeoEye-1, QuickBird and WorldView-2 are used for comparison. The spatial resolutions of the associated multispectral and panchromatic bands of these sensors are 200cm, 240cm and 200cm, respectively; and 50cm, 60cm and 50cm, respectively. For the analysis of the RPAS as well as the satellite images, traditional statistical pattern-recognition techniques, as well as more recently-developed methods, are used to classify present riverine habitats. Classification is performed via ISODATA, Maximum Likelihood, and an image-segmentation algorithm based on Full Lambda Schedule. A photogrammetrically-derived digital surface model is used as auxiliary information to enhance classification accuracy. Field reference data are used for accuracy assessment. To gain

knowledge about the spatio-temporal characteristics of the different restoration measures, an object-based change detection is performed using RPAS data.

The result of this research project is an overall quality and suitability assessment of a small RPAS-based multi-sensor platform for high-resolution spatio-temporal monitoring of vegetation and geomorphological change in dynamic river environments. Furthermore, recent satellite systems are compared to the RPAS platform, and possibilities and limitations for different application areas are demonstrated for both remote sensing systems.

Keywords

VHR Remote Sensing, Earth Observation, Unmanned Aerial Vehicle, Image Classification, Change Detection, Habitat Mapping, Environmental Monitoring, River Restoration

ACKNOWLEDGEMENT

This project would not have been possible without the support of several people, foundations and companies. I would like to take this opportunity to thank them all.

First of all I want to thank my advisors in Austria, FH-Prof. Mag. Dr. Gernot Paulus MSc, MAS and FH-Prof. Dr.-Ing. Karl-Heinrich Anders, as well as my supervisors in Texas, Dr. Anthony M. Filippi and Dr. Inci Güneralp, for their time, technical discussions and assistance meanwhile the whole project time.

My stay at Texas A&M University would not have been possible without the financial support of the Austrian Marshallplan Foundation.

The DigitalGlobe Foundation thankfully provided all satellite images used in the present project.

The Austrian company Revital provided reference data of the vegetation in the project sites collected in the field and through image interpretation.

Thankfully, the Carinthian government made high resolution aerial images derived by airplane available for change detection purposes.

The companies ic Flussbau and Viewcopter provided river cross sections and very high resolution RPAS aerial images, respectively.

Finally, I want to thank the experts of the German company Leitsch, namely Karsten Jocksch, Andreas Steiger und Katja Trimpl, for their time and effort to interpret the ultra-high resolution aerial RPAS images for tree mapping purposes.

To all of you and all other people who motivated me, helped me developing new ideas or supported me in any other way:

THANK YOU.

TABLE OF CONTENTS

Statutory Declaration.....	I
Abstract	II
Acknowledgement.....	IV
Table of Contents	V
List of Tables.....	VIII
List of Figures.....	X
List of Abbreviations	XII
1. Introduction	1
1.1. Motivation	1
1.2. Problem Definition	3
1.3. Objective and Research Question	4
1.4. Expected Results	5
2. Theoretical Principles	7
2.1. European Legal Basis	7
2.1.1. Habitats Directive.....	8
2.1.2. Water Framework Directive.....	9
2.1.3. Legal Regulations for Agriculture	10
2.2. Remote Sensing	11
2.2.1. Earth Observation with Satellite Systems.....	13
2.2.2. Remotely Piloted Aircraft Systems	14
2.2.3. Multispectral and Hyperspectral Data	15
2.2.4. Photogrammetry	16
2.2.5. Visual Image Interpretation.....	17
2.2.6. Image Classification	19
2.3. Biotic and Abiotic Principles.....	20
2.3.1. River Vegetation	20
2.3.2. Geomorphology of Rivers.....	26

3.	Related Work.....	30
3.1.	CORINE Land Cover and Copernicus.....	31
4.	Test Sites and Data Basis.....	33
4.1.	Location and Description of Project Sites	33
4.2.	Satellite Imagery	37
4.3.	RPAS and Data.....	40
4.4.	Aerial Imagery	41
4.5.	Reference Data	43
4.6.	Elevation Data.....	45
4.7.	Summary Data Used	47
5.	Methodology.....	49
5.1.	Concept.....	49
5.2.	Preprocessing	50
5.3.	Visual Interpretation Methods.....	52
5.4.	Classification Procedures	53
5.4.1.	ISODATA Algorithm	54
5.4.2.	Image Segmentation	55
5.4.3.	Maximum Likelihood Classification Algorithm	56
5.4.4.	Validation.....	58
5.5.	Improvement of Classification.....	59
5.6.	Change Detection Techniques	62
5.7.	Comparison Strategy	63
6.	Application	64
6.1.	Visual Interpretation Results.....	64
6.2.	Preprocessing satellite imagery.....	66
6.3.	Preprocessing RPAS imagery	67
6.4.	Classification Results	68
6.4.1.	Satellite Data	71
6.4.2.	RPAS Data	76

6.4.3. Comparison	78
6.5. Change Detection Results	79
7. Evaluation	84
7.1. Accuracy Assessment	84
7.2. Quantitative Assessment	87
7.3. Error Analysis	88
8. Discussion	89
8.1. Conclusion	91
8.2. Outlook.....	92
References	i
ANNEX A	xiii
ANNEX B	xxii
ANNEX C	xxxvii

LIST OF TABLES

Table 1: NATURA 2000 sites in Austria, 2012 (European Environment Agency, 2012)	9
Table 2: VHR Satellite Systems (DigitalGlobe, 2013a, 2013b and Satellite Imaging Corporation, 2015)	13
Table 3: Comparison of pioneer and climax tree species (Leitsch, 2012)	22
Table 4: Neophytes in Austria (Austrian Federal Environment Agency, 2015 and NOBANIS, 2015, the images are from the NOBANIS fact sheets, Stiftung Hessischer Jaegerhof, 2015 and Intermountain Region, 2015)	23
Table 5: Main soil types and their grain diameters (Roth-Kleyer, 2009)	28
Table 6: Sensor bands of WorldView-2 (DigitalGlobe, 2013b)	37
Table 7: Sensor bands of GeoEye-1 (DigitalGlobe, 2015a)	38
Table 8: Sensor bands of QuickBird-2 (DigitalGlobe, 2015b)	38
Table 9: Overview of all data sources used in the present project.....	47
Table 10: Correctly classified results of visual image interpretation.....	65
Table 11: Final RMSEs of the satellite images after geometric correction.....	67
Table 12: Available classes in the project site Gail	68
Table 13: Combination of classes to reach 15 classes for Maximum Likelihood classification	70
Table 14: Combination of classes to reach 11 classes for Maximum Likelihood classification	70
Table 15: Combination of classes to get 11 ISODATA classes	71
Table 16: Classification results of the GeoEye-1 satellite image at the river Gail (number of classes achieved)	73
Table 17: Classification results of the GeoEye-1 satellite image at the river Gail without agricultural classes.....	74
Table 18: Classification accuracy of the RPAS-derived images at the river Gail (number of classes)	77
Table 19: Transformed Divergence separability values for Maximum Likelihood signatures.....	78
Table 20: Post classification change detection result RPAS-derived ortho-photos	82
Table 21: Post classification change detection result airplane-derived ortho-photos	83

Table 22: Example of a confusion matrix evaluating the accuracy of eleven example classes	85
Table 23: Overall accuracy values for the 11 ISODATA classes of the example in Table 22.....	86

LIST OF FIGURES

Figure 1: Electromagnetic spectrum and its use for remote sensing (Albertz, 2007 with modifications)	11
Figure 2: Spectral signatures of different materials (Ashraf et al., 2011)	15
Figure 3: Partial key to identification of tree species in southern Oregon and northern California on large-scale, color aerial photographs (Ciesla and Hoppus, 1990)	18
Figure 4: Four main tree species in above and laterally view (Engleder, 2004 with modifications)	19
Figure 5: Birch Forest representing Pioneer Species (Arnoldius, 2012)	21
Figure 6: Beech representing Climax Species (Augsburger Allgemeine, 2013)	21
Figure 7: Vegetation sequence of an idealized cross section of a bed load carrying river with dominant summer high water in Central Europe (Ellenberg and Leuschner, 2010 with modifications)	27
Figure 8: Soil texture triangle to determine soil type (Bellingham, 2007)	28
Figure 9: Project site I at the river Gail (KAGIS, 2015 and Glanznig, 2006)	35
Figure 10: Project site II at the river Drau (KAGIS, 2015 and Glanznig, 2006)	36
Figure 11: Satellite Imagery: A = WorldView-2 Drau, B = QuickBird Drau, C = WorldView-2 Gail, D = GeoEye Gail	39
Figure 12: Bramor rTK RPAS produced by C-Astral (C-Astral, 2015)	40
Figure 13: RPAS Imagery A = RGB Drau 12/2013, B = RGB Gail 09/2014, C = RGB + NIR Gail 06/2015	41
Figure 14: Aerial Imagery A = Drau 2006, B = Drau 2013, C = Gail 2010, D = Gail 2013	42
Figure 15: Reference data A = Drau 2004, B = Drau 2011, C = Gail 2014	44
Figure 16: Elevation data A = DTM Gail, B = DSM Gail 2014, C = DSM Gail 2015	46
Figure 17: Overview about the image processing workflow	50
Figure 18: Levels of detail evaluated for visual image interpretation	53
Figure 19: Image processing workflow VHR multispectral satellite data	54
Figure 20: Image processing workflow RPAS-derived data	54
Figure 21: The Image Segmentation classification performed in different levels of detail, becoming coarser from A to D	56

Figure 22: The problem of finding an n-dimensional decision boundary to separate major classes in a spectral distribution of data in n bands (here just 1 band) (Jensen, 2005)	58
Figure 23: Comparison of pan-sharpening algorithms for a GeoEye-1 satellite image	61
Figure 24: Visual image interpretation result and reference data, A = interpretation results expert 2, B = reference data subset 2.....	64
Figure 25: GeoEye-1 classification results, A = FLS-based Image Segmentation, B = Maximum Likelihood classification, C = ISODATA.....	72
Figure 26: Result of the river classification in the WorlView-2 winter scene at river Gail	75
Figure 27: Result of the river classification in the WorlView-2 winter scene at river Drau	76
Figure 28: Maximum Likelihood classification results RPAS-derived data.....	77
Figure 29: Probability of change between RPAS RGB images 2014 and 2015 at the river Gail	80
Figure 30: Probability of change between RGB ortho-photos from 2010 and 2013 at the river Gail.....	81

LIST OF ABBREVIATIONS

CLC	CORINE Land Cover
BMLFUW	Austrian Federal Ministry of Agriculture, Forestry, Environment and Water Management
DEM	Digital Elevation Model
DSM	Digital Surface Model
EC	European Commission
EP	European Parliament
EU	European Union
GCP	Ground Control Point
HCS	Hyperspherical Color Space
IR	Infrared
ISODATA	Iterative Self-Organizing Data Analysis Technique
LIDAR	Light Detection And Ranging
LISA	Land Information System Austria
NASA	National Aeronautics and Space Administration
NIR	Near-Infrared
NOBANIS	European Network on Invasive Alien Species
RGB	Red Green Blue
RMSE	Root Mean Square Error
RPAmSS	Remotely Piloted Aircraft multi Sensor System
RPAS	Remotely Piloted Aircraft System
UAS	Unmanned Aerial System
UAV	Unmanned Aerial Vehicle
VHR	Very High Resolution
VTOL	Vertical Take-Off and Landing

1. INTRODUCTION

After significant river regulations especially in the first half of the 20th century in recent decades the field of river restoration and management has developed enormously. While earlier reasons for the straightening of rivers had been to gain land for agriculture or settlement nowadays an increased recognition of river ecological values, river functions and ecosystem services appear (Carbonneau et al., 2012). Additionally new requirements on flood safety caused by global warming and changes of the frequency and intensity of extreme weather events gave an impulse to rethink river regulation. In the European Union (EU) certain directives regulate the development of ecosystems. The Water Framework Directive has been issued to ensure water quality and quantity and also states which streams need to be restored to reach more natural states (EU Water Framework Directive, 2000). On the other hand the Habitats Directive has the aim to ensure biodiversity of wild flora and fauna throughout the EU (EU Habitats Directive, 1992). But to ensure a high water quality and biodiversity the protected regions have to be monitored regularly to detect changes and avoid degradation. One problem that persists still lies with the ability to reliably acquire environmental data in dynamic river environments.

1.1. MOTIVATION

With an average precipitation of 1,100 mm per year (BMLFUW, 2015d) Austria is among the countries of Europe most richly endowed with water resources. To ensure a certain drinking water quality all water bodies are monitored regularly according to the Water Framework Directive. Natural riverine environments have a high potential of being used as habitats for different flora and fauna and therefore are often specifically protected for the purpose of maintaining biodiversity.

In 2010 the Austrian Federal Ministry of Agriculture, Forestry, Environment and Water Management (BMLFUW) in cooperation with the EU started the Gail LIFE Nature Conservation project. Aim of this project with a duration of five years was to restore a monotonously regulated river section of the river Gail into a nature-near but still flood-safe stream. Different actions have been realized in three river sections to show how the water reacts on diverse restoration

methods and which action improve the ecological situation most sustainably without restricting flood safety. The results gained in the Gail LIFE project should now further be adapted to other river environments in similar situations. Additionally to the river bed itself the surrounding areas have been improved concerning quality and quantity to create wetlands of high ecological value (BMLFUW, 2015a). The location of the project site had been chosen because additionally to the river shape and the highly biodiverse surrounding the project site is from supraregional importance as it acts as resting place for migratory birds. The project was finished successfully at the end of 2014 (BMLFUW, 2010). Another project performed by the BMLFUW is the LIFE project Life Vein – Upper Drau River. Starting in 2006 this project was finished in 2011 with the aim to continue the successful revitalization to sustainably integrate the upper Drau River as life vein for the region. Furthermore, the project was used to highlight solutions for managing ecologic problems and difficulties that are relevant in terms of water management. With high biodiversity this project site is accounted for NATURA 2000 protection site (BMLFUW, 2015b).

Because of their high relevance as NATURA 2000 sites and the recent processing and high amount of data available, the Gail LIFE project site as well as the area of the Drau LIFE project are chosen for the current work as project sites for river monitoring with the help of earth observing satellites as well as with Remotely Piloted Aircraft Systems (RPAS). The different multispectral sensors are used for data collection in these protected areas of high ecological value to assess their suitability for environmental monitoring applications.

Another important project related to the present work is the cooperation & innovation project New Environmental Robotic Services with a Remotely Piloted Aircraft Multi Sensor System for Environmental Monitoring (RPAmSS) funded by the Austrian Research Promotion Agency. The cooperative RPAmSS project has the major goal to develop, apply and quantitatively assess the capabilities of a civil, low-cost unmanned aerial multi-sensor system for the fast and high-resolution capture of multidimensional environmental data. With a project duration of two years the RPAmSS project will combine state of the art RPAS technology with on the one hand the latest innovations in the field of airborne remote sensing presented as a hyperspectral camera and on the other a new standardized sensor system for capturing weather and air quality data. The outcome of this project is expected being the development of new and innovative services based on high quality validated multidimensional data of

dynamic river environments, weather conditions and air quality for long-term monitoring and change detection.

This present work cooperates with the RPAmSS project in having the major goal to perform an analysis on data acquired from different remote sensors regarding river vegetation and geomorphology and compare the informational content of products derived from the different sensors. Therefore, the RPAS infrastructure of the RPAmSS project is used and the analyses are done for the same project sites.

1.2. PROBLEM DEFINITION

To fulfil the requirements of the European directives concerning environmental protection and biodiversity conservation each member state has to define specific protection sites with high ecologic value. Those protection sites need to be monitored regularly every six years to detect changes and maintain natural states. Additionally the surface waters are obliged to be monitored in a time interval of six years as well in all European member states to inspect their qualitative and quantitative state.

Currently, field sampling and measurement methods for river vegetation and geomorphology are time-consuming and therefore expensive, especially when it comes to change detection and other long-term environmental monitoring tasks. On the other hand, Earth-observation satellites are able to acquire data covering large areas within a short period of time, but with lower ground resolution. Very high-resolution (VHR) satellite systems indeed provide high spatial resolution with up to 31 cm but with a spectral resolution of only 4 spectral bands (8 bands for World View-2 and -3, respectively). Systems with high spectral resolution like Hyperion with 220 bands only provide low spatial resolution, i.e. 30 m for Hyperion (Thenkabaill et al., 2012). The temporal resolution of satellite systems is also rather low with a nominal revisit interval of several days.

Also known under the names Unmanned Aerial Vehicle (UAV), Unmanned Aerial System (UAS) or drone the RPAS market worldwide is currently developing extremely quickly. With high agility and relatively low costs RPAS technology is applicable in almost every area to be monitored. The potential improvement in the temporal resolution of images captured by RPAS is likely to be a key factor in their expanding usage since it allows for monitoring at monthly or even daily or sub-daily timescales. Additionally, choosing the altitude of flight and

thus adjusting the ground resolution leads to an almost free choice of spatial resolution. Such monitoring methods with both high temporal and spatial resolutions are crucially needed in river sciences and monitoring (Fonstad, 2012).

1.3. OBJECTIVE AND RESEARCH QUESTION

The main goal of the present work is to analyze and compare environmental data concerning river vegetation and geomorphology gained out of different sensors. For the data acquisition traditional earth observation satellites as well as the RPAmSS, a fixed-wing RPAS loaded with multiple environmental sensors, are used. To support the achievement of this objective the major research question is formulated as follows:

- *How usable are the different sensors for monitoring riverine environments in terms of informational content and accuracy?*

The research question results in other sub-questions that are associated with various science fields and are additionally treated in this project. One of these additional problems goes into detail about the classification of multispectral data to research on the possibility to differentiate between different vegetation species and to even distinguish different varieties. This information then can further be used to detect pioneer species in plant communities, simulate their spreading and predict their influence on restoration measures and natural habitats in river environments like gravel banks. Furthermore the detection of species/varieties is useful in the field of natural conservation to identify and keep invasive neophytes in check and therewith protect indigenous vegetation. Another sub-problem of this research project is integrated in the field of river hydrology and geomorphology. According to the Water Framework Directive the EU member states especially have to monitor water quality and quantity to make statements about the natural state of flowing waters. Additionally morphologic changes are tried to be detected to understand how the riverbed changes over time. Efforts are being expanded to complement the analysis to the field of grain size distribution and to research on the possibility of classifying soils based on their granulometric composition with the help of remote sensing.

These further research questions are the following:

- *To what scale is it possible to distinguish between different plants using multispectral and Red Green Blue (RGB) aerial images?*
- *Which statements can be made about water quality and quantity of the monitored rivers?*
- *How far can the geomorphology of flowing rivers be described using the sensors mentioned before?*
- *Is the spatial resolution of currently operating earth observation satellite systems high enough to fulfil environmental monitoring tasks according to EU directives?*
- *Is it possible and in which application areas is it appropriate to use a RPAS for environmental monitoring tasks?*

These questions will be answered by analyzing and validating the appropriate data and comparing the results to the requirements of the European directives in the field of conservation and environmental monitoring.

1.4. EXPECTED RESULTS

The major goal of this master's project is to perform an analysis on data acquired from different remote sensors regarding river vegetation and geomorphology and compare the informational content of different sensors. To achieve this objective, the following intermediate results are expected:

- Overall quality and suitability assessment of a small RPAS-based multi-sensor platform for high-resolution spatiotemporal monitoring of dynamic river environments in the context of vegetation and geomorphology
- Evaluation of classification results for vegetation and geomorphic landforms
- Comparison of the different remote sensing systems
- A large quantity of environmental data sets generated by multiple missions during the project period

Firstly, one of the most important expected results is an overall quality and suitability assessment of the applicability of a RPAS for monitoring tasks of river environments. This will be achieved by analyzing the results of a variety of test

flights in two different project sites and comparing these results to the requirements in environmental monitoring. Next the evaluation of classification results regarding vegetation and geomorphic landforms is expected. This is realized through the validation of the analyzed data gained during multiple missions in comparison to data of the same regions collected by Austrian domain experts with visual image interpretation and field methods. The comparison of the different data types acquired by RGB and multispectral sensors will be attained based on accuracy and informational content. Finally a large quantity of multi-temporal environmental data sets generated during multiple RPAS flights for the appropriate Austrian project sites is expected as result.

2. THEORETICAL PRINCIPLES

This chapter covers the main fields relevant for the present work and provides a theoretical background of the different disciplines. Starting with the European legal basis the most important directives and legal regulations asking for regularly environmental monitoring are presented. Altogether this section justifies the need to research in this area of environmental monitoring and to develop an RPAS to fulfil the requirements of the EU. The next main field is the science of remote sensing. This part deals with general important definitions concerning remote sensing, the functionality of earth observation satellite systems and the development of RPASs and their use for environmental monitoring. As one aim of this work is to combine satellite data with data received during RPAS missions this part provides the theoretical background of both systems. The last disciplines covered in this chapter are biology and geology with a look at biotic and abiotic principles. This part is fundamental to understand typical European river environments and their geomorphology for data evaluation.

2.1. EUROPEAN LEGAL BASIS

With 28 member states and 6 candidate countries the EU forms a large community that promotes the participating European countries in building an economic and social cohesion, equating men and women, protecting the environment and supporting the scientific and technical progress. Understandably such a large community needs rules to regulate the cohabitation. Therefore, the European Commission (EC) has the possibility of new legislation in cooperation with the European Parliament (EP) and the Council of the EU. In the following subchapters the most important legal basics of the EU for the current work are summarized. At first the Habitats Directive that has the aim to ensure the maintenance of biodiversity in Europe is explained shortly. After that the Water Framework Directive to improve or obtain water quality in the European member states is described. The final subchapter deals with the requirements of monitoring agricultural.

2.1.1. HABITATS DIRECTIVE

The COUNCIL DIRECTIVE 92/43/EEC of 21 May 1992 on the conservation of natural habitats and of wild fauna and flora, also known as Habitats Directive, was published for all European member states in 1992. The directive has the aim to preserve and protect wild species and natural habitats and to build a connection between habitats all over Europe. The major goal of this Habitats Directive is to support the maintenance of biodiversity taking into account economic, social, cultural and regional requirements of each member state. To ensure the restoration or maintenance of natural habitats protected areas need to be defined that have a connection all over Europe to build a network of continuous natural habitats. After the DIRECTIVE 2009/147/EC of the EP and of the Council of 30 November 2009 on the conservation of wild birds the European member states additionally are asked to define specially protected areas for all wild birds naturally occurring in the European Union (EU Birds Directive, 2009). The Birds Directive is only mentioned for the sake of completeness as the protection areas defined in the Habitats Directive together with those defined in the Birds Directive build a network of natural habitats known as NATURA 2000 protection territories. Those NATURA 2000 protected areas have the aim to preserve and maintain wild flora and fauna of high conservation value and thereby sustainably ensure the natural biodiversity in Europe. Species with high conservation value are defined in the appendix of the Habitats Directive and have to be protected in all member states where they occur. These definitions of habitat types with high ecologic value are attached in ANNEX A. To fulfil the ecologic requirements of protected species and ensure their maintenance a system of interlinked biotopes is essential. Once the NATURA 2000 sites have been accepted a regularly control of the conservation status as well as the monitoring of actions for improvement has to take place every six years (EU Habitats Directive, 1992). In order to enable reliable assessments extensive information concerning the unique habitats and species, their development status and possible threats is needed. With accession into the EU in 1995 Austria agreed to implement the European directives and thus the conservation and maintenance of natural biodiversity. Due to the legal situation in Austria the legislative and executive jurisdiction of conservation falls under the competence of the nine provinces. Therefore, both directives have been implemented in corresponding national laws like the Nature Conservation-, the Hunting-, the Fisheries-, the National Park-, the Regional Development Act and others. The site selection process was done by

the provinces having regard to the habitat types or species mentioned in the Habitats- and Birds Directive. In 2012 Austria had nominated 218 NATURA 2000 sites that take in total 15 % of the Austrian territory and from which 167 are legally ordered (Federal Environmental Agency, 2015). The distribution of NATURA 2000 sites over the Austrian provinces can be seen in Table 1.

Table 1: NATURA 2000 sites in Austria, 2012 (European Environment Agency, 2012)

Austrian Province	Number of NATURA 2000 sites	NATURA 2000 Areas	Share of the Province's Area
Burgenland	14	1,100 km ²	27.7 %
Carinthia	33	557 km ²	5.8 %
Lower Austria	36	4,414 km ²	23.0 %
Salzburg	29	1,091 km ²	15.3 %
Styria	41	2,557 km ²	15.6 %
Tyrol	13	1,836 km ²	14.5 %
Upper Austria	25	744 km ²	6.2 %
Vienna	4	55 km ²	13.2 %
Vorarlberg	23	211 km ²	8.1 %
Austria in total	218	12,565 km²	15.0 %

Consequently, to fulfil the requirements of the Habitats Directive as well as those of the Birds Directive Austria has to regularly monitor the area of 12,565 km² with a resolution high enough to detect the development status of natural habitats and species and possible future threats of their maintenance.

2.1.2. WATER FRAMEWORK DIRECTIVE

In 2000 the Water Framework Directive printed as the DIRECTIVE 2000/60/EC OF THE EP AND OF THE COUNCIL of 23 October 2000 establishing a framework for community action in the field of water policy has been published. The main goals of the directive are the sustainable management and the protection of freshwater resources to ensure a stable quality and quantity. Through the Water Framework Directive the EU regulates the abstraction of freshwater and develops an integrated water policy in the European community. Additionally to the protection and improvement of the water quality the Water Framework Directive requests the protection and improvement of directly adjacent

aquatic and terrestrial ecosystems and wetlands. All member states are required to reach at least a good water status. If a good status already exists this needs to be maintained. Due to a defined time frame the Water Framework Directive has to be implemented until 2015 – in exceptional cases until 2027. To analyze the freshwater status the member states are asked to monitor the water development on a systematic and comparable basis every six years (EU Water Framework Directive, 2000).

In Austria the Water Framework Directive has been implemented in 2003 in the Water Rights Act. With the Monitoring of the Quality of Water Bodies Regulation in 2006 all Austrian monitoring programs have been adapted to the requirements of the European directive. Three different types of monitoring programs have been formed: the surveillance-, the operational- and the investigative monitoring program. The surveillance monitoring is used to distinguish large scale trends in water quality while the operational monitoring especially takes care of the water bodies that have been rated in the inventory with “not clear” or “unlikely” in reaching the quality goals. The investigative monitoring program is used if the cause of appearing pollution is unknown or if accidental pollution occurs.

2.1.3. LEGAL REGULATIONS FOR AGRICULTURE

When the council of the EU legislated the COUNCIL REGULATION (EC) No 1782/2003 of 29 September 2003 establishing common rules for direct support schemes under the common agricultural policy and establishing certain support schemes for farmers, a link between agriculture and conservation has been built. Considering other regulations this regulation predicates agricultural direct payments with the compliance of regulations in the field of conservation, feed and food safety, animal health and plant health. Due to the cross compliance of this regulation cropland has to be maintained in good agricultural and environmental conditions. Good agricultural and environmental conditions mean among others the maintenance of soil organic matter, prevention of erosion and the regeneration of brownfield sites (EU Single Farm Payment Regulation, 2003). Especially the monitoring of the agricultural areas can be linked with the requirements of the Habitats- and the Water Framework Directive as all three ask for a regularly, areal monitoring.

2.2. REMOTE SENSING

Remote Sensing is defined as the science to derive information about the earth's surface through a sensor that is not in physical contact with the observed object. In order to accomplish remote sensing of an object the reflected and emitted electromagnetic radiation of the earth's surface in multiple regions of the electromagnetic spectrum is measured (Campbell, 2002). The whole range of the electromagnetic spectrum is shown in Figure 1. As can be seen the light visible for the human eye is only a minor part of the spectrum and ranges from about 400 nm to 700 nm. Because the different ranges of the electromagnetic spectrum are overlapping and have no sharp boundary differences can be found in literature. The whole idea of remote sensing is based on the fact that each material reflects, absorbs, transmits and emits electromagnetic radiation in a unique way.

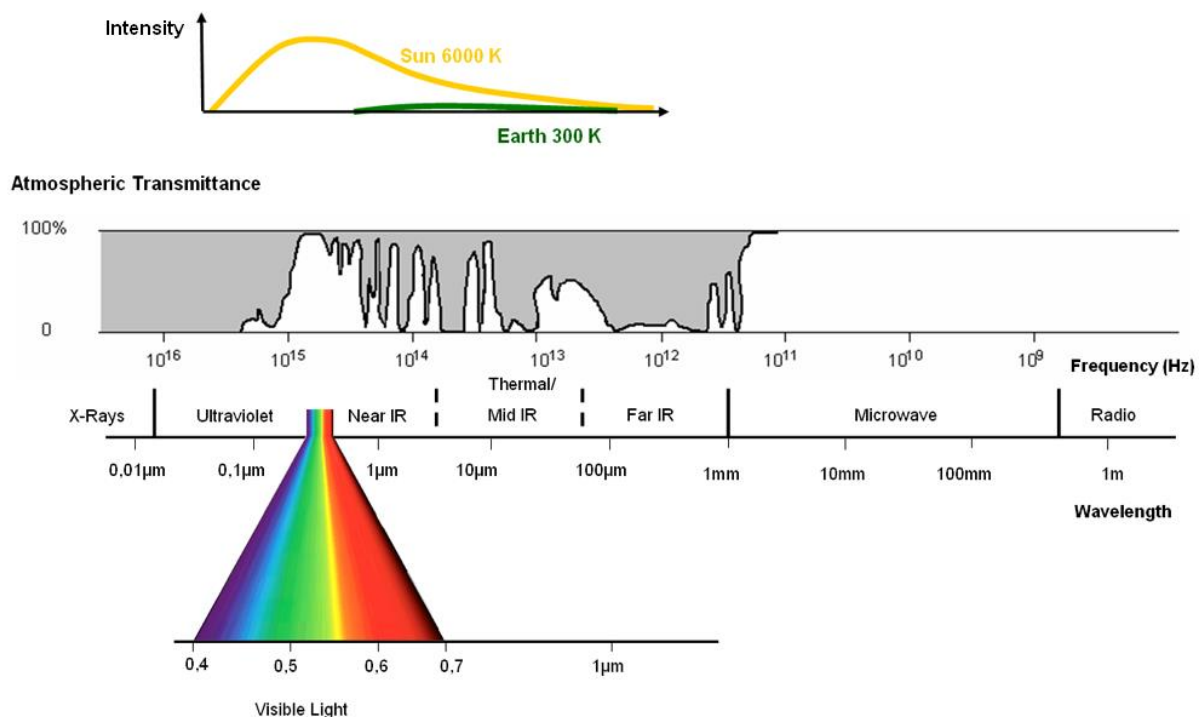


Figure 1: Electromagnetic spectrum and its use for remote sensing (Albertz, 2007 with modifications)

Although the light visible for a human eye makes only a small part of the whole spectrum this part is very important and mainly used in remote sensing. However, short-wave radiation like ultraviolet radiation or X-rays is not useful for remote sensing. The range above 700 nm includes infrared (IR) and thermal radiation as well as micro- and radio-waves. Optical sensors measure radiation reflected by the earth's surface in the range from near-IR (NIR) to far-IR while

non-optical sensors, in the narrow sense radar sensors, collect data about objects on the earth mainly using microwaves (Albertz, 2007).

When in the middle of the 19th century the Frenchman FÉLIX TOURNACHON took the first aerial images from a hot-air balloon (Löffler et al., 2005) the idea of remote sensing was born and started developing. In the following years the field of remote sensing derived benefit from technical progress in aviation and photo technology. After World War II the first colored aerial images have been taken (Matusch, 2009). When in 1972 the National Aeronautics and Space Administration (NASA) launched Landsat-1 the first earth observation satellite for cartography started operating (USGS, 2015).

In general remote sensing includes two major recording techniques which are active and passive procedures. While passive systems use the sun as source for radiation, active systems work independently from solar light by having an own radiation source on board. On the way from the sun to the earth and back to the sensor incident radiation is affected by disturbing influences especially in the atmosphere. The effect of absorption means the transformation of radiation into a different energy form which leads to a loss for remote sensing. However, scatter describes the effect of distraction and dispersion of radiation caused by aerosols. Both influences, together called extinction, reduce the measurable radiation. Naturally active systems are subject to the same disturbing atmospheric influences. To counter this, long-wave radiation of 1,000 mm is used, as the degree of atmospheric transmission depends on the wavelength of radiation (Albertz, 2007).

Another important factor is the atmospheric transmittance which is also included in Figure 1. Only in the atmospheric windows remote sensing can be applied. Another factor also having a large influence for the results of optical sensors are clouds. The high cloud density in some regions complicates a high resolution long-term monitoring a lot, wherefore radar systems are mostly used in these areas.

Nowadays the monitoring tasks of the EU member states required by legal regulations are mostly fulfilled using earth observation satellite systems. Therefore, the monitoring results of satellite systems especially in terms of vegetation classification, geomorphology and change detection are evaluated in the present work. By introducing a small RPAS for further environmental monitoring task the classification results are tried to be improved. The following subchapters will go into detail about the possibilities of

earth observation with satellite systems as well as the advantages of using RPASs.

2.2.1. EARTH OBSERVATION WITH SATELLITE SYSTEMS

Since the first earth observation satellite was launched more than forty years ago the constructors of satellites continually improved the spatial resolution. Caused by novel technologies and rapid development the US American Landsat series with a spatial resolution of 30 m has been exceeded by the French SPOT satellites with a resolution of 10 m but also they have been surpassed by the Indian satellites IRS 1C and 1D with a nominal resolution of 5 m in the panchromatic spectral range within a few years. Nevertheless, when IKONOS delivered the first images with a spatial resolution below 1 m the world was surprised about the resolution comparable to an ortho-photo in an image that had been taken from 680 km altitude (Mansberger and Eisl, 2009).

Through continuous further development currently operating Civil Earth-observation satellites deliver data with ground resolutions down to 50 cm/pixel (in part data with higher detail, currently down to 30 cm/pixel, is acquired but not provided to customers due to limitations of the US law). A summary of the specifications of the data acquired by current VHR satellite systems is given in Table 2. Most current systems of this type provide high spatial-resolution data in only four spectral bands (3 visible, 1 near infrared), thus allowing for composition of near-real color image products and false-color infrared image products for vegetation applications, for example. To date, only WorldView-2 and WorldView-3 go beyond this by providing 8 multispectral bands each, significantly increasing the potential to discriminate among various land-cover classes.

Table 2: VHR Satellite Systems (DigitalGlobe, 2013a, 2013b and Satellite Imaging Corporation, 2015)

System	Ground resolution ms (pan)	Spectral Resolution (Bands)	Swath width
IKONOS	3.20 m (0.82 m)	4 MS + 1 PAN	11.3 km
GeoEye-1	1.65 m (0.41 m)	4 MS + 1 PAN	15.3 km
QuickBird	2.16 m (0.55 m)	4 MS + 1 PAN	14.9 km
WorldView-2	1.85 m (0.46 m)	8 MS + 1 PAN	16.4 km
WorldView-3	1.24 m (0.31 m)	8 MS + 1 PAN	13.1 km
Pleiades (1A and 1B)	2.00 m (0.50 m)	4 MS + 1 PAN	20.0 km
Eros B	- (0.70 m)	1 PAN	7.0 km

Particularly regarding hyperspectral satellites, which are significantly more suitable for multidimensional remote-sensing tasks because they combine spectroscopy and imaging, only a very limited number of civil space borne hyperspectral instruments are operating so far. For instance, the Hyperion sensor onboard NASA's scientific Earth Observing-1 (EO-1) platform is acquiring data in 220 bands, but with a spatial resolution of only 30 m/pixel (Thenkabaill et al., 2012).

The use of satellite systems for environmental monitoring mainly depends on three factors: spatial, spectral and temporal resolution. As a rule satellite systems with a high spatial resolution in most cases only have a low spectral resolution and vice versa. The temporal resolution of a satellite system is determined by its orbit which usually defines a time of revisit of several days.

2.2.2. REMOTELY PILOTED AIRCRAFT SYSTEMS

The development of RPASs started in the 1950s with main focus on military use where the RPASs could demonstrate their operational capacity. But RPASs additionally have a great potential for civil applications and are expected to bring important benefits into a wide variety of applications (EC, 2012).

In general small RPAS platforms can be roughly divided into Vertical Take-off and Landing (VTOL) Systems, mainly implemented as quadro- or octo-copter systems and fixed-wing systems. VTOL Systems are mainly used for surveillance, real-time video streaming, perspective imaging for touristic applications and point-related sensor measurements. They are very well-suited for local problems and short-time missions. Due to their available payload capacity of up to one kg, they are also suitable for carrying sensors of such mass for short mission duration of up to approximately 30 minutes. A significant disadvantage of these VTOL systems is their vulnerability against adverse weather conditions, especially including higher wind speeds. However, fixed-wing systems fly comparably stable even in adverse weather conditions and therefore are more suitable for environmental monitoring tasks.

Compared to satellite systems for environmental monitoring RPAS platforms have some significant advantages. Using a RPAS the spatial resolution can be adjusted by changing the altitude of flight and therefore can easily be adapted to the user's needs. The spectral resolution depends on the camera sensor that is mounted on the system but the temporal resolution can also be adapted because the system is not dependent on an orbit and is operational whenever the user wants to take images. Additionally to the comparison

between satellite systems and RPASs for environmental monitoring, the present project researches on the potential of both systems.

2.2.3. MULTISPECTRAL AND HYPERSPECTRAL DATA

The whole idea of remote sensing is based on the fact that each material reflects, absorbs, transmits and emits electromagnetic radiation in a unique way. Through remote sensing the reflectance of each material can be measured in different regions of the electromagnetic spectrum. Thereby a reflectance value of 100 % means that the whole light striking an object is reflected from the object and is detected by the sensor. Contrariwise the reflectance value is said to be 0 % if none of the energy returns to the sensor. Through the principle of reflecting light with different percentage values in the diverse regions of the electromagnetic spectrum each material creates its own spectral signature. Figure 2 shows spectral signatures of different materials. For instance the spectral signature of green grass stays relatively low in the visible light. As it has its highest value in the visible spectrum of green light it appears to look green for the human eye. But in the NIR light the spectral signature of green grass suddenly increases to a reflectance value of about 40 %. After another lower peak in the mid-IR it decreases again. Because the spectral signature contains much more information than detectable in visible light, it can be used to differentiate more precisely between different materials. As shown in Figure 2 with the green and red graph the spectral signature makes it possible to even differentiate between green and dry grass as the reflectance values differ a lot in the electromagnetic spectrum.

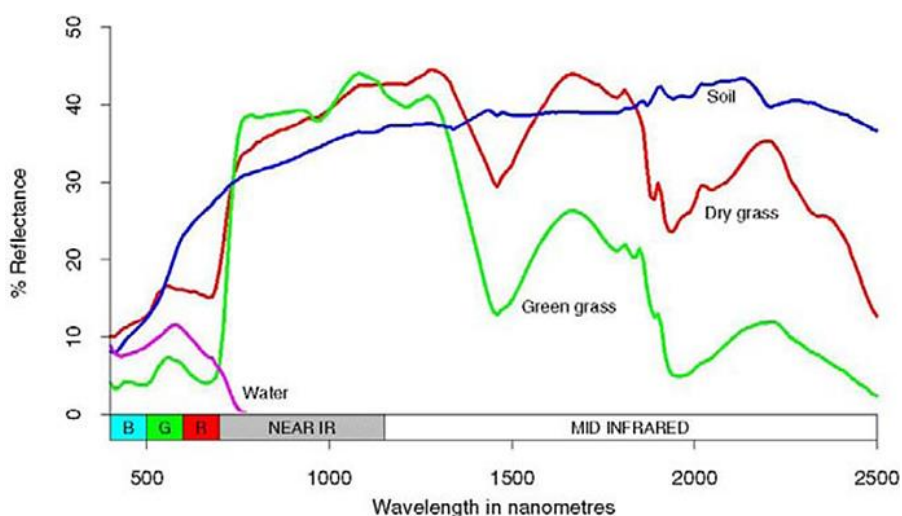


Figure 2: Spectral signatures of different materials (Ashraf et al., 2011)

Based on this idea of each material having a unique spectral signature the difference between multispectral and hyperspectral sensors can be explained. While multispectral sensors usually have only four, in exceptional cases (WorldView-2 and WorldView-3) eight bands, hyperspectral sensors have hundreds of continuous spectral bands available. For instance, the Hyperion sensor onboard NASA's scientific Earth Observing-1 platform is acquiring data in 220 bands with a bandwidth of 10 nm each (Thenkabaill et al., 2012). Understandably a complicated spectral signature can be approximated much better with 220 available values than with four (or eight). Therefore, hyperspectral data are more suitable to extract specific objects from the data set.

In general multispectral image pixel vectors have poorer information than hyperspectral image pixel vectors. For that reason multispectral image processing is mainly based on image spatial information and correlation to compensate insufficient spectral resolution. Therefore, spatial domain-based techniques predominate in multispectral image processing. However, with the introduction of hyperspectral sensors materials that cannot be made visible with multispectral sensors are now analyzed from hyperspectral data. Consequentially application areas for multispectral and hyperspectral data differ according to target and objects to be analyzed. While for multispectral data land cover is from major interest on the contrary the objects of interest in hyperspectral data are mainly targets with particular spectral characteristics. Generally these types of targets appear either as a mixture of different materials or as a mixed pixel due to their size being smaller than the sensor's spatial resolution. Additionally these types of targets usually have a low probabilistic of occurrence. For that reason image processing techniques for multispectral data usually perform pattern classification and analysis assuming that each pixel belongs to one particular spatial class. On the other hand targets of hyperspectral data analysis can only be detected at mixed or subpixel level and traditional spatial domain based image classification algorithms may not be suitable. Algorithms for hyperspectral data analysis need to extract targets based on their spectral profile and have to perform target based detections (Chang, 2013).

2.2.4. PHOTOGRAMMETRY

As another form of remote sensing, photogrammetry started developing between 1850 and 1900 with the plane table photogrammetry, the analysis of

complexly manufactured visualizations of the landscape (Linder, 2005). After Slama (1980) photogrammetry is defined as an art, science and technology of obtaining reliable information about physical objects and the environment through processes of recording, measuring and interpreting photographic images and patterns of recorded radiant electromagnetic energy and other phenomena. Photogrammetry can be divided into four categories based on the camera position (Ahmad, 2013):

- Aerial Photogrammetry; the camera is positioned at > 300 m altitude
- Close-Range Photogrammetry; defined as < 300 m altitude
- Terrestrial Photogrammetry; the photo is taken near to the ground
- Outer Space Photogrammetry; the photo is taken from space

For the present project close-range photogrammetry is used to calculate a Digital Surface Model (DSM) from the highly overlapping RGB data collected during RPAmSS missions. The calculation is done using the Software Agisoft PhotoScan. The DSMs of the project sites are then used as additional information to support the classification procedures. Besides the use of the original multispectral, RGB and Near Infrared (NIR) data for classification the height information of the photogrammetrically-derived DSM in combination with the original data is used to achieve a better classification result.

2.2.5. VISUAL IMAGE INTERPRETATION

Meanwhile the Second Italian War of Independence in 1859 and the American Civil War in 1861-65 the idea of taking aerial images from a balloon and later from other aerial vehicles started developing. Simultaneously, the visual image interpretation has been established. Early on, the applicability of aerial images not only for military applications has been recognized. While petroleum industries have been one of the most consistently using aerial image interpretation, nowadays especially forestry is taking advantage of this technique (Hagen, 1950).

Visual image interpretation in forestry and other arboricultural application areas is useful to extract information about tree height, volume of wood growing, tree species and others. Although the preparation takes some time, this technique is especially useful for mapping larger areas. Mapping tree species requires an interpretation key to build a connection between the appearance of an object in nature and how the same object is visualized in

the image. Of main importance for identification purposes are therewith color, texture, shape of the shadow if visible and size of the object. The normal procedure for visual image interpretation aiming in vegetation species is to start in the field and map the vegetation in a representative sample area. Preferably, each species of the complete study site should be present in the smaller sample area at least once. After the species are mapped and their location is known an interpretation key is developed using all available information. An example of a tree interpretation key for forestry in southern Oregon and northern California can be seen in Figure 3. Finally, each object in the image is identified according to the interpretation key (Oester, 2003).

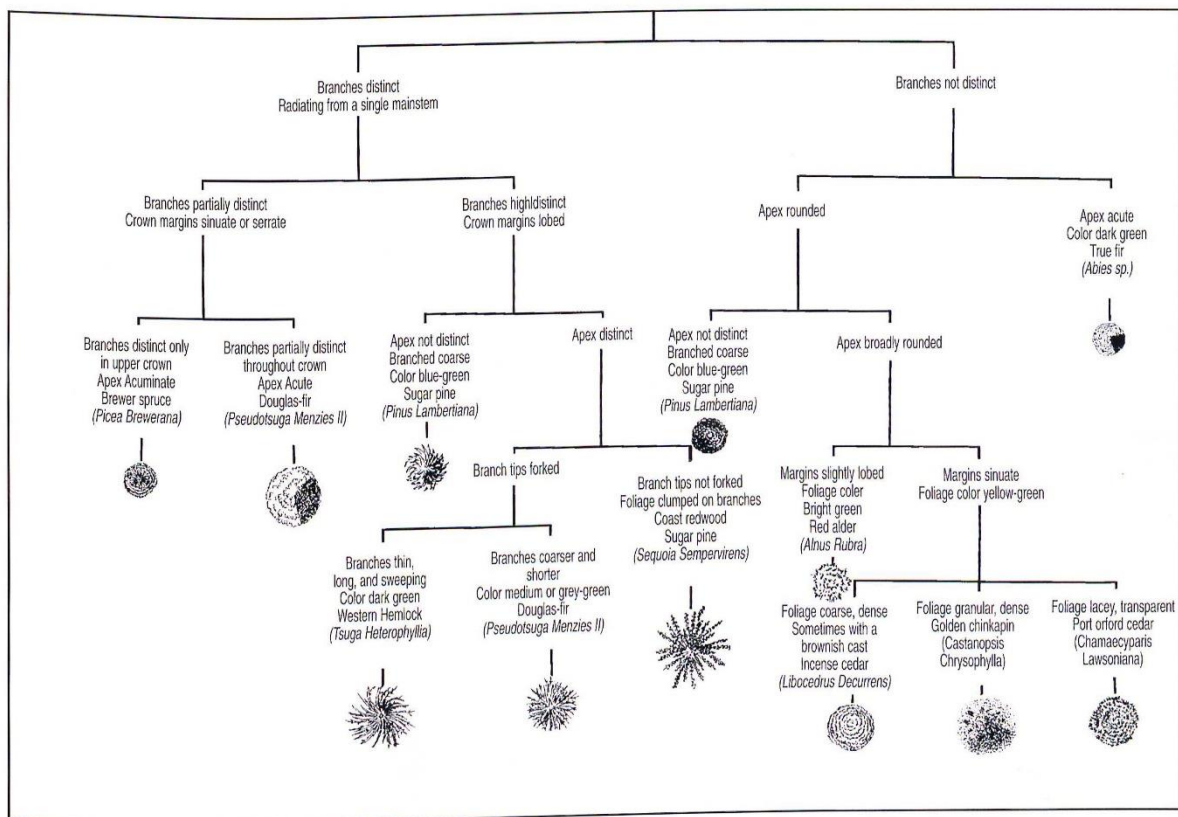


Figure 3: Partial key to identification of tree species in southern Oregon and northern California on large-scale, color aerial photographs (Ciesla and Hoppus, 1990)

The main difficulty in visual tree identification based on aerial images is the missing information compared to profile view. While in aerial images each tree crown appears more or less circular, laterally viewed crown shapes differ enormously between species. Figure 4 shows four main tree species of central Europe and their appearance in above and laterally view. Other information an expert would consider outside in the field for tree identification are bark structure, leaf shape and bud appearance. Although some of these information might not be visible caused by seasons and tree location, there are

always some characteristics to at least identify the species. Due to camera angle and limited resolution these information are not included in most aerial images. Therefore, the interpreter needs to change his habit of tree identification and develop and use an interpretation key to ensure proper identification. Visual image interpretation should always be conducted by experts in the field of interest as they have experience how different objects appear and are able to develop and apply a meaningful interpretation key. In this project visual image interpretation is used on the one hand as part of the reference data acquisition and on the other to examine the interpretability of VHR RGB RPAS-derived images.

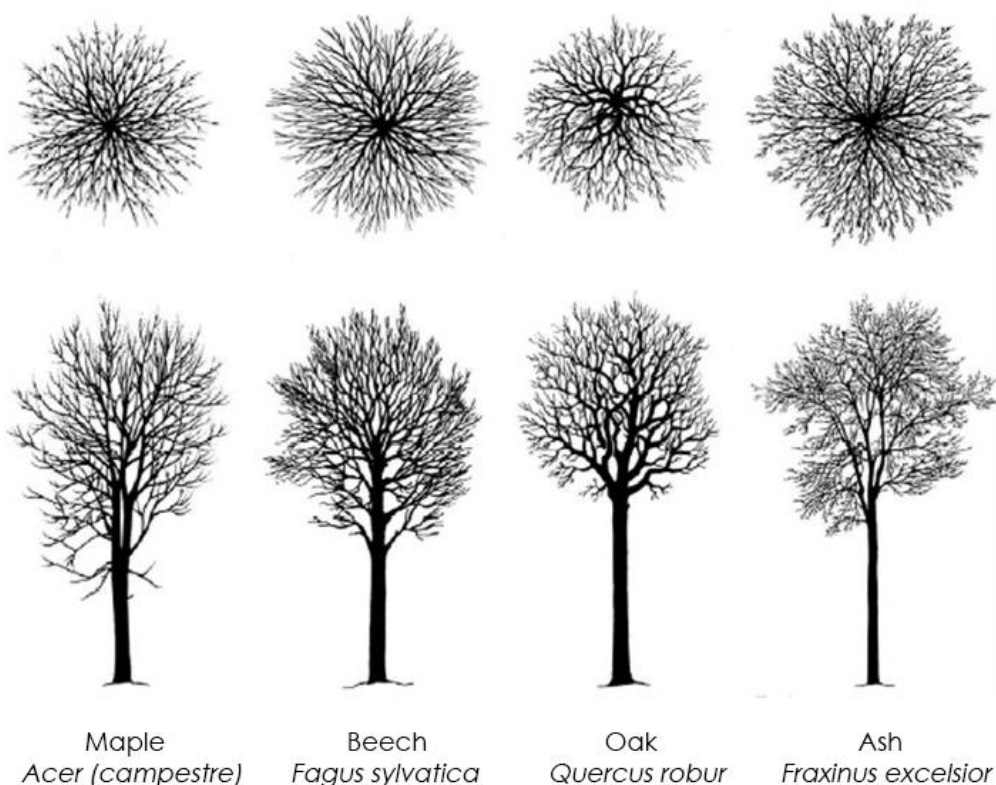


Figure 4: Four main tree species in above and laterally view (Engleder, 2004 with modifications)

2.2.6. IMAGE CLASSIFICATION

Classification is the process of sorting pixels into a defined number of categories according to their data values. A class or category includes all pixels that satisfy a set of certain criteria. Depending on the type of information that should be extracted from the original data, classes can either represent areas with different appearance or be associated with known features on the ground. In general two different classification methods can be applied: unsupervised and supervised training (Jensen, 2005).

Unsupervised classification is the process where the user specifies some parameters which the computer uses to find statistical patterns. These patterns are detected based on the clustering of pixels with similar spectral characteristics and do not necessarily stand in the context of the analyzed scene. Unsupervised classification is mostly used when there is less knowledge about the data and possible classes. However, supervised training gives the analyst more control by selecting single pixels and assign them to certain classes. To classify data using supervised classification, at first the computer needs to be trained to be able to recognize patterns. Therefore, reference data are required. According to the selected pixels the computer identifies other pixels with similar characteristics to form classes. To make use of this method, knowledge about the data and the aimed classes is required. The result of the training phase is a signature for each class containing data to define the content of the class. Based on the signature a mathematical algorithm, known as decision rule, is formulated and applied to data for classification (Jensen, 2005).

2.3. BIOTIC AND ABIOTIC PRINCIPLES

As every ecosystem natural flowing rivers are characterized by biotic as well as abiotic factors. Plants growing adjacent to rivers have a significant influence on its dynamic and sediment load but otherwise are dependent on the flood delivering nutrients. Pioneer species with their capacity of rapid spread populate newly formed banks and therewith create landing zones for softwood meadows. Invasive neophytes displace species, endanger indigenous biotopes and disturb the natural equilibrium. The stability of a river regarding morphologic changes depends on the relation between water flow, sediment load and bed grain size. To determine a river's ecological value and predict the future drainage basin among others the soil type of the river bed needs to be included as important factor.

2.3.1. RIVER VEGETATION

For long-term survival trees need to make high investments because of relatively slow growth, long life duration and the need to adapt to evolving locational factors because of immobility. Therefore, different tree species have developed their own survival strategy and thus two major survival strategies have been established. Pioneer tree species are those tree species that

populate open spaces at first using their high spread potential, like willow (*Salix*), birch (*Betula*), pine (*Pinus*), ash (*Fraxinus*), poplar (*Populus*) and alder (*Alnus*). A birch forest as an impression of pioneer species is shown in Figure 5. On the contrary, climax tree species appear much later in the regeneration cycle and focus on the strategy to respond the pressure in the competitive environment. Climax tree species usually have a high life expectancy like beech (*Fagus*) and oak (*Quercus*). Figure 6 shows a beech as representative of the climax tree species. Another group is formed by the tree species that neither belong to the pioneer- nor the climax tree species. This group is called transition tree species and includes trees like maple (*Acer*), lime tree (*Tilia*) and hornbeam (*Carpinus*).



Figure 5: Birch Forest representing Pioneer Species (Arnoldius, 2012)



Figure 6: Beech representing Climax Species (Augsburger Allgemeine, 2013)

Table 3 has a comparative look at the characteristics of pioneer- and climax tree species. This table highlights the major goal of the different survival strategies. While pioneer species aim to secure the survival of the species in having high regrowth potential, a low life expectancy and a high spread potential in being dispersed by the wind, climax species aim to secure the survival of the individual. Climax species ensure this with a high life expectancy, high competitive strength and a high shade tolerance. Seeds are distributed slowly using conservative dispersion pattern that only reach the surrounding area. The CODIT (**c**ompartmentalization **o**f **d**ecay **i**n **t**rees, in the 1990s reformulated to compartmentalization of *damage* in trees) model developed by Shigo and Marx (1977) explains the process of compartmentalization of

decay in trees. With regard to the CODIT model pioneer species are sensitive to damages because they have a low compartmentalization while climax species have a high compartmentalization and therewith are able to deal better with decays and damages.

Table 3: Comparison of pioneer and climax tree species (Leitsch, 2012)

Pioneer Tree Species	Climax Tree Species
High regrowth potential	Low crown elasticity
Low life expectancy	High life expectancy
High spread potential	Slow spread
Low shade tolerance	High shade tolerance
Broad site amplitude	High competitive strength
Low compartmentalization	High compartmentalization
High risk tolerance	Conservative strategy
Aim: Secure survival of the species	Aim: Secure survival of individual





Pioneer species are from certain interest for natural conservation because they usually expand first on open spaces and for this reason can have a disturbing effect to executed actions in the field of river restoration. Water flow and sedimentation experience a braking effect caused by the root penetration of newly established species. Another vegetation group having an influence on the existing flora are the invasive neophytes.







Caused by globalization and export of goods around the whole world exogenous species are introduced into local landscape either purposely as ornamental or useful plant or accidentally as innocent bystander in global transportation. Because of climate change good conditions are offered for some of these invasive plants and they begin to spread. These neophytes which manage to establish permanently are an issue for natural conservation because they displace indigenous species and have an impact on the natural equilibrium. Furthermore, in river environments invasive plants can impair flood protection in endangering stability of the embankment zones. After the Federal Environment Agency (Essl & Rabitsch 2002) in Austria 17 invasive neophytes exist which are relevant from a nature conservation perspective. Additionally 18 species are declared as potentially invasive and are expected to cause problems in the future. All of these 17 neophytes grow more or less as a matter of priority in river environments. All invasive species of Austria are introduced in







Table 4 (Magnes, 2012 and German Federal Office of Nature Conservation, 2015).

The European Network on Invasive Alien Species (NOBANIS) was developed as a result of the recommendations formulated on the Convention on Biological Diversity's 6th meeting of the Conference of Parties in 2002. Aim of NOBANIS is the establishment of a database including all invasive species that are currently present or might become invasive in the future in the participating countries (NOBANIS, 2015). As another database DAISIE (Delivering Alien Invasive Species Inventories for Europe) funded by the sixth framework program of the EC includes many exogenous species growing in European countries (DAISIE, 2015).

Table 4: Neophytes in Austria (Austrian Federal Environment Agency, 2015 and NOBANIS, 2015, the images are from the NOBANIS fact sheets, Stiftung Hessischer Jaegerhof, 2015 and Intermountain Region, 2015)

Name	Botanic Name	Description	Impression
Ash-leaved maple	<i>Acer negundo</i>	Small tree, grows amongst others in alluvial forests, danger of displacement of indigenous species	
Tree of heaven	<i>Ailanthus altissima</i>	Appears predominantly in urban areas but grows also in alluvial forests, builds monocultures and displaces species	
Flat-leaved aster	<i>Aster novi-belgii</i>	Herbaceous plant, displacement of indigenous species through rapid expansion	
Lancet-leaved aster	<i>Aster lanceolatus</i>	Perennial plant, displacement of indigenous species through rapid expansion	

Common tickseed	<i>Bidens frondosa</i>	Annual herbaceous plant, displacement of indigenous species	
American waterweed	<i>Elodea canadensis</i>	Aquatic plant, displacement of pondweeds through rapid expansion	
Hairy willow-weed	<i>Epilobium ciliatum</i>	Perennial herbaceous plant, potential risk of hybridization with indigenous species	
Japanese knotweed	<i>Fallopia japonica</i>	Up to 3 m high shrub, spread through rhizomes, danger of destabilization of banks	
Green ash	<i>Fraxinus pennsylvanicum</i>	Deciduous tree, occurrence in alluvial forests, overgrows flood channels, displacement of indigenous species	
Topinambour	<i>Helianthus tuberosus</i>	Perennial herbaceous plant used for agriculture, occurrence in riverine areas leads to displacement of species	

Giant hogweed	<i>Heracleum mantegazzianum</i>	Perennial herbaceous plant, forms photo toxically-effective substance, displacement of indigenous species	
Himalayan balsam	<i>Impatiens glandulifera</i>	Annual tall shrub, displacement of indigenous species through rapid expansion	
Canadian poplar	<i>Populus x canadensis</i>	Deciduous tree, especially displacement of the black poplar (<i>Populus nigra</i>), genetically influences black poplar	
Locust tree	<i>Robinia pseudoacacia</i>	Deciduous tree, mostly occurs in urban areas but also in river environments, displacement of species through enrichment of soils with nitrogen	
Cut-leaved daisy	<i>Rudbeckia laciniata</i>	Perennial herbaceous plant, displacement of indigenous species	
Canadian goldenrod	<i>Solidago canadensis</i>	Herbaceous plant, displacement of indigenous species through rapid expansion	

Late
goldenrod

Solidago
gigantea

Herbaceous plant,
displacement of
indigenous species
through rapid
expansion



While most of the invasive neophytes hold the risk to displace indigenous species caused by their massive spreading, some neophytes like the giant hogweed are additionally toxic for humans. Others like the Japanese knotweed destabilize river banks with their missing establishment of fine roots. Locust trees sustainably change soil compositions by enriching them with nitrogen collected from the air. And other invasive plants like the hairy willowweed and the Canadian poplar genetically influence other subspecies. For natural conservation it is important to know about the occurrence of neophytes to keep them in bay and protect indigenous species.

The probably most significant spectral characteristic of Austrian neophytes is their individual flowering time. However, the flowering time is highly influenced by seasonal conditions and some neophytes only bloom inconspicuously. But plants comply with the phenological calendar and therefore, the flowering time of each species will always follow a certain order.

2.3.2. GEOMORPHOLOGY OF RIVERS

The zonation of dynamic rivers in general depends on the ground water and duration of flood events. As natural retention basins alluvial forests are important for flood safety and their soils fulfil filter functions to clear water. Contrariwise flood events are of major importance for alluvial forest because they enrich soils with nutrients and contribute to a genetic exchange caused by the current and transposition of species. Figure 7 displays the cross zonation of an ordinary flowing water in Europe. Hereby low water describes the situation when the water level lies significantly below an as normal declared status. As a consequence of meteorologically related lack of precipitation low water is subject to seasonal fluctuations. The zone covered with water in a low water phase is called water zone and usually characterized by a soil consisting of gravel and brash. In rivers with a natural dynamic the riverbed often changes through erosion and sedimentation. The water meadow zone of a natural river is situated directly adjacent to the water. Therefore, this zone is frequently flooded throughout the year. Dividing the water meadow zone again in three

parts, the part closest to the river mainly is populated by annual species. Above low growing grasses and herbs settle and finally the third part is characterized by river reeds and tall grasses. The sediments are coarser grained caused by the increased current and mainly consist of gravel, brush and partly sand. The sandy-gravelly soils of the softwood meadow are flooded up to 190 days per year. Additionally to the mechanical tension and pressure of the water the trees need to compensate oxygen deficiency at the roots. Therefore, the trees have developed different strategies to absorb oxygen and the most frequently represented species of this zone are willows and gray elders. Caused by the missing river dynamics nowadays softwood meadows are often replaced by hardwood meadows which leads to a loss of these habitats and therewith certain species. The hardwood meadow zone is characterized by shorter flooding time and more mature soils because of the larger distance to the water body. Typical species in a hardwood meadow are oaks and elms but also ashes and field maples. These species usually have to tolerate a flooding time of up to three months per year caused by the peak flood. The rich soil in a hardwood meadow consists of fine grained components, mainly clay and sand. Nowadays most remaining hardwood meadows are no longer flooded regularly but have at best a groundwater connection (Roth-Kleyer, 2009 and 2011 and Scheidegger et al., 2012).

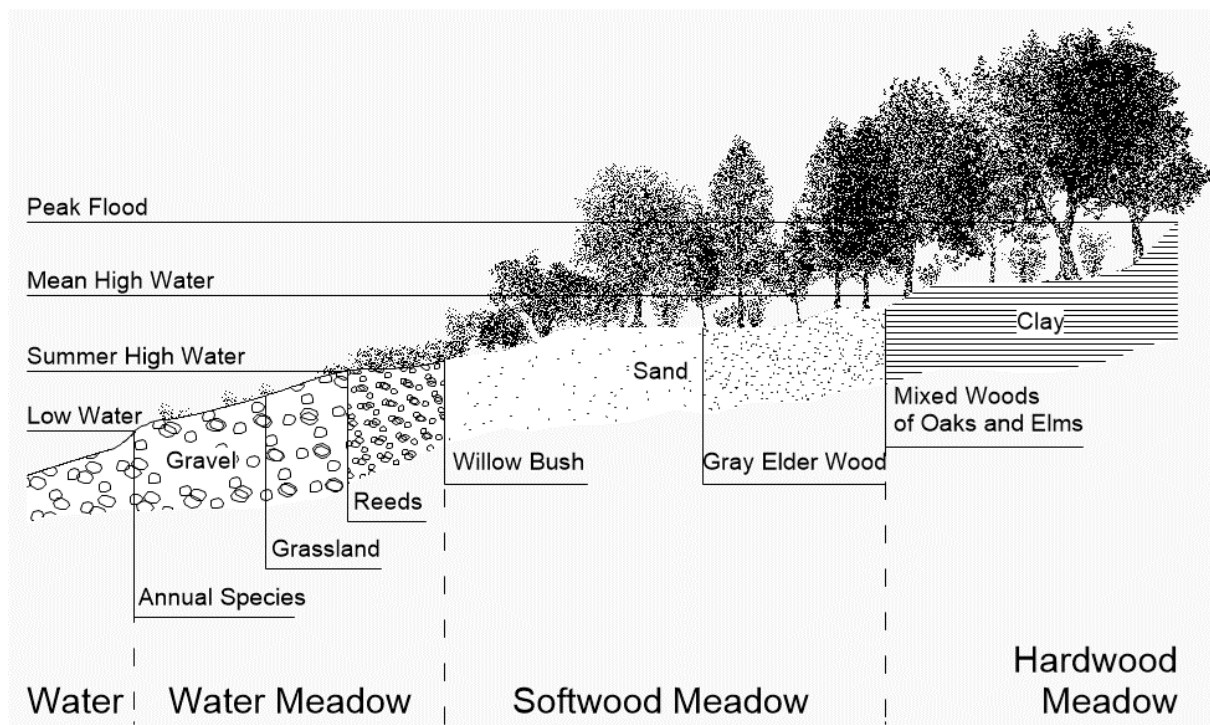


Figure 7: Vegetation sequence of an idealized cross section of a bed load carrying river with dominant summer high water in Central Europe (Ellenberg and Leuschner, 2010 with modifications)

Soils are composed of solid, liquid and gaseous components whereby the solids are of organic and inorganic nature. Additionally to the separate grain sizes of the basic material newly formed clay minerals and salts belong to the inorganic components. The grain size distribution of a soil mainly depends on its basic material and past weathering processes. The organic components of soil include living organisms as well as plant roots and dead organic materials like plant residues and dead micro-organisms. Liquid soil water fulfils the function of a solvent and transporting agent for plant nutrients and colloid substances. Besides soil water soil vapor fills the pores and ensures oxygen supply of the plant roots and life of soil organisms. In general soils are classified based on their percentage content of main soil types which are gravel, sand, silt and clay. The grain diameters of the main soil types are stated in Table 5. Figure 8 displays a soil texture triangle which is used to classify the soil based on its content of each main soil type.

Name		Grain Diameter
Stones, blocks		> 60 mm
gravel	Coarse gravel	20-60 mm
	Medium gravel	6-20 mm
	Fine gravel	2-6 mm
sand	Coarse sand	0.6-2 mm
	Medium sand	0.2-0.6 mm
	Fine sand	0.06-0.2 mm
silt	Coarse silt	0.02-0.06 mm
	Medium silt	0.006-0.02 mm
	Fine silt	0.002-0.006 mm
clay		< 0.002 mm

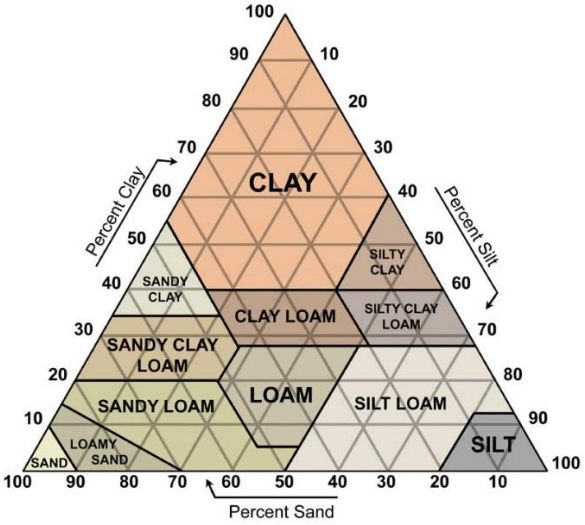


Table 5: Main soil types and their grain diameters (Roth-Kleyer, 2009)

Figure 8: Soil texture triangle to determine soil type (Bellingham, 2007)

The morphology and dynamics of a fluvial system are controlled by several interrelated variables. After Lane (1954) river channels are formed, maintained, and altered based on two main influences: flows and sediment loads. Equilibrium is achieved through a balance of the four factors sediment load, bed sediment size, stream discharge and stream slope. For that reason

equilibrium occurs when the streamflow power is constant over the length of the stream resulting in no changes in the shape.

Caused by seasonal precipitation and other factors natural dynamic rivers usually not reach equilibrium but change morphologically. The soil type of a river bed can provide information about the river bed's stability. While clayey or rocky bed and banks usually indicate high stability silty, sandy or gravely bed and banks normally form less stable systems with high morphologic change potential. Through sedimentation of particles in calmer regions and erosion in regions with strong current a natural river forms its bed, promotes high biodiversity and fulfils its ecosystem function. Sediment rearrangement is important for the species in alluvial forests and to build temporal gravel- and sand banks with high ecologic value (Scheidegger et al., 2012).

3. RELATED WORK

Due to the rapid development of the RPAS market in combination with the requirements of the European Union for environmental monitoring a variety of different related research projects have been performed. Salamí et al. (2014) focused on the survey of vegetated areas with a RPAS and concluded that these remote systems are especially useful for precision agriculture and their high potential for diverse application areas presently only is limited by legal restrictions.

In 2009 Rango et al. researched on the applicability of a RPAS for rangeland monitoring. Besides the use of traditional classification algorithms they gave the aerial images to experts in the field of rangelands for visual interpretation. With their experiments they showed that the RPAS is directly applicable to operational agency needs for measuring and monitoring rangelands.

As a service center of the Utah Water Research Laboratory at Utah State University the AggieAir Flying Circus has developed a RPAS called AggieAir. This platform is able to acquire multispectral data for riparian and wetlands applications. In different projects the AggieAir Flying Circus has proven the applicability of the AggieAir platform for fish habitat mapping and monitoring (Jensen et al., 2011) and mapping and predicting the growth of invasive plant species in wetlands (Zaman et al., 2011).

Although the principles of river restoration are now quite well established, some aspects like the monitoring process still need to improve (Palmer et al., 2005). As Carbonneau et al. (2012) showed in a recent review in the area of fluvial remote sensing radar, Light Detection And Ranging (LiDAR) and RPAS approaches represent the most recent and least used and completed systems for applied uses in river environment. To counter this a research project was performed by Dufour et al. in 2013 with the aim to illustrate recent developments and perspectives for riparian vegetation monitoring purposes. Therefore, they used three different image sources: LIDAR, radar and RPAS. Because of the high overlap of RGB images collected by RPAS they could be used to photogrammetrically derive local DSMs. They concluded that LiDAR, radar and RPAS images notably allow a three dimensional characterization of vegetation through DSM regarding RPAS, point cloud concerning LiDAR and Shannon entropy for radar.

In 2006 Frick published her thesis (PhD) about the utilization of highest resolution satellite systems for environmental monitoring after the Habitats Directive. She

presented a semi-automatic method for habitats classification in the northeastern part of Germany. After Frick the use of satellite images is a good way to improve large aerial environmental monitoring tasks. Additionally automatic classification facilitates and improves visual interpretation.

Concerning geomorphology in 2013 Güneralp et al. delineated river-flow boundaries from digital aerial photography and ancillary images using Support Vector Machines. They found that Support Vector Machines perform satisfactory delineations of the boundaries using a multiscale evaluation scheme to not only evaluate the performance for the whole river reach but also for subriver sections.

Lucas et al. published in 2014 their results of the development of an Earth Observation Data for Habitat Monitoring system. The aim of the system is to consistently map habitats of high ecologic value and monitor biodiversity throughout the EU. The highly automated system has been tested on VHR satellite data in NATURA 2000 sites in different member states. The results prove the applicability and transferability of the monitoring system to the natural conditions in different member states.

Other related researches focus on automatic analyses of forest stands using remote sensing. In 2002 Atzberger and Schlerf presented their tool to automatically estimate stem density in coniferous forests from high resolution black-white ortho-photos. The method works with an accuracy of approximately ± 65 trees per hectare for stem densities varying between 200 and 800 trees per hectare. Another study conducted by Lefsky et al. (2002) concentrates on the application of LIDAR remote sensing for ecosystem studies. The authors conclude that LIDAR remote sensing is an extremely accurate method for measuring topography, vegetation height and cover as well as more complex attributes of canopy structure and functions.

These and much more projects have been used to get an overview about current works in the field of VHR remote sensing and habitats monitoring.

3.1. CORINE LAND COVER AND COPERNICUS

The CORINE (Coordination of Information on the Environment) Land Cover (CLC) project as part of the European CORINE program was intended to provide geographic information on the land cover in the EU member states and other European countries. The inventory was initiated in 1985 because the environmentally relevant data available at the time have not been comparable with regard to both content and structure. The CLC project is

supervised by the European Environment Agency and uses satellites to acquire land cover data in a scale of 1:100,000 (Federal Environmental Agency, 2014). The land cover inventory has been taken place in the years 1990, 2000, 2006 and 2012. While the first two recordings have been taken with the American Landsat-5 and Landsat-7 satellites, CLC2006 and CLC2012 used the imagery of the Indian ResourceSat-1 and in addition the French SPOT-4 and -5 satellites for CLC2006 and the German RapidEye satellite for CLC2012 (Copernicus, 2015). Since the latest update in 2012 the CLC project monitors the land cover in 39 states with a minimum mapping unit of 25 ha and a minimum width of linear elements of 100 m. The standard CLC nomenclature consists of 44 land cover classes (Federal Environmental Agency, 2014). CLC data sets provide spatio-temporal data of land cover and land use information of Europe used to monitor changes of the earth's surface.

The objective of the European Copernicus land monitoring service is to provide information on land cover and land use to responsables in the field of environmental and other terrestrial application areas. Previously known as Global Monitoring for Environment and Security (GMES) the Copernicus program started with the initial operations in 2011 with the objective of being fully operational by 2016 and is managed by the EC. Overall Copernicus consists of six thematic areas: land, marine, atmosphere, climate change, emergency management and security. The project uses earth observation satellites as well as *in situ* sensors such as ground stations, airborne and sea-borne sensors to collect data from multiple sources (EC, 2015).

Since 1992 the CLC project is performed in Austria under the responsibility of the Federal Environmental Agency. With the project Land Information System Austria (LISA) which was started in 2009 the basis for the computer-aided evaluation of ortho-photos has been created in Austria. Forming three phases the LISA project was finished in June 2015 as Austrian contribution to Copernicus. LISA uses earth observation imageries for analyzing and monitoring land cover and land use in Austria (LISA, 2015).

4. TEST SITES AND DATA BASIS

The project has the aim to perform analyses on data captured with different remote sensing systems to evaluate their use for environmental monitoring of river environments according to the European legal situation. Therefore, the project sites should represent different natural characteristics to cover as much different land cover types with high ecologic value as possible. In the following both project sites at the river Gail and Drau in Carinthia, Austria, are described based on their natural characteristics. Additionally reasons for the choice of the VHR satellite systems WorldView-2, GeoEye-1 and QuickBird-2 as well as the systems' characteristics are stated. Finally the RPA platform with its technical specifications, the reference data and the elevation data used are described. For acquiring the reference data traditional field sampling methods are performed by Austrian domain experts. In the end of this chapter Table 9 gives a summary of all data used in the present project.

4.1. LOCATION AND DESCRIPTION OF PROJECT SITES

For the choice of the project sites certain criteria concerning natural characteristics and location have to be fulfilled. Because the major aim of the survey is to test its applicability for the European directives the project areas should cover as much different monitoring requirements mentioned in the directives as possible. As stated in chapter 2 the Habitats Directive together with the Birds Directive asks for the monitoring of interconnected NATURA 2000 protection sites while each directive on its own already requires a regularly monitoring of natural habitats. Additionally, after the Water Framework Directive all rivers and their directly adjacent ecosystems have to be monitored to ensure high water quality and quantity. For agriculture a bundle of related regulations ensures the maintenance or establishment of good environmental and agricultural conditions by linking the requirements to the agricultural direct payments.

In recent years two different LIFE projects have been performed by the BMLFUW in NATURA 2000 protected sites at the rivers Gail and Drau. Both project sites are not only of importance in the sense of the Habitats Directive but additionally have a relevance for the Birds Directive as migratory birds use the areas for resting. In addition the Water Framework Directive can be applied to

both project areas because they include dynamic rivers. Being surrounded by agricultural fields both LIFE project sites cover all of the four presented legal regulations that ask for monitoring in the EU and demonstrate comparability as both of them have the same legal characteristics. Therefore, the LIFE project sites Gail and Upper Drau River are chosen as study sites in the present project. In the following their natural characteristics are described in detail.

The first project site is the area of the Gail LIFE Nature Conservation project performed by the Austrian BMLFUW. Simultaneously this project site is accounted for NATURA 2000 site. The test area is located in Gailtal east of Hermagor and in between Pressegger See and Nötsch in Carinthia. An overview of the spatial spread of the project site is given in Figure 9. The project site has a total area of 83 ha and is located at an altitude of 580-600 m above the Adriatic Sea. The directly adjacent floodplain areas are represented by calcareous, sandy and silty soils and loamy and sandy soils while the soils far away from the river Gail are predominantly formed as fen soils rich in humus and lime-free transitional peat bogs. The river Gail traverses the project site as potentially meandering and braided river. In the project site the river is regulated with a trapezoidal- or duplicate trapezoidal profile. Through the reduction of the outflow's cross sectional area the discharge capacity gets restricted and therewith the danger of flooding caused by the bursting of the dam increases. The fauna of the project site is comparatively well explored and with an amount of at least 35 species with high conservation value after the Habitats Directive the NATURA 2000 site is one of the most important protected areas in Carinthia. Additionally the project site is used by migratory birds as a resting place and therewith reaches supraregional significance (BMLFUW, 2015a).

For the second project side a part of the LIFE project Life Vein – Upper Drau River is chosen. The whole LIFE project area has a size of 977 ha and is located at an altitude of 525-640 above the Adriatic Sea (BMLFUW, 2015b). The NATURA 2000 protection site includes Austria's largest gray elder alluvial forest, in total 19 indigenous fish species and extremely rare plant species like the German Tamarisk and the Dwarf Bulrush. Additionally the area residents more than 140 bird species and is used as resting place by migratory birds on their crossing of the Alps (BMLFUW, 2015c). The extent of the second project site at the river Drau is shown in Figure 10.

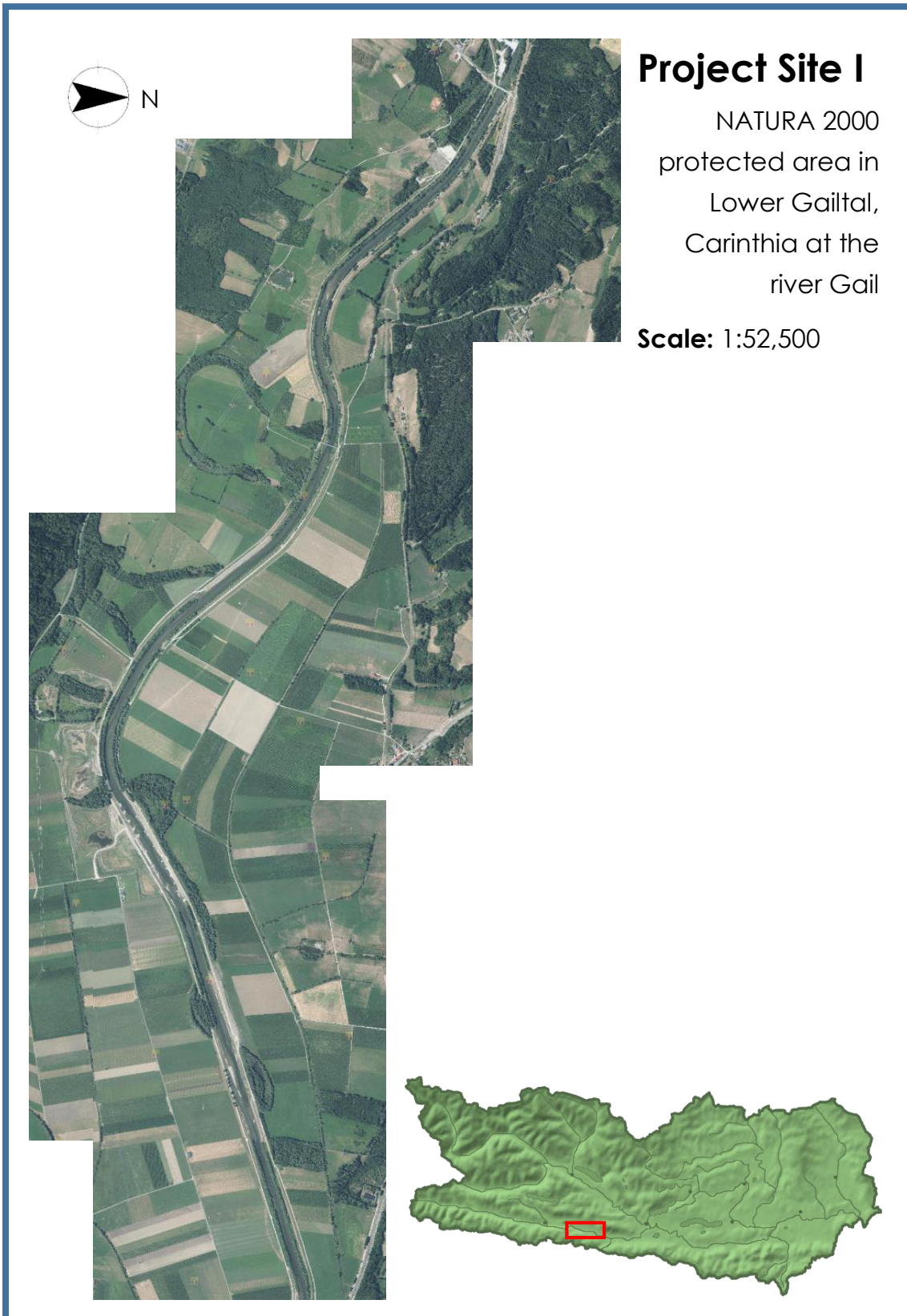


Figure 9: Project site I at the river Gail (KAGIS, 2015 and Glanznig, 2006)

Project Site II

Part of NATURA
2000 protected
area at Upper
Drau River,
Carinthia

Scale: 1:30,000



Figure 10: Project site II at the river Drau (KAGIS, 2015 and Glanznig, 2006)

4.2. SATELLITE IMAGERY

To have a comparison between the collected RPAS and satellite data a satellite system needs to be chosen. Although Hyperion provides an interesting possibility of using a hyperspectral sensor with 220 bands the spatial resolution of 30 m is too low for the research purposes of the present project. Looking at the available VHR satellite systems WorldView-3 offers data with the highest spatial resolution of up to 31 cm in panchromatic range. Additionally this system has one of the highest spectral resolution with eight multispectral and one panchromatic bands. But data of WorldView-3 covering the project sites were not available in the starting phase of this project. As another VHR satellite system WorldView-2 is the main choice for resampling data collected with earth observation methods for environmental monitoring. With its high spatial resolution this system is especially suitable for local analysis as treated in this project.

Launched in October 2009 by DigitalGlobe WorldView-2 was the first VHR satellite system recording in eight multispectral bands. With an operating altitude of 770 km and a sun synchronous orbit the system provides 46 cm spatial resolution in panchromatic and 1.85 m in multispectral range at nadir. Due to US law the high spatial resolution has to be re-sampled by DigitalGlobe for panchromatic and multispectral bands to 50 cm and 2 m, respectively. The temporal resolution is specified with an average revisit time of 1.1 days. Besides the four standard colors blue, green, red and NIR1 WorldView-2 provides four additional colors coastal, yellow, red edge and NIR2 for precise change analyses and mapping. Table 6 specifies the spectral ranges and bandwidths of WorldView-2's nine sensor bands (DigitalGlobe, 2013).

Table 6: Sensor bands of WorldView-2 (DigitalGlobe, 2013b)

Panchromatic	450-800 nm		
Multispectral:			
Coastal	400-450 nm	Red	630-690 nm
Blue	450-510 nm	Red Edge	705-745 nm
Green	510-580 nm	NIR1	770-895 nm
Yellow	585-625 nm	NIR2	860-1040 nm

But there is only one WorldView-2 image of each project site available, acquired in March 2013 which shows snow cover in both project areas. The

snow covering the landscape distorts the spectral signature of underlying land cover and therefore these images have a limited use for classification purposes. Nevertheless, it is used to find out about the usability of snow images for classification purposes.

Thankfully DigitalGlobe provided one additional satellite image for each project area without snow cover. GeoEye-1 was launched in September 2006 and is collecting data in four multispectral and one panchromatic bands, which are specified in Table 7. With a sun-synchronous orbit in 681 km altitude GeoEye-1 delivers data in 41 cm in the panchromatic and 1.65 cm in multispectral bands spatial resolution at nadir. Due to US law all images are resampled to 50 cm and 2 m, respectively. The images from GeoEye-1 are used in the project site at the river Gail. The imagery was acquired in August 26, 2011 and shows the river reach before the restoration project started.

For the project site at the river Drau the data from QuickBird-2 of September 9, 2006 are chosen and show the project area before the restoration started. This satellite was launched in October 2001 and collects data in one panchromatic and four multispectral bands which are specified in Table 8. The spatial resolution is given as 55 cm and 2.16 m at nadir, acquired in 400 km altitude. An overview about the different multispectral satellite images used in this project is given in Figure 11.

Table 7: Sensor bands of GeoEye-1 (DigitalGlobe, 2015a)

Panchromatic	450-800 nm
Multispectral:	
Blue	450-510 nm
Green	510-580 nm
Red	655-690 nm
NIR	780-920 nm

Table 8: Sensor bands of QuickBird-2 (DigitalGlobe, 2015b)

Panchromatic	405-1053 nm
Multispectral:	
Blue	430-545 nm
Green	466-620 nm
Red	590-710 nm
NIR	715-918 nm

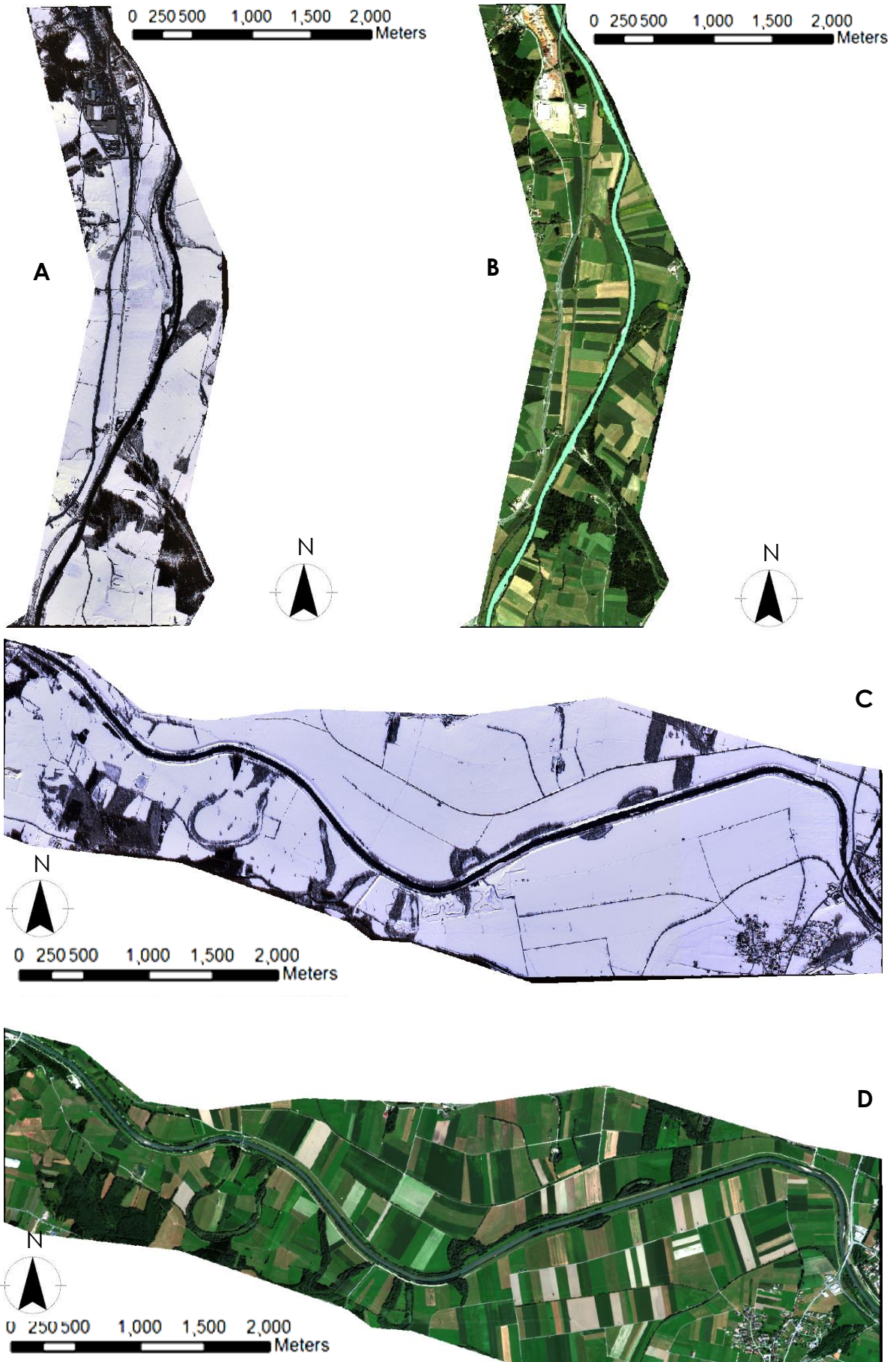


Figure 11: Satellite Imagery: A = WorldView-2 Drau, B = QuickBird Drau, C = WorldView-2 Gail, D = GeoEye Gail

4.3. RPAS AND DATA

For achieving the objective of comparing high resolution RPAS data with data collected from a satellite system, first of all a RPAS platform needs to be chosen. The system should meet the requirements of flying stable even in adverse weather conditions and under wind influence, being easily controllable for inexperienced pilots and providing the possibility of mounting all necessary sensors. With a safe catapult launch, an autonomous flight following predefined waypoints and an automatic parachute landing the chosen Bramor rTK RPAS produced by the Slovenian company C-Astral is easily controllable. Being a fixed-wing system the platform is characterized by rain proofing and wind resistance up to a wind speed of 60 km/h. With a wingspan of 230 cm and a total weight of 4.5 kg the system has a command and control range of 40 km and the battery's endurance is specified with 2.5 h (C-Astral, 2015). A RGB Sony Advanced Photo System type C sensor is mounted on the platform for the RGB imagery acquisition and an additional Sony Alpha 6000 reconstructed as NIR sensor is used for data acquisition in IR spectra. On a second system a hyperspectral camera from the Finnish company Rikola is planned to be mounted in future for hyperspectral data acquisition. Working based on a Fabry-Perot Interferometer the spectral range of this camera can be selected in the range from 400-950 nm and the maximum spectral image dimensions are specified with 1024 x 1024 pixels. The two mirrors of the interferometer create an optical resonator. Constructive interference allows certain wavelengths to be transmitted through the interferometer whereas other wavelengths are reflected (Mäkeläinen et al., 2013). The weight of less than 600 g allows it to attach the camera sensor to the RPAS (Rikola, 2015). While Figure 12 shows the RPAS, in Figure 13 the RPAS-derived data used in this project can be seen.



Figure 12: Bramor rTK RPAS produced by C-Astral (C-Astral, 2015)

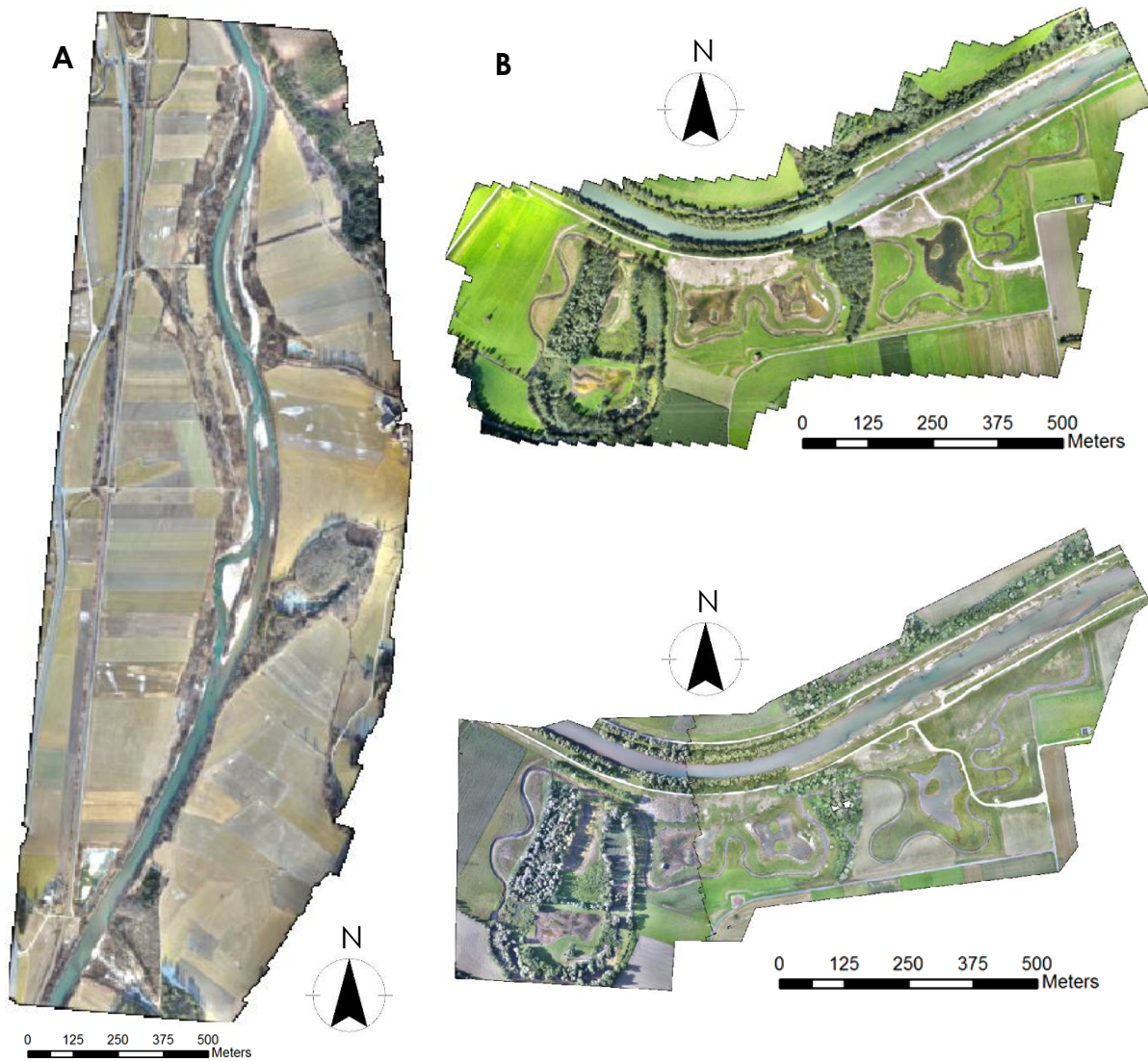


Figure 13: RPAS Imagery A = RGB Drau 12/2013, B = RGB Gail 09/2014, C = RGB + NIR Gail 06/2015

4.4. AERIAL IMAGERY

One goal of this master's project is to evaluate the effect of the different actions performed during restoration with different change detection techniques. To detect change between two images it is from crucial importance to keep spectral and seasonal conditions as similar as possible. As there is a temporal lack of several months between the satellite and RPAS images and the spectral resolutions differ as well, these data sets are not suitable for change detection purposes.

For that reason, airborne ortho-images acquired before and after the restoration are used for change detection. These images have a spatial resolution of 20 cm, have been collected by the Carinthian government and are shown in Figure 14. For the study site at the river Drau the recording times of the ortho-images used for change detection are July 2006 and August 2013 and for the Gail site images were acquired in July 2010 and August 2013.

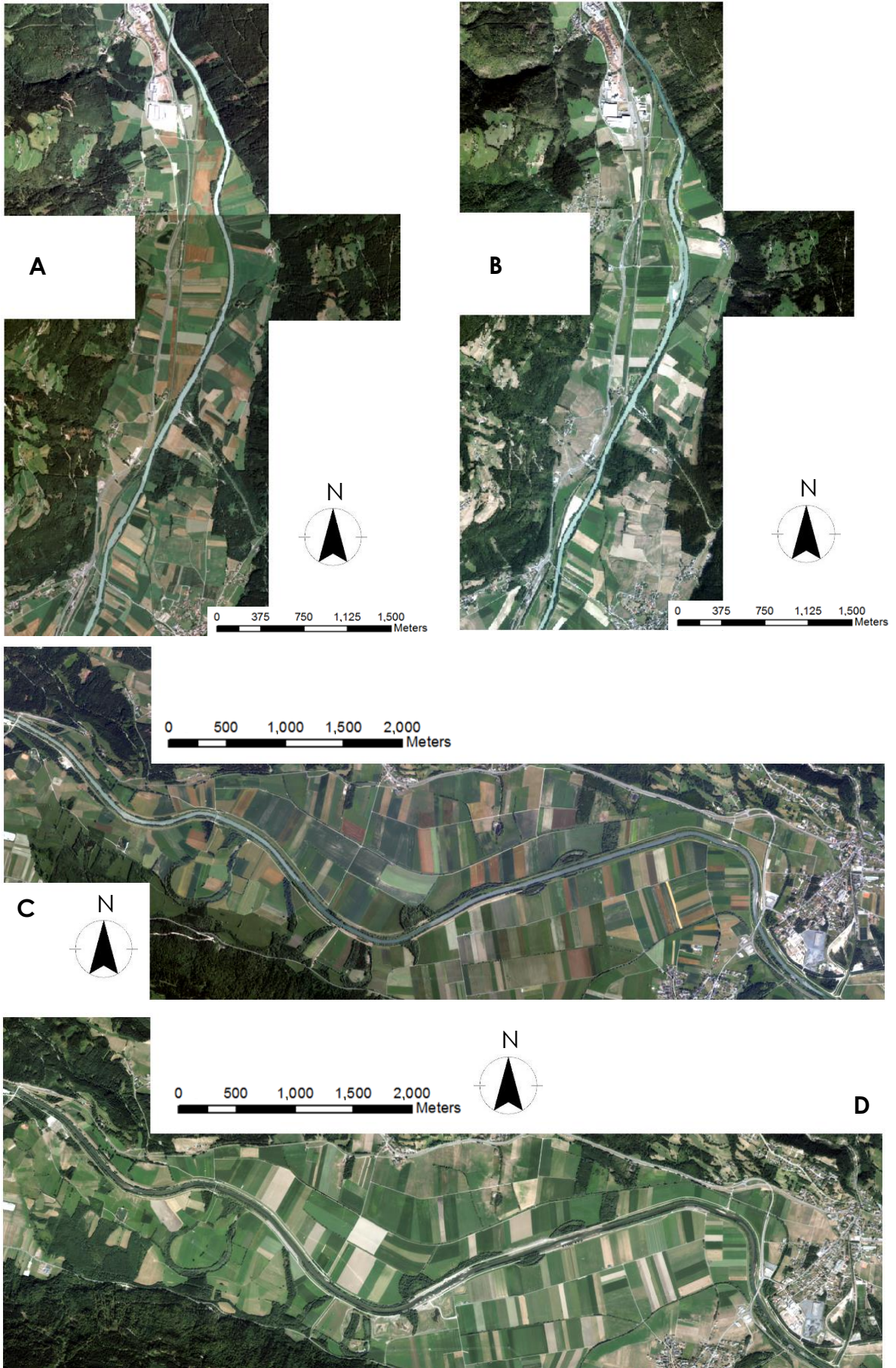


Figure 14: Aerial Imagery A = Drau 2006, B = Drau 2013, C = Gail 2010, D = Gail 2013

4.5. REFERENCE DATA

For the river Gail the first field mapping was done in 2010 based on current ortho-photos of the same year and the existing mapping of the NATURA 2000 protected area. Identified classes as well as areas without available data have been validated and mapped in the field. The second field mapping was performed after the restoration project has been finished in 2014. This time ortho-photos from 2013 were overlaid with the field mapping results of 2010 and classes were assigned by visual interpretation. For validation the results were checked in the field and the state of the habitats was reported.

The spatial base data of the project site at the river Drau was collected in a similar way as for the river Gail. The current NATURA 2000 mapping was compared to ortho-photos of the years 2006/2007. In areas where a significant mismatch was found the habitat type was checked in the field. In 2011 a second comparison between the mapping and ortho-photos from 2010 was performed. If necessary the classes have been adapted due to the current ortho-photo.

Using field methods and comparison to ortho-photos the experts have performed a vegetation classification in both project sites according to the natural habitat types defined after the Habitats Directive. The specific natural habitat types with high ecologic value can be found in ANNEX A. Besides the Habitats Code after the Habitats Directive with the associated description and a unique number for identification the vector data set includes attributes specifying a more detailed internal vegetation typification as numerical as well as descriptive value. Additionally information about the use of the habitats and the presence of deadwood are provided. Another attribute includes a note about the habitat to describe exceptional characteristics and the status of the natural habitat. The reference data with the internal habitat classes are shown in Figure 15.

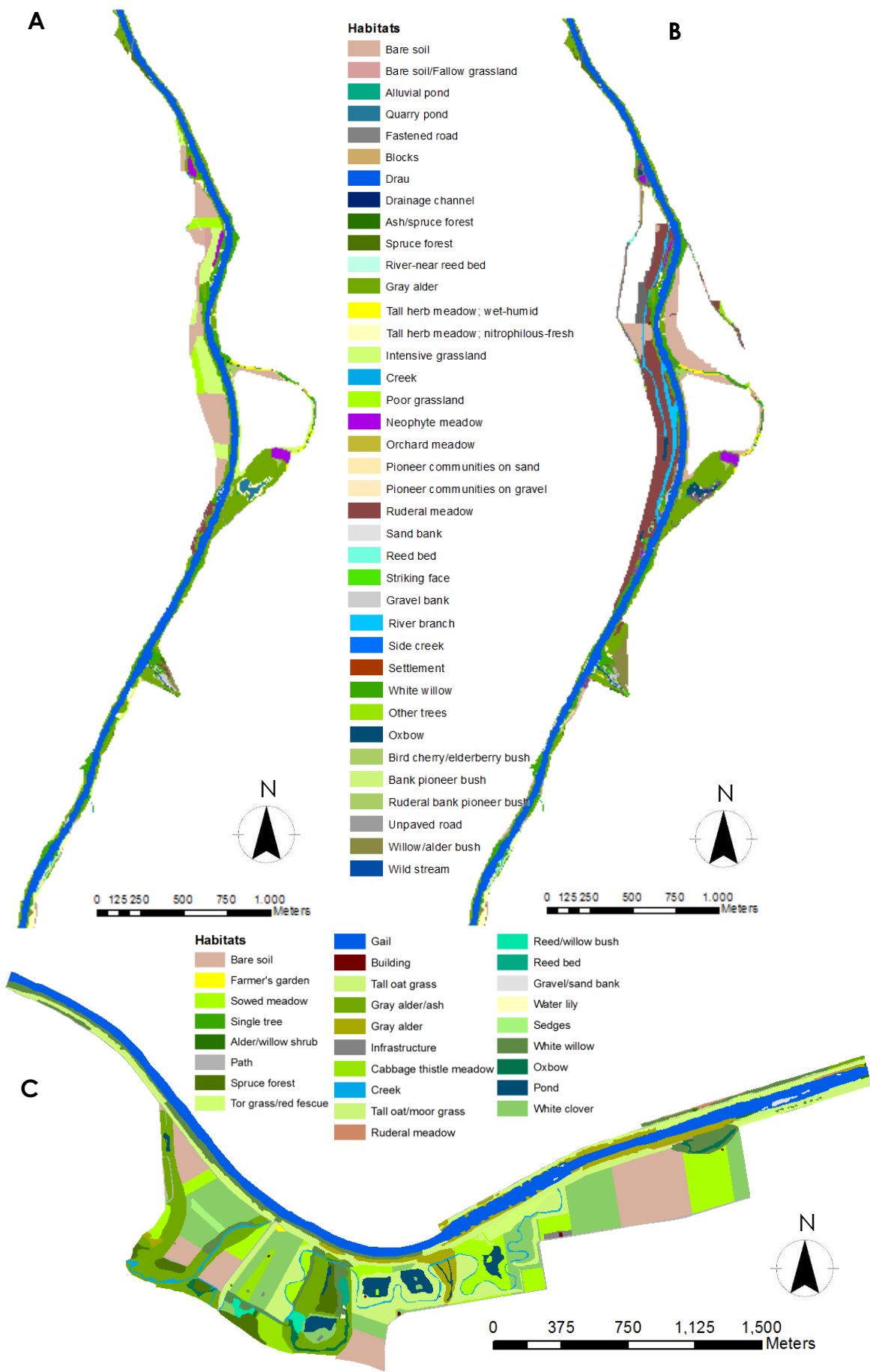
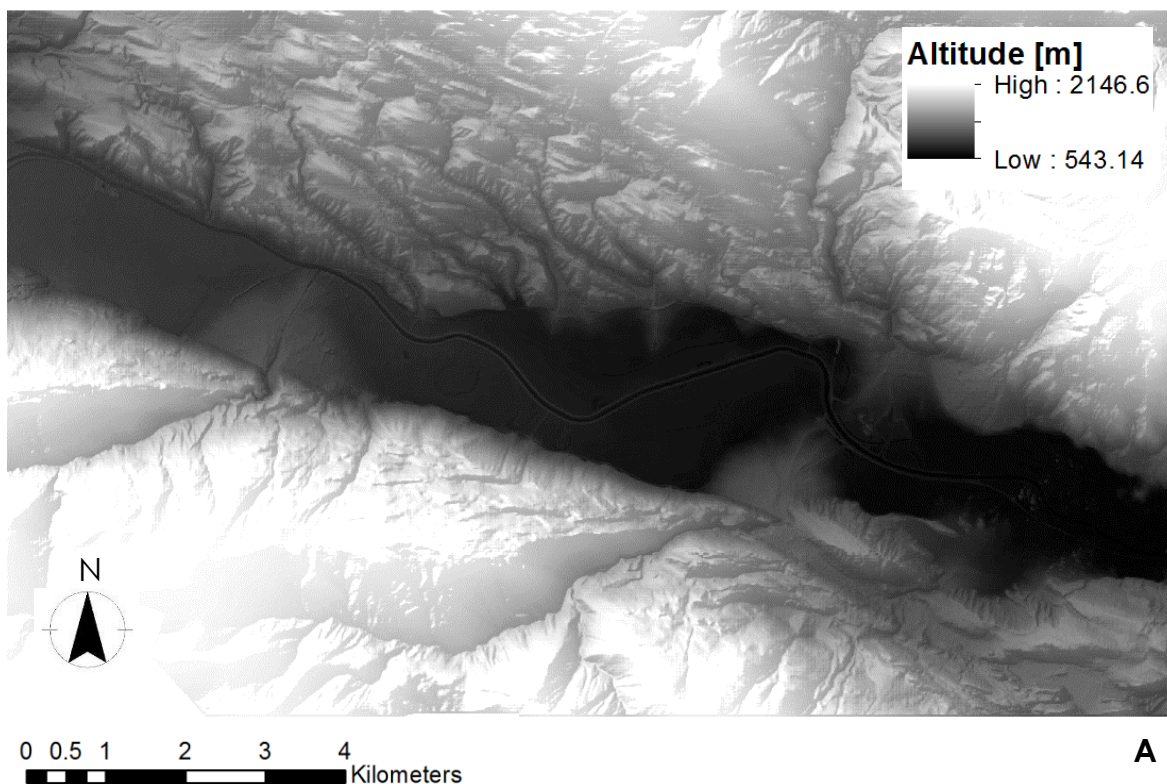


Figure 15: Reference data A = Drau 2004, B = Drau 2011, C = Gail 2014

4.6. ELEVATION DATA

In addition to the before mentioned data other data sources are used to enrich the available information. The Austrian government provides current data open for everyone and accessible through the internet. Thereof the national digital elevation model (DEM) is used to include elevation information and ortho-rectify the satellite images. The data set has a spatial resolution of 10 m and has been derived by airborne laser scanning in 2013. The horizontal position accuracy is stated with 20 cm and the vertical elevation accuracy with 7.5 cm. Additionally DSMs are calculated based on the high overlap between the RPAS-derived images and used as auxiliary information to improve classification. The different elevation data can be seen in Figure 16.



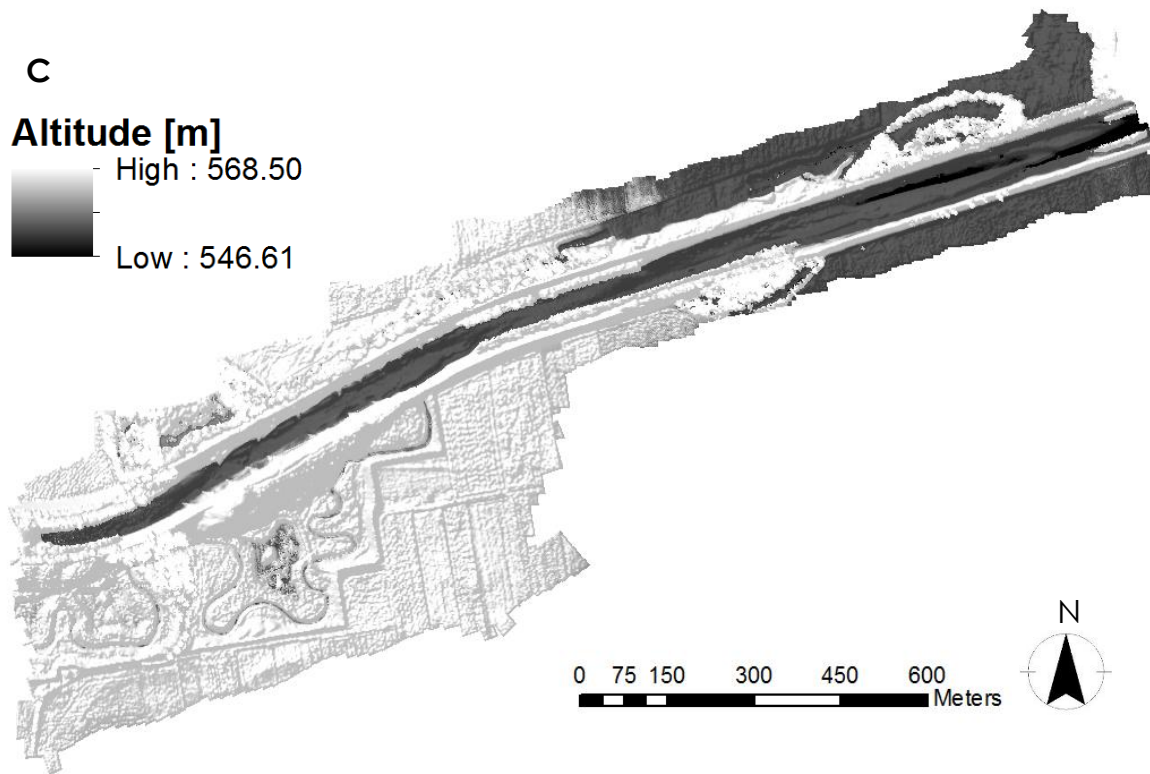
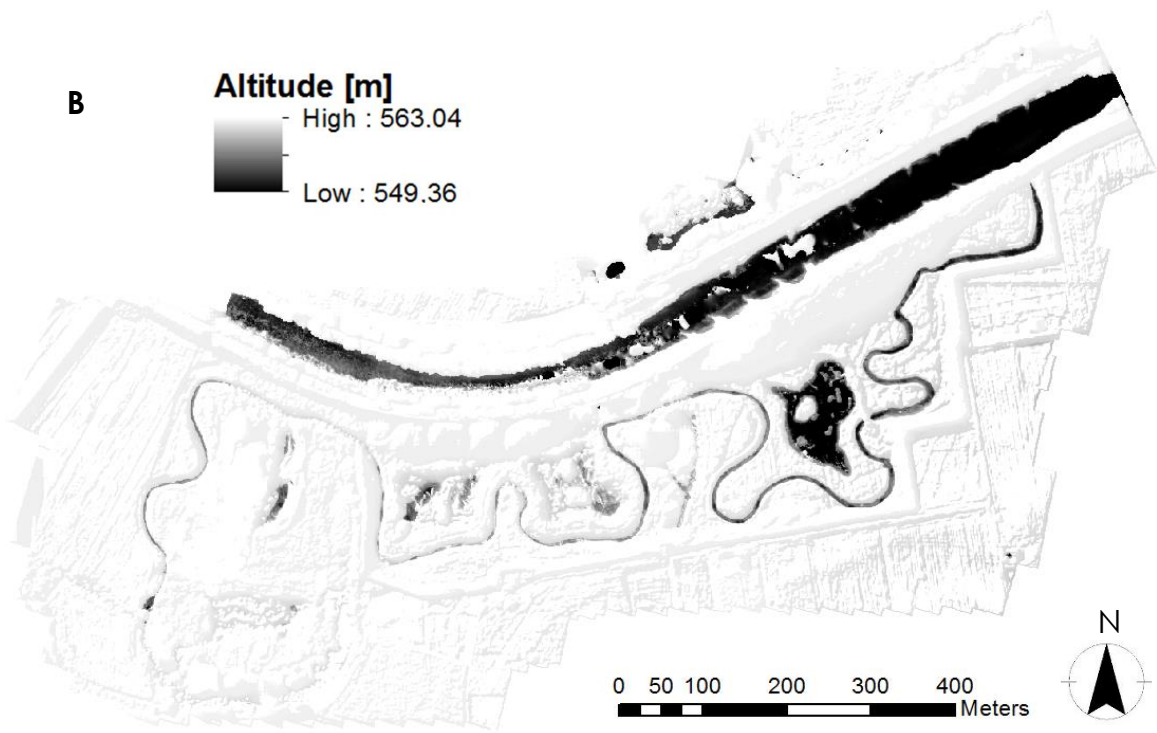


Figure 16: Elevation data A = DTM Gail, B = DSM Gail 2014, C = DSM Gail 2015

4.7. SUMMARY DATA USED

Table 9: Overview of all data sources used in the present project

Restoration performed				
	Start	End		
Drau	09/2006	08/2011		
Gail	01/2010	12/2014		
Satellite Imagery				
	Acquisition Date	Spectral Resolution	Spatial Resolution MS/PAN	Project site
QuickBird	09/09/2006	4 MS+1 PAN	2.00m/0.51m	Drau
GeoEye-1	08/26/2011	4 MS+1 PAN	2.43m/0.60m	Gail
WorldView-2	03/01/2013	8 MS+1 PAN	2.00m/0.50m	Both
RPAS Imagery				
	Acquisition Date	Spectral Resolution	Spatial Resolution	Project site
Sony Alpha 6000	12/30/2013	RGB	7 cm	Drau
Sony Alpha 6000	09/24/2014	RGB	5 cm	Gail
Sony Alpha 6000	06/29/2015	RGB	3 cm	Gail
Sony Alpha 6000	06/29/2015	NIR	3 cm	Gail
Aerial Imagery				
	Acquisition Date	Spectral Resolution	Spatial Resolution	Project site
Pre-restoration	07/17-19/2006	RGB	20 cm	Drau
Post-restoration	08/17-09/25/2013	RGB	20 cm	Drau
Pre-restoration	06/24-07/14/2010	RGB	20 cm	Gail
Post-restoration	08/16/2013	RGB	20 cm	Gail
Reference Data				
	Acquisition Date	Source	Project site	
Vegetation	2004	Field mapping, aerial image	Drau	
Vegetation	2011	Field mapping, aerial image	Drau	
Vegetation	2010	Field mapping, aerial image	Gail	
Vegetation	2014	Field mapping, aerial image	Gail	

Elevation Data

	Acquisition Date	Source	Spatial Resolution	Project site
DTM	2013	Airborne Laser Scanning	10 m	Both
DSM	09/24/2014	Photogrammetrically calculated using RPAS RGB	5 cm	Gail
DSM	06/29/2015	Photogrammetrically calculated using RPAS RGB	3 cm	Gail

5. METHODOLOGY

The following subchapters are intended to give an overview about the methodical approach followed to analyze the different data types of the project sites. Starting with the overall concept the explanations go into detail about each of the planned steps. Additionally methods to improve the classification result are discussed. The photogrammetrically-derived DSM is used in the classification process to test if the additional altitude information helps improving the classification result. Another approach to increase the accuracy of classification is to pan-sharpen the medium resolution multispectral satellite images based on their corresponding high resolution panchromatic images. Different algorithms for pan-sharpening as well as classification and change detection are applied to the data to find the best suitable for the present research problem.

5.1. CONCEPT

After acquiring the data in the project sites with the help of satellite and RPA systems, the first step of the image analysis is the data preprocessing. The preprocessing part includes the correction of geometric, radiometric and atmospheric deficiencies and the removal of data errors. The preprocessing process makes the images comparable and therefore needs to be finished before the classification and change detection analyses can start. When all data sets are preprocessed the next step is to classify all different images. For the classification three different classification algorithm are applied to test their suitability and find the most accurate one for gaining information related to the specific monitoring questions. In the change detection phase images with different time stamps are compared to analyze the spatio-temporal aspect of the project sites. At last after analyzing each and every data type an overall evaluation and accuracy assessment is performed to find out about the suitability of different data for environmental monitoring tasks. Therefore, the results of the analyses of different data types are compared based on accuracy and informational content. The whole image processing workflow is explained in detail in the following subchapters and visually summarized in Figure 17.

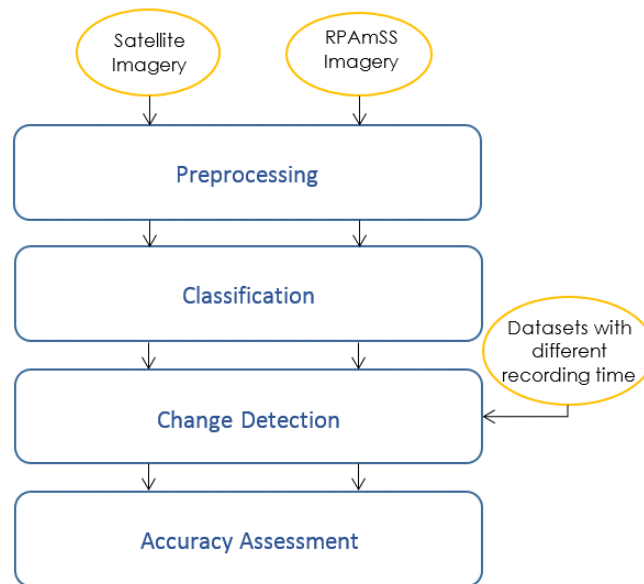


Figure 17: Overview about the image processing workflow

5.2. PREPROCESSING

According to the general explanations of chapter 2.2 data acquired with the help of remote sensing include diverse disturbances and blurs. Before starting with the analysis and evaluation of data these deficiencies need to be filtered out or compensated. In general it can be differentiated between geometric and radiometric correction.

Radiometric correction includes the compensation of errors caused by the recording sensor, the sun angle and topography of the study site and the atmosphere. To perform a complex atmospheric correction data of the atmospheric composition at the time of data acquisition is required. To compensate disturbances caused by the sensor its camera signal noise needs to be taken into consideration. Diffusely reflectance resulting in sun spots and shading can be corrected by estimating a shading curve and knowing the angle of solar radiation to identify shaded areas (Murai, 1993).

For the geometric correction the shape of the images is modified but the original color values stay unchanged. Geometric correction procedures are used to compensate distortion and geometric errors and to geo-reference the images for further use in a geographic information system. For referencing into a certain coordinate system usually ground control points (GCP) are used. GCPs are clearly discernible points of the distorted image whose positions are then either given in ground coordinates or measured from a map or geo-referenced image. Based on the identified GCPs the images are then

transformed using mathematical operations. The accuracy of the geo-referenced result mainly depends on the amount of selected GCPs, their distribution over the image area and the types of objects identified (Eltohamy & Hamza, 2009). The preprocessing steps for the satellite images are summarized in Figure 19.

To correct distortions and errors in the aerial images of the project sites different correction methods need to be applied for the various sensors. WorldView-2, GeoEye-1 and QuickBird-2 data is already geometrically and radiometrically corrected by DigitalGlobe before delivered to customers. The geometric correction has been done based on a coarse DEM with a resolution of 90m/pixel and resulted in a root mean square error (RMSE) of 2.3 m. Nevertheless, the satellite data do not match well the other data sets and therefore several preprocessing steps are performed for improvement.

Additionally, the images gained during RPAS missions need to pass different preprocessing steps to become comparable to the satellite data and among themselves. For spatial registration the RPAS data are geometrically corrected with the help of the software Agisoft PhotoScan on the basis of predefined GCPs with known coordinates. Through this step of geometric correction additionally the next step including image registration is fulfilled. With getting geo-referenced the diversified images recorded on the flight of the fixed-wing RPAS are matched together based on their location and then are mosaicked to an ortho-photo. A visual summary of the performed preprocessing tasks on the RPAS-derived data are shown in Figure 20.

Whenever the NIR camera in addition to the RGB camera acquires data, this has to be done in two different flights because of payload and space limitations of the system. Although both times the RPAS follows the same defined route and there usually only is a small time interval in between, small wind influences and change of conditions lead to significant differences in spatial locations of the images. These small offsets are hard to correct as they appear very locally in the mosaicked ortho-photo. Nevertheless, one NIR image is geo-referenced to detect the degree of improvement. The results are described in chapter 6.3.

5.3. VISUAL INTERPRETATION METHODS

Visual interpretation of high resolution aerial images can be a helpful addition to field mapping in diverse application areas. However, the usefulness of an interpretation result is mainly dependent on the problem to solve, the data material and the interpreter. To assess the visual interpretability of the very high resolution RPAS images, smaller subsets of the imagery are generated including trees of different species each and handed to experienced experts in the field of tree assessment, arboriculture and forestry. The experts excel in long-lasting experience in identifying trees and checking their traffic safety. Each expert works on a dissimilar subset area to test the identifiability of different tree species. The experts are asked to mark single tree locations and write down as much information as possible about each tree. All the experts know about the aerial image subset is acquisition date, scale and location. These information are provided to allow them using their experience in terms of vegetation cycles like flowering time, soil necessities and relative crown size. However, an interpretation key is by purpose not handed to the experts as aim is to examine the interpretability of the collected raw image without further time-consuming preparation.

The evaluation takes into account not only the accuracy of classification but also the level of detail achieved. While the lowest level of detail is defined as identifying single tree locations, a higher level is to differentiate between coniferous and deciduous trees. A pretty high level of detail is to be able distinguishing different species and finally the highest level is to differentiate between diverse varieties. The different levels of detail defined for visual image interpretation are shown in Figure 18.

The results are then digitized in ArcMap and compared to reference data collected in the field in July 2015. The reference data include the tree species in each subset area, the appropriate tree group and their locations in the field. The tree species have been identified by the author, who holds a B. Eng. In landscape architecture and is certified as tree inspector by the German FLL (Research Society for Landscape Development and Landscaping). The comparison is done concerning the distance between the point features of the reference and the expert data set to find out about the accuracy of single tree locations. All features without any distance between the data sets are counted and divided by the total number of features in the reference data set to get the percentage of correctly located trees. For the tree group the appropriate attributes are compared using an if-statement. All correctly identified tree

groups are counted and divided by the total number of trees in the subset area. The accuracy of identifying the species and variety are assessed in the same way.

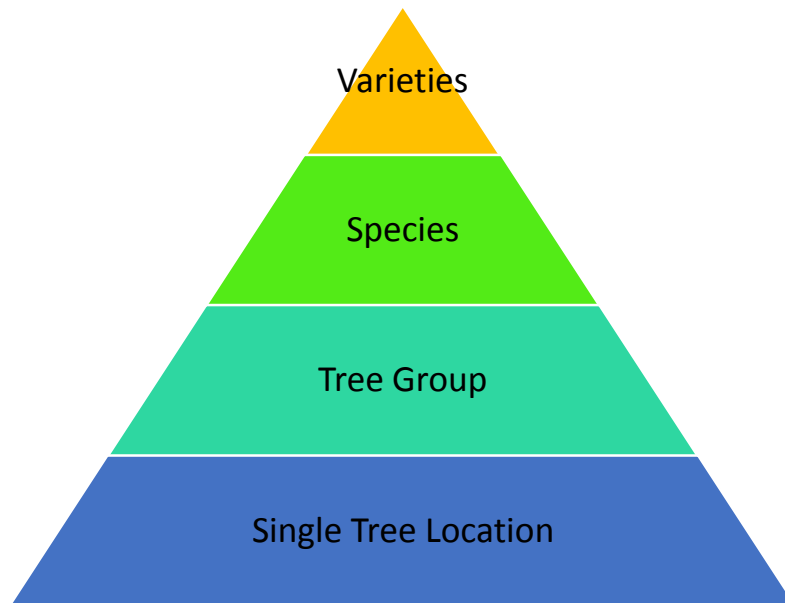


Figure 18: Levels of detail evaluated for visual image interpretation

5.4. CLASSIFICATION PROCEDURES

For the present project all different data types need to be analyzed to evaluate the applicability of the particular remote sensing technique in terms of riverine environmental monitoring. To compare the results, first of all a classification has to be performed on the different data sets. As mentioned in chapter 2.2.3 traditional statistical pattern recognition techniques primarily have been developed to evaluate spatial domain-based phenomena like land cover, while analyses of hyperspectral data have the goal to extract targets with particular spectral characteristics. However, in this project the pattern recognition techniques are applied to the multispectral satellite data and also to the RGB and NIR RPAS data because they contain a maximum number of four bands and therefore do not map very detailed spectral signatures. The concept of the classification procedure of the different data is shown in Figure 19 and Figure 20.

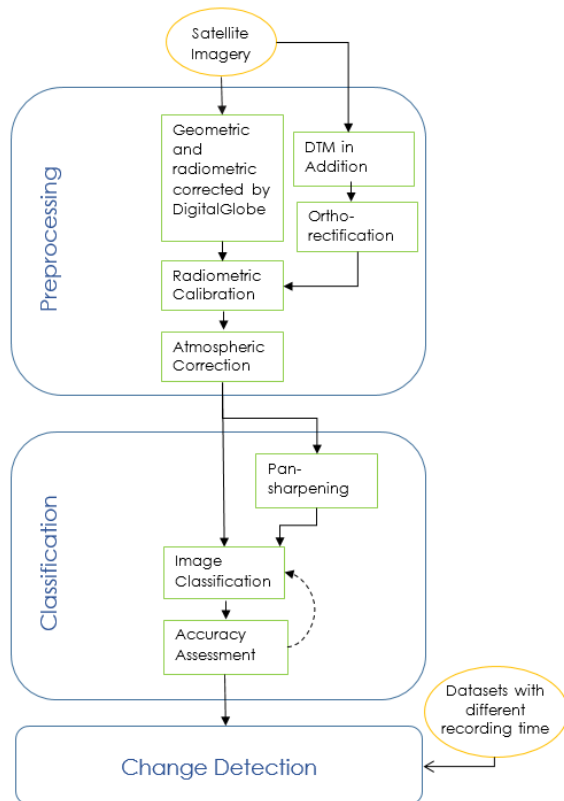


Figure 19: Image processing workflow VHR multispectral satellite data

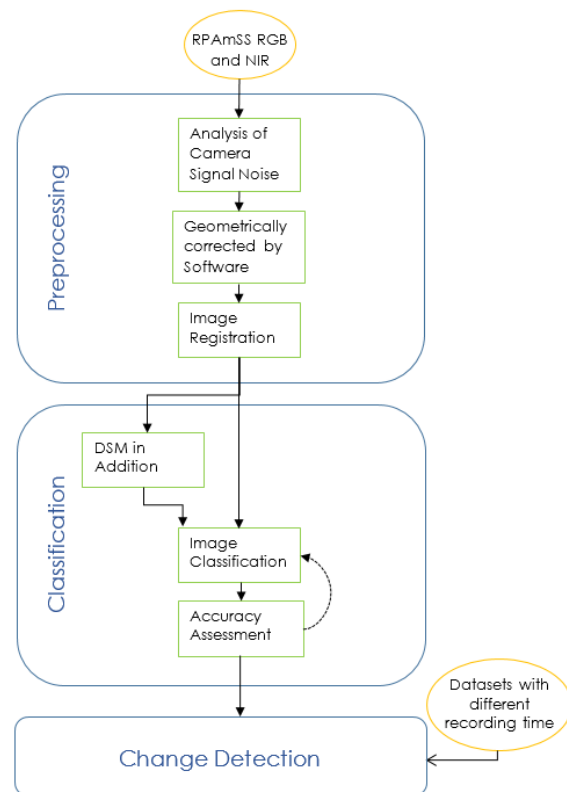


Figure 20: Image processing workflow RPAS-derived data

5.4.1. ISODATA ALGORITHM

Probably the most often used unsupervised classification algorithm, the Iterative Self-Organizing Data Analysis Technique (ISODATA) is a further development of k-means algorithm and uses statistical calculations to find spectrally similar, spatially close clusters. ISODATA starts with either arbitrary initial class centers or centers loaded from a signature set. Each cell is assigned to the classes with the minimum Euclidean distance and based on the class sizes a new center is calculated using the mean vector. But in difference to k-means, at the beginning of each iteration, large classes might be split based on different factors like the maximum standard deviation of the class, the average distance of class cells from the center and the total amount of class cells. A combination of classes takes place when the distances between their centers fall below a defined threshold. Iterations continue until there is no or only little change in the locations of class centers or the predefined maximum number of iterations is reached. To run this algorithm the analyst has to specify the parameters: minimum number of classes, maximum iterations, maximum standard deviation, minimum distance to combine, minimum cluster cells and

minimum distance for chaining (Jensen, 2005 and Leica, 2006). The main challenge in applying ISODATA algorithm is to find a significant number of clusters to be created. In merging and splitting the resulting clusters the analyst then is able to acquire the classes he is interested in. Post classification of this classifier is the allocation of clusters into their appropriate classes.

5.4.2. IMAGE SEGMENTATION

The German psychologist Kurt Koffka formulated the maxim “the whole is other than the sum of its parts” that is used by the Gestalt theory and describes the human ability of perceiving structures and ordering principles (Tuck, 2010). In machine learning the principles of Gestalt theory are implemented in algorithms that aim to find clusters in an image like e.g. ISODATA and Image Segmentation.

As another concept of unsupervised classification Full Lambda Schedule (FLS) based Image Segmentation segments an image into meaningful clusters. Image Segmentation is based on the idea of dividing an image into smaller sections of spatially close pixels with similar spectral characteristics instead of assigning each pixel to one class. First of all, edge detection is performed on the raster image to find boundaries between dissimilar pixel groups. These edges are then used to form the segments. After computing the mean spectral values for each adjacent segment of each band the Euclidean distance between the segments is computed. This is done using FLS algorithm (Intergraph, 2013b). Based on a combination of spatial and spectral information adjacent segments are merged to form categories. Merging occurs if the algorithm finds adjacent segments where the merging costs are lower than a defined threshold lambda value (Exelis Visual Information Solutions, 2015). The user directly controls the segment sizes in setting the minimum and maximum size constraint as well as the pixel to segment ratio that specifies an average number of pixels forming one segment. Furthermore, the merge cost function is executed based on user-defined weights for spectral, texture, size and shape components. The spectral component is measured as the mean of the digital number values of all pixels in the segment. Texture is measured as the standard deviation of all digital number values of the pixels in a segment. The size component is defined as the number of pixels being included in one segment and finally the shape component is a measurement of the shape complexity of the segment (Hexagon Geospatial, 2015a).

The challenge in using the Image Segmentation algorithm implemented in ERDAS Imagine is to find the best suitable scale to get segments that best approximate meaningful areas in the image. An example of Image Segmentation in different levels of detail is shown in Figure 21.

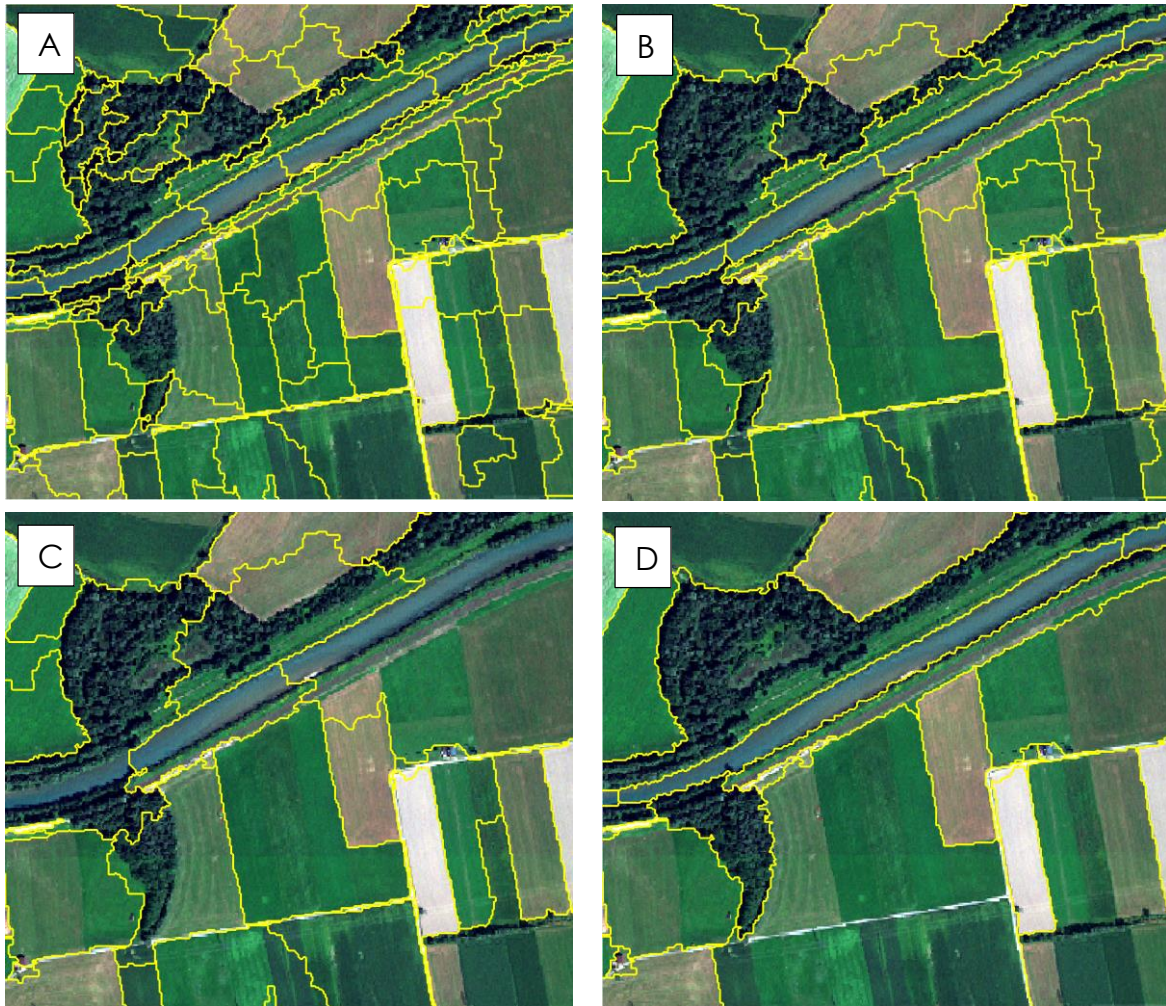


Figure 21: The Image Segmentation classification performed in different levels of detail, becoming coarser from A to D

5.4.3. MAXIMUM LIKELIHOOD CLASSIFICATION ALGORITHM

The second field of classification techniques is the field of supervised classification. Applying supervised classification requires some knowledge about the classes and their distribution in the study sites. Usually the data set to be classified is divided into training and test data. Thereby, care should be taken to select representative areas of the class. While training data is used to learn identifying similar pixels in the image, test data later is used for validation. Although most methods have been developed to analyze multispectral data,

they can also be applied to hyperspectral data if the number of features has been reduced to a similar level (Thenkabaill et al., 2012).

Maximum Likelihood Classification is the by far most commonly used supervised classification method if data are Gaussian distributed. Based on the Bayes classification rule the conditional probabilities of the test data are estimated and then used to develop the decision rule. To obtain reasonable accuracy a large amount of training samples is required (Thenkabaill et al., 2012). The basic equation assumes an equality of probabilities for all classes and a normal distribution of the input bands but can be adapted due to user's prior knowledge about the data.

To evaluate the separability of the trained classes their divergence is computed. Divergence is a measure to evaluate the suitability of the training pixels to represent the appropriate class. The basic problem of spectral pattern recognition is demonstrated in Figure 22 where just one band and two classes are visualized. The more bands are used the higher is the probability of using redundant information. The two major errors that result of the overlap of classes are on the one hand the error of commission that appears when a pixel is assigned to a class to which it does not belong. And on the other, the error of omission describes the case of a pixel not being assigned to its appropriate class. To decrease these errors and find training data with high separability the transformed divergence is computed using the mean and covariance matrices. Thereby, signature separability is a statistical measure between two signatures. Because separability can be calculated for every combination of bands that is used in the classification, unnecessary bands can be detected and eliminated based on the best average separability (Hexagon Geospatial, 2015b). The resulting transformed divergence values rank from 0 to 2000 for the different class combinations. While a value of 2000 expresses excellent class separability, >1900 means good separability and values <1700 indicate a poor separability between the classes (Jensen, 2005).

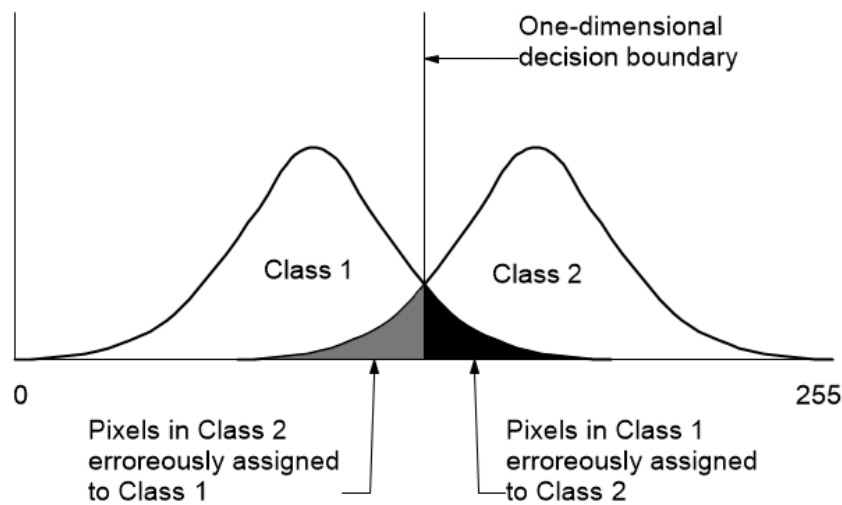


Figure 22: The problem of finding an n -dimensional decision boundary to separate major classes in a spectral distribution of data in n bands (here just 1 band) (Jensen, 2005)

5.4.4. VALIDATION

To detect which of the algorithms delivers the highest accuracy of classification results, each classification result needs to be evaluated and compared. Therefore, an accuracy assessment is performed for a pixel-by-pixel comparison. For this technique the classified image as well as the appropriate reference data reflecting the land cover is accurately compared to examine the correctness of classification. The result of the evaluation is displayed in form of a confusion matrix; overall accuracy and Kappa coefficient are calculated. The confusion matrix, sometimes also called error matrix, is a confrontation of actual against predicted classes to visualize true and false positive as well as true and false negative classified objects. The confusion matrix helps to better understand the classification errors that occur by analyzing the correlation between classes. Overall accuracy is achieved by dividing the total number of correctly classified pixels of one class by the total number of reference pixels of the same class. Thereby, it is differentiated between producer's and consumer's accuracy or error of omission and error of commission. While producer's accuracy represents how well reference pixels are classified the consumer's accuracy represents the probability that a pixel classified into a given class actually represents that class on the ground. The Kappa coefficient of the error matrix is an evaluation how well the data set was classified compared to a randomly generated data set. The Kappa coefficient ranks between -1 and 1 whereas 0 denotes a random accordance and means that

the classification result is equal to a randomly generated data set. Positive values point out the classification as being more precise than a random data set whereby 1 means perfect classification. And negative values identify the classification being worse than a randomly generated image (Congalton & Green, 2009).

5.5. IMPROVEMENT OF CLASSIFICATION

To improve the classification results different auxiliary information are added to the data sets and the new results are compared and evaluated. In a first attempt the NIR band of the RPAS NIR image is added to the RPAS RGB record to achieve an image comparable to the GeoEye-1 satellite image. Afterwards, the photogrammetrically-derived DSM is added to the multispectral RPAS data to simplify the separability of different objects based on their height. Furthermore the panchromatic band is used to improve the classification of the multispectral satellite images. Although the panchromatic band misses the color information, the spatial resolution usually is much higher than in the multispectral bands. The process of merging medium resolution multispectral with high resolution panchromatic images is called pan-sharpening.

The result of a pan-sharpening operation is a multispectral image with the same resolution and extent as the panchromatic image. While a huge amount of pan-sharpening algorithms has been published, only a few outstanding algorithms have been adapted by industry (Mishra and Zhang, 2013). In a first analyzing step different pan-sharpening techniques provided by ERDAS Imagine are tested with the GeoEye-1 satellite data to compare the results and find the best fitting method. After the best pan-sharpening technique for the satellite images is found a classification is conducted and compared to the classification results of the original data set.

Because there is no consensus on quantitative evaluation methods for pan-sharpening algorithms (Mishra and Zhang, 2013), Figure 23 shows the original data as well as four suitable pan-sharpening methods for visual comparison. While the multispectral image has a coarser resolution, the color information is missing in the panchromatic image. The pan-sharpening algorithm should combine both images in maintaining the color as well as the high resolution. Hyperspherical Color Space (HCS) Pan Sharpening was specifically designed having WorldView-2 in mind. The advantage of HCS pan-sharpening algorithm

is that it handles any number of input bands. Mathematically it uses the transformation from native into hyperspherical color space and back again (Padwick, 2010). The result shows clear colors and a significantly higher quality in terms of resolution.

The principal components resolution merge uses a principal components transformation of the low resolution image. The first principal component is assumed to contain the intensity variation in the image. The radiometric response of the high resolution image is adjusted so that the histogram shape is kept constant with the same numeric range of the low resolution intensity channel. The high resolution image is substituted for the first principle component, and the inverse principle component transform is applied to generate an enhanced image. The resulting imagery is visually sharper; however, there is some loss of spectral quality (Goforth, 1998).

Especially designed for the merge of QuickBird, Ikonos, and Formosat data the Subtractive Resolution Merge is from high interest for the present project as one satellite image from QuickBird is used. This method is limited to dual sensor platforms with specific band ratios between the high resolution panchromatic image and the lower resolution multispectral image (Ashraf et al., 2013). But although resolution information is well used in the result, color is almost completely lost.

A similar problem can be seen for the High Pass Filter (HPF) Resolution Merge. Thereby, a high pass convolution filter kernel is created and applied to filter the high resolution input data. The result is then weighted relative to the standard deviation of each multispectral band and added to each band (Gangkofner & Holcomb, 2008).

The pan-sharpening results of the before described algorithms for the GeoEye-1 satellite image can be found in Figure 23. To conclude, HCS resolution merge and resolution merge deliver the best pan-sharpening results in terms of resolution and color. While HCS resolution merge achieves bright contrasts, the colors in the resolution merge result seem pale. For that reason HCS resolution merge is chosen as pan-sharpening algorithm to find out if the classification of the pan-sharpened result ends up with higher accuracy or informational content.

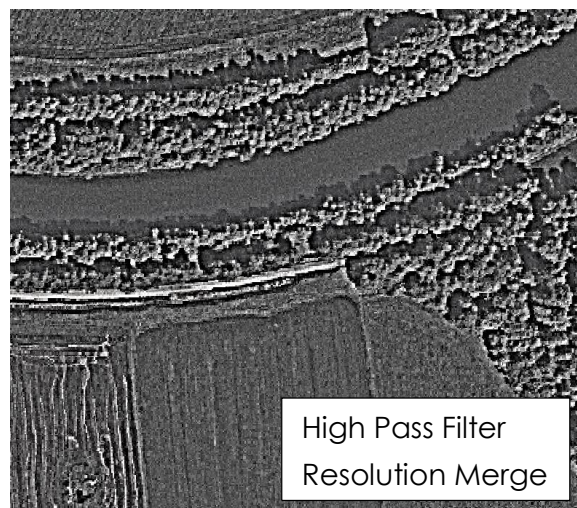
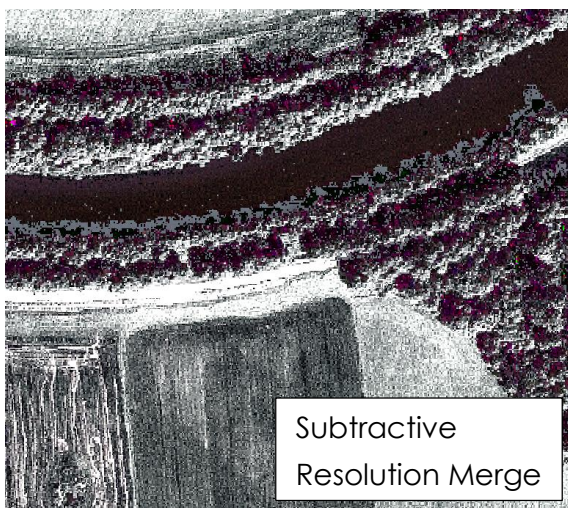
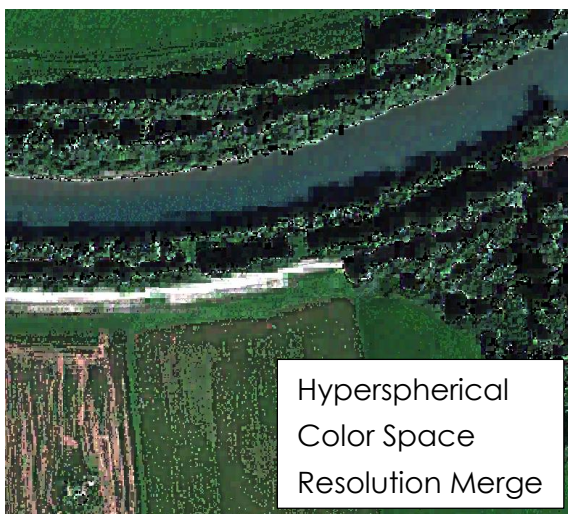
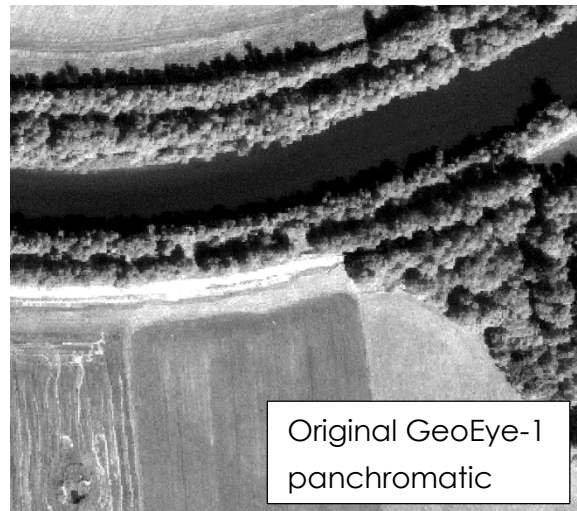


Figure 23: Comparison of pan-sharpening algorithms for a GeoEye-1 satellite image

5.6. CHANGE DETECTION TECHNIQUES

The multi-temporal analysis of the project sites is especially from interest to detect the way of natural adjustment after a river restoration has taken place. Through the change detection analysis the establishment of vegetation species as well as the geomorphological adoption of the river can be highlighted. The comparison of two data sets with different recording times highlights the spreading of neophytes and pioneer species on open spaces and visualizes changes in the course of the river.

Pixel-based change detection algorithms take the subtraction or ratio of two raster images with different recording times to detect whether a change has taken place or not. A threshold value is useful to counteract the impact of random factors. The main disadvantage of both methods is the loss of reflectance of changes between classified categories (Shaoqing & Lu, 2008). On the other hand post-classification change detection techniques involve the comparison between independently produced and classified data sets. In comparison to differencing and ratioing methods post-classification techniques depict a complete descriptive matrix containing changes between two time stamps. Caused by the independently produced classification of each data set the different atmospheric conditions at recording time as well as geometric inaccuracies are compensated much better (Sohl, 1999).

With their research on the effects of image misregistration on the accuracy of remotely sensed change detection Dai and Khorram (1998) have proven that a registration accuracy of less than one-fifth of a pixel is required to achieve a change detection error of less than 10%. Because of the high geometric inaccuracies between the satellite data and the data acquired with the RPAS change detection cannot be used for comparison between these images. For that reason regarding change detection the focus is put on RPAS-derived images from 2014 and 2015 and airplane-derived ortho-photos of the Carinthian government of 2010 and 2013.

5.7. COMPARISON STRATEGY

The final methodical step in the data analysis is the comparison between the classification results of the different data types to find out about their suitability for various environmental monitoring tasks. For the comparison different categories are created according to the research questions formulated in chapter 1.3. To represent the accuracy of each data type the results of the data validation, explained in chapter 5.4.4, are used. The percentage of overall classification accuracy derived from the Accuracy Totals is calculated for the classified data set that was acquired temporarily closest to the data of the reference data collection for the multispectral, RGB and NIR data each. If two data sets of one type with the same distance of time exist, the mean accuracy value and standard deviation are calculated. To make statements about the quantity of classification and evaluate the informational content the classification accuracy values are finally compared for each of the defined categories, which are:

1. Accuracy of classification after the Habitats Directive
2. Accuracy of classification in accordance to the more detailed internal habitat type classification
3. Accuracy of classification of single vegetation species
4. Accuracy of classification of single vegetation varieties
5. Accuracy of classification of soil types

The Habitats Directive defines natural habitat types of community interest which are described in ANNEX A. Based on the accuracy of detecting these habitats compared to the reference data set the accuracy values of the different data types are compared in this category. The next category presents the accuracy of classifying the internal habitat types which are provided in the reference data and offer more detail about present vegetation. To validate the accuracy of classifying single vegetation species and varieties reference data will be collected for a representative part of the complete project sites. For the geomorphologic aspect in this project the accuracy of classifying different soil types for the different data types will be compared.

6. APPLICATION

This chapter summarizes the application following the methodology as described in chapter 5. Besides evaluating the results of visual image interpretation, the preprocessing processes for satellite and RPAS data are described in detail. Furthermore, the classification results are stated and compared and finally the results of the change detection analysis can be found at the end of this chapter.

6.1. VISUAL INTERPRETATION RESULTS

After the experts finished working on the tree identification of their aerial subset, their work has been digitized to automatically compare the trees and their locations with the reference data collected in the field. Figure 24 shows exemplary the interpretation results of expert 2 in comparison of the appropriate reference data. All the other results can be found in detail in ANNEX B.

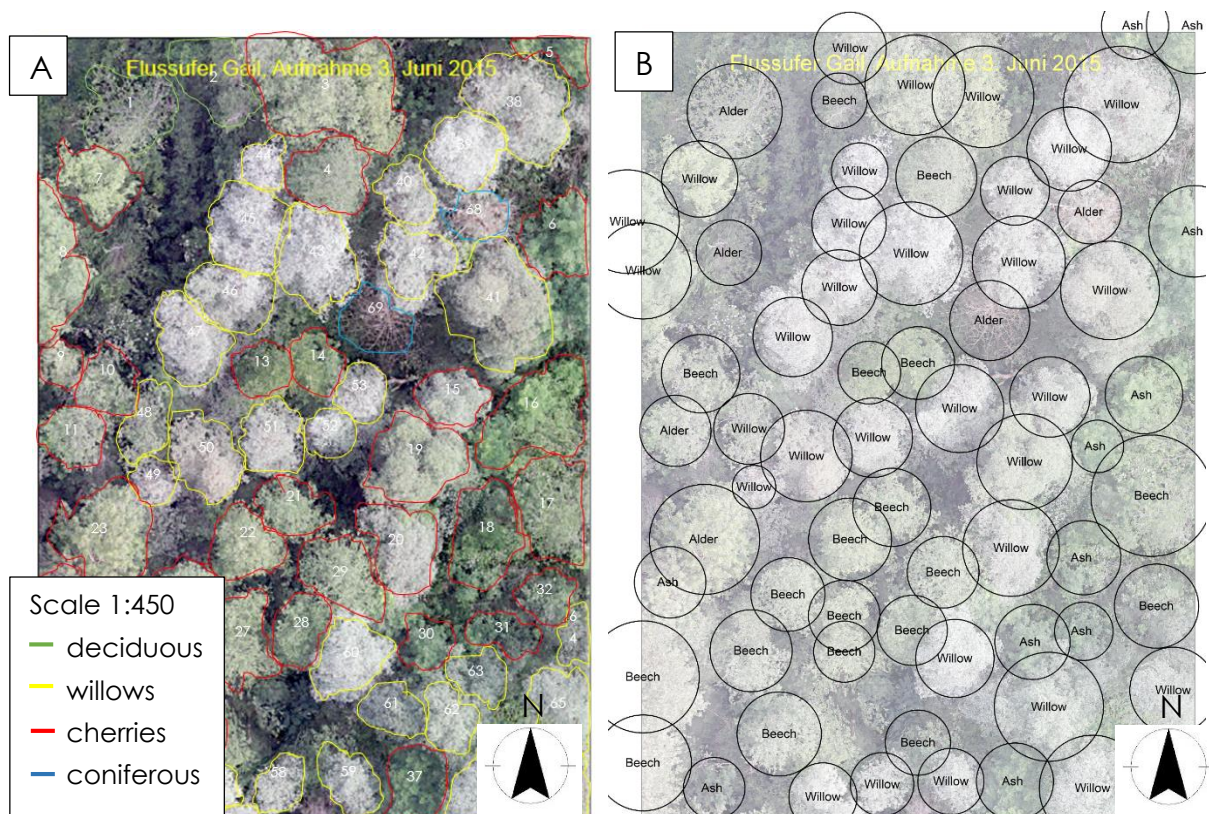


Figure 24: Visual image interpretation result and reference data, A = interpretation results expert 2, B = reference data subset 2

The results of the visual image interpretation by experts of forestry and arboriculture show different percentages of correctly classified tree species, tree groups and tree locations that can be seen in Table 10. As can be seen

the highest level of tree varieties was not reached by any of the experts. However, the second level, tree species, could be differentiated by most experts. While expert 2 only found the correct species of 7 of 68 trees and therewith identified species with 10.29 %, expert 3 only differentiated between willows and general tree groups. With 44 correctly classified willows out of 166 trees, he reached an accuracy of 26.51 % regarding tree species. Although all trees he marked as willows are correctly classified, he still missed some other willows in the sample area and did not identify all the other species. Level three, the tree group, meaning the difference between coniferous and deciduous trees, could be distinguished fairly well from all three experts. Expert 3 had some problems and confused many ashes with coniferous trees. Expert 1 correctly identified 12 out of 52 trees regarding their group and therewith achieved an accuracy of 23.08 %. His problem was that he missed a lot of trees in the area. With a percentage of 85.29 % expert 2 correctly classified 58 out of 68 tree groups. And finally expert 3 correctly identified 58 from 166 trees regarding their group and therewith achieved an accuracy of 34.94 %. Finally, the location of single trees has been identified with the highest accuracy of all experts. While expert 1 identified 21 of 52 trees with their correct location and resulted in an accuracy value of 40.38 %, experts 2 correctly located 60 out of 68 and therewith 88.24 % trees in the area. Finally, expert 3 correctly located 96 from 166 trees and therewith achieved an accuracy of 57.83 %. Additionally, the processing time for the RPAS images was at most half the time needed for collecting the reference data. In terms of time visual image interpretation is much faster than acquiring data in the field.

Table 10: Correctly classified results of visual image interpretation

	Expert 1	Expert 2	Expert 3
Tree variety	-	-	-
Tree species	-	10.29 %	26.51 %
Tree group	23.08 %	85.29 %	34.94 %
Single tree location	40.38 %	88.24 %	57.83 %

To conclude, the experts had some issues in visually interpreting the RPAS-derived RGB images. As they usually have a laterally view on the trees they inspect, more experience and training with aerial images could probably improve the results. While statements about the varieties could not be made at all, the species have only been identified with poor accuracy. With decreasing categorical detail, the accuracy of identification increased. Thus, the single

tree location could be identified with the highest accuracy from all experts. Besides the processing time for the RPAS images was always shorter than the time needed to collect the appropriate reference data in the field.

6.2. PREPROCESSING SATELLITE IMAGERY

For the radiometric correction the pixel values are calculated as a function of the spectral radiance entering the sensor's aperture and the instrument's conversion of radiance into a digital signal. To normalize the pixel values a radiometric calibration is performed using ENVI 5.1 software. The therewith achieved top-of-atmosphere spectral radiance depends on the earth-sun distance, the solar zenith angle, the topography of the project site and atmospheric effects (Elsharkawy et al., 2012). Furthermore, an atmospheric correction is performed using FLAASH tool of ENVI 4.8. As atmospheric model Mid-Latitude Winter is chosen for the WorldView-2 images and Mid-Latitude summer for the other satellite data. The aerosol model is specified as Rural. Atmospheric correction normalizes the reflectance of objects by removing distortions caused by the atmospheric composition.

The satellite imagery comes already preprocessed by DigitalGlobe. For the geometric correction the images have been orthorectified using a DEM with 90 m resolution. But even with geo-referencing based on GCPs it is not possible to get a location accuracy of pixel resolution or less. Therefore, the not preprocessed raw data are taken and orthorectified using the 10 m DEM of Carinthia. Comparing this result to the images being orthorectified with the coarser DEM, the location accuracy is higher, but still not high enough to work with per pixel comparison techniques between the satellite and even higher resolution RPAS images. The required accuracy of more than one-fifth pixel (Dai and Khorram, 1998) could not be achieved in the available satellite data.

After Hoja et al. 2008 there is no significant difference concerning accuracy of the orthorectification results between software like ERDAS Imagine and ENVI. Therefore, to simplify matters, the satellite images are orthorectified using ERDAS Imagine. Orthorectification is the process of removing spatial distortions caused by terrain relief and off-nadir image acquisition and locating the features to their positions in a planimetric map. For that purpose a DEM needs to be added containing altitude information. ERDAS Imagine provides a rational polynomial coefficient model for each of the satellite sensors used in

this research project. As elevation source the Austrian national DEM with a 10 m spatial resolution is used.

To finalize the geometric correction all satellite images are geo-referenced with a second order polynomial transformation using clearly discernible and well distributed GCPs. The geo-referencing procedure is performed based on the Austrian national ortho-photo with a pixel resolution of 29 cm and a position accuracy of 20 cm RMSE. The final results of the preprocessing process have a geometric accuracy that is shown in Table 11. Bovolo et al. (2009) explain the high residual registration noise of the VHR satellite images with the ability of the satellite systems to acquire images in different view angles resulting in different geometrical distortions. These distortions even stay after proper registration and strongly affect the geometric precision.

Table 11: Final RMSEs of the satellite images after geometric correction

	Drau		Gail	
	Number of GCPs	RMSE [m]	Number of GCPs	RMSE [m]
GeoEye-1	-	-	75	3.59
QuickBird	59	2.88	-	-
WorldView-2	51	3.07	50	4.05

6.3. PREPROCESSING RPAS IMAGERY

To improve geometric accuracy between RGB and NIR data, the NIR image is geo-referenced using 100 GCPs. Before geo-referencing offsets of 1.80 m between the two data sets are found. After geo-referencing the NIR image the highest offset found is 0.15 m which is still three times the pixel resolution. The RMSE is 1.34×10^{-6} m with a 2nd order polynomial transformation. Although geo-referencing lead to a significant improvement concerning location accuracy, there is still a shift of up to three pixels between RGB and NIR images. The combination of RGB and NIR data therewith often leads to a wrong spectral signature of small materials and materials in border areas of different classes. Despite this serious error, RGB and NIR bands are merged into a multispectral image to test if there is an improvement in the classification.

6.4. CLASSIFICATION RESULTS

Due to the nature of the different classification computations, the algorithms used result in different numbers of classes. To result in similar classes, a hierarchical structure is defined. Broader classes are reached in merging some or all underlying classes. To clarify what lies behind the class names, a brief description of the classes can be found in Table 12. The numeric code of the column "Hierarchy" is further used to state which classes are merged to get these broader classes.

Table 12: Available classes in the project site Gail

Hierarchy	Class Name	Description
1	Natural eutrophic lakes with Magnopotamion or Hydrocharition-type vegetation	Habitats Directive Habitat Type 3150
1.1	Oxbow	Part without connection to main branch
1.2	Reed bed	Habitat type, consisting of tall, reed-like plants
1.3	Pond/standing water	Artificial or natural standing water
1.4	Water lily	Standing water covered with water lily
2	Alpine rivers and the herbaceous vegetation along their banks	Habitats Directive Habitat Type 3220
2.1	Gravel/sand bank	River banks of gravel and/or sand
2.2	River	Flowing water
3	Water courses of plain to montane levels with the <i>Ranunculion fluitantis</i> and <i>Callitriche-Batrachion</i> vegetation	Habitats Directive Habitat Type 3260
3.1	Creek	Creek created to develop a side arm
4	Semi-natural dry grasslands and scrubland facies on calcareous substrates (<i>Festuco Brometalia</i>)	Habitats Directive Habitat Type 6210
4.1	Tor grass/red fescue semi-dry grassland	Grassland, mainly consisting of tor grass and red fescue
5	Lowland hay meadows (<i>Alopecurus pratensis</i> , <i>Sanguisorba officinalis</i>)	Habitats Directive Habitat Type 6210
5.1	Purple moor/tall oat grass	Grassland mainly consisting of purple moor and tall oat grass

5.2	Tall oat grass	Grassland, mainly consisting of tall oat grass
5.3	Sedges/hassock	Grassland, mainly consisting of sedges and hassock
6	Alluvial forests with <i>Alnus glutinosa</i> and <i>Fraxinus excelsior</i> (<i>Alno-Padion</i> , <i>Alnion incanae</i> , <i>Salicion albae</i>)	Habitats Directive Habitat Type 91E0
6.1	Gray alder alluvial forest	Alluvial forest mainly consisting of gray alder
6.2	White willow alluvial forest	Alluvial forest mainly consisting of white willow
6.3	Gray alder/ash alluvial forest	Alluvial forest mainly consisting of gray alder and ash
6.4	Alder/willow shrub	Shrub mainly consisting of alder and willow
6.5	Reed/willow bush	Bush mainly consisting of reed and willow
7	other classes	Present classes of the study sites that are not mentioned in EU directive
7.1	Agricultural field/bare soil	Agricultural field without growing plants
7.2	Sowing meadow	Grassland, composition of grass species not known in detail
7.3	Single tree	Deciduous individual tree
7.4	Path	Footpaths, streets, bridges
7.5	Spruce forest	Coniferous forest, mainly spruce
7.6	Building	Building
7.7	Infrastructure	Power pole, power line
7.8	Cabbage thistle meadow	Meadow, mainly consisting of cabbage thistle
7.9	White clover/ryegrass meadow	Meadow, mainly consisting of white clover and ryegrass
7.10	Agriculture 1	Agricultural field, crop not known in detail
7.11	Agriculture 2	Agricultural field, crop not known in detail
7.12	Agriculture 3	Agricultural field, crop not known in detail

To get the high accuracy value in the Maximum Likelihood classification, the original classes are merged in the following way to 15 classes (Table 13):

Table 13: Combination of classes to reach 15 classes for Maximum Likelihood classification

Class	Combination of original classes
Standing water and water plants	1.1, 1.3, 1.4
Alluvial forest	1.2, 6.1, 6.2, 6.3, 6.4, 6.5, 7.3
Gravel/sand bank	2.1
River	2.2
Tor grass/red fescue	4.1
Purple moor/tall oat grass	5.1, 5.2
Agricultural field/bare soil	7.1
Sowing meadow	7.2
Path	7.4
Spruce forest	7.5
Building/infrastructure	7.6, 7.7
White clover	7.9
Agriculture 1	7.10
Agriculture 2	7.11
Agriculture 3	7.12

To become comparable to the ISODATA result, the 15 Maximum Likelihood are merged to 11 classes in the following way (Table 14):

Table 14: Combination of classes to reach 11 classes for Maximum Likelihood classification

Class	Combination of original classes
Standing water and water plants	1.1, 1.3, 1.4
Alluvial forest	1.2, 6.1, 6.2, 6.3, 6.4, 6.5, 7.3
Gravel/sand bank	2.1
River	2.2
Grassland	4.1, 5.1, 5.2, 5.3, 7.2, 7.8
Agricultural field/bare soil	7.1
Manmade structure	7.4, 7.6, 7.7
Spruce forest	7.5
White clover	7.9
Agriculture 1	7.10
Agriculture 2	7.11, 7.12

The following classes are merged to get 11 ISODATA classes (Table 15):

Table 15: Combination of classes to get 11 ISODATA classes

Class	Combination of original classes
Standing water and water plants	1.1, 1.2, 1.4, 6.5
Alluvial forest	1.3, 6.1, 6.2, 6.3, 6.4, 7.3
Gravel/sand bank	2.1
River	2.2
Grassland	4.1, 5.1, 5.2, 5.3, 7.2, 7.8
Agricultural field/bare soil	7.1
Manmade structure	7.4, 7.6, 7.7
Spruce forest	7.5
White clover	7.9
Agriculture 1	7.10
Agriculture 2	7.11, 7.12

6.4.1. SATELLITE DATA

After applying all preprocessing steps that are described in chapter 5.2 the satellite images are classified based on the classification algorithms described in chapter 5.4. in detail. As the best result concerning both, classification accuracy and informational content, Figure 25 A shows the result of the FLS-based Image Segmentation algorithm including 23 classes with an overall accuracy of 77.18 % at the study site Gail. The final parameters for the Image Segmentation algorithm are the following: Pixel:Segment Ratio: 700 (boundaries: 10-1,400), Relative Weights: spectral: 1, texture: 0, size: 0, shape: 0, Size Limit: Minimum: 100, Maximum 100,000. The result of the Maximum Likelihood classification with 15 classes and an overall accuracy of 76.73 % can be seen in Figure 25 B. And Figure 25 C shows the result of the classification based on ISODATA resulting in 11 classes and an overall accuracy of 39.64 % both at the river Gail as well. The method of calculating overall accuracy is explained in chapter 7.1.



A



B



C

- | | |
|--------------------------------|------------------------|
| ■ agricultural field/bare soil | ■ pond/standing water |
| ■ agriculture 1 | ■ reed bed |
| ■ agriculture 2 | ■ reed/willow bush |
| ■ agriculture 3 | ■ river |
| ■ alder/willow shrub | ■ single tree |
| ■ building | ■ sowing meadow |
| ■ gravel/sand bank | ■ spruce forest |
| ■ gray alder | ■ tall oat/moor grass |
| ■ gray alder/ash | ■ tor grass/red fescue |
| □ infrastructure | ■ water lily |
| ■ oxbow | ■ white clover |
| ■ path | ■ white willow |

0 250 500 1,000 1,500 2,000 Meters



Figure 25: GeoEye-1 classification results, A = FLS-based Image Segmentation, B = Maximum Likelihood classification, C = ISODATA

A summary of the classification accuracies of the GeoEye-1 satellite image for different amounts of classes is given in Table 16 and Table 17. The different numbers of classes are achieved by nature of the diverse algorithms and merged to result in meaningful classes. The five Habitats classes are derived by merging all subclasses as described in Table 12 to their appropriate higher hierarchical class. For ISODATA classification it was not possible to reach all five habitats classes. Evaluating these five habitat classes gives information about how accurate the habitats, defined according to the Habitats Directive, can be classified with the different algorithms. While 11 is the highest number of classes being reached with ISODATA, Maximum Likelihood results in 15 classes showing high classification accuracy and with the segmentation algorithm it is even possible to differentiate between 23 classes. To be able to better compare the different accuracy values, the Image Segmentation and Maximum Likelihood classes are merged to the 11 ISODATA classes. Surprisingly, accuracy decreases for these algorithms, especially for Maximum Likelihood. This is caused by the fact that classes with low classification accuracy that are not merged with other classes become more meaningful relative to classes with high accuracy that are merged together. Table 17 shows the classification results without including the agricultural classes as they are not mentioned in the reference data.

Table 16: Classification results of the GeoEye-1 satellite image at the river Gail (number of classes achieved)

	ISODATA	Maximum Likelihood	Segmentation
Overall accuracy	51.22 % (4)	35.60 % (5)	81.60 % (5)
Kappa	0.2894 (4)	0.3027 (5)	0.7700 (5)
Overall accuracy	39.64 % (11)	43.27 % (11)	74.55 % (11)
Kappa	0.3360 (11)	0.3643 (11)	0.7200 (11)
Overall accuracy	-	76.73 % (15)	-
Kappa	-	0.7507 (15)	-
Overall accuracy	-	33.30 % (23)	77.18 % (23)
Kappa	-	0.2951 (23)	0.7614 (23)

Table 17: Classification results of the GeoEye-1 satellite image at the river Gail without agricultural classes

	ISODATA	Maximum Likelihood	Segmentation
Overall accuracy	34.07 % (9)	41.08 % (12)	84.00 % (20)
Kappa	0.2583 (9)	0.3613 (12)	0.8316 (20)

Finally the pan-sharpened GeoEye-1 image is classified using the segmentation algorithm, as it delivers the best results in terms of accuracy and informational content. After the segments are merged, 22 classes are found. The overall accuracy is 70.73% with a corresponding Kappa coefficient of 0.6941 and therewith slightly lower than the accuracy of the original image. Although there are several parameters that affect the function of the algorithm and could partly explain this behavior, there is no trend of improvement visible. To conclude the process of pan-sharpen VHR multispectral satellite images does not improve the classification result significantly.

Because of the snow coverage in the WorldView-2 satellite images, their use for habitat classification is limited. But the leaf-off situation not only has disadvantages. No leaves hide the riverbank in winter and therefore the shape of the river is much better visible. Using this fact, a classification of the WorldView-2 images is performed aiming to achieve an accurate shape of the river course. Problematic is in this case the validation. The change of water level has a significant influence on the river's shape and unfortunately there is no ground truth data about the river available at recording time. For these reasons the river classification results are only visually evaluated based on the winter scenes. In a further step the hydraulic model of the river could be used for validation.

Figure 26 shows two parts of the river with the superimposed shapes of riverbank classification. In image A all three algorithms agree all in all on the line of riverbank. Only ISODATA classifies a part of the surrounding alluvial forest as river while Maximum Likelihood leads to a slightly smaller river bed in not classifying the shallower bank regions as river. Finally, impression B shows a part with a sand bank in the river. As can be seen Maximum Likelihood classifier again considers the shallower parts as not belonging to the water body while the other algorithms more or less agree on the shape of the larger sand bank. However, the smaller sand bank is not recognized at all by Image Segmentation classifier. This is caused by the user defined pixel to segment ratio and the boundary of a minimum number of pixels per segment.

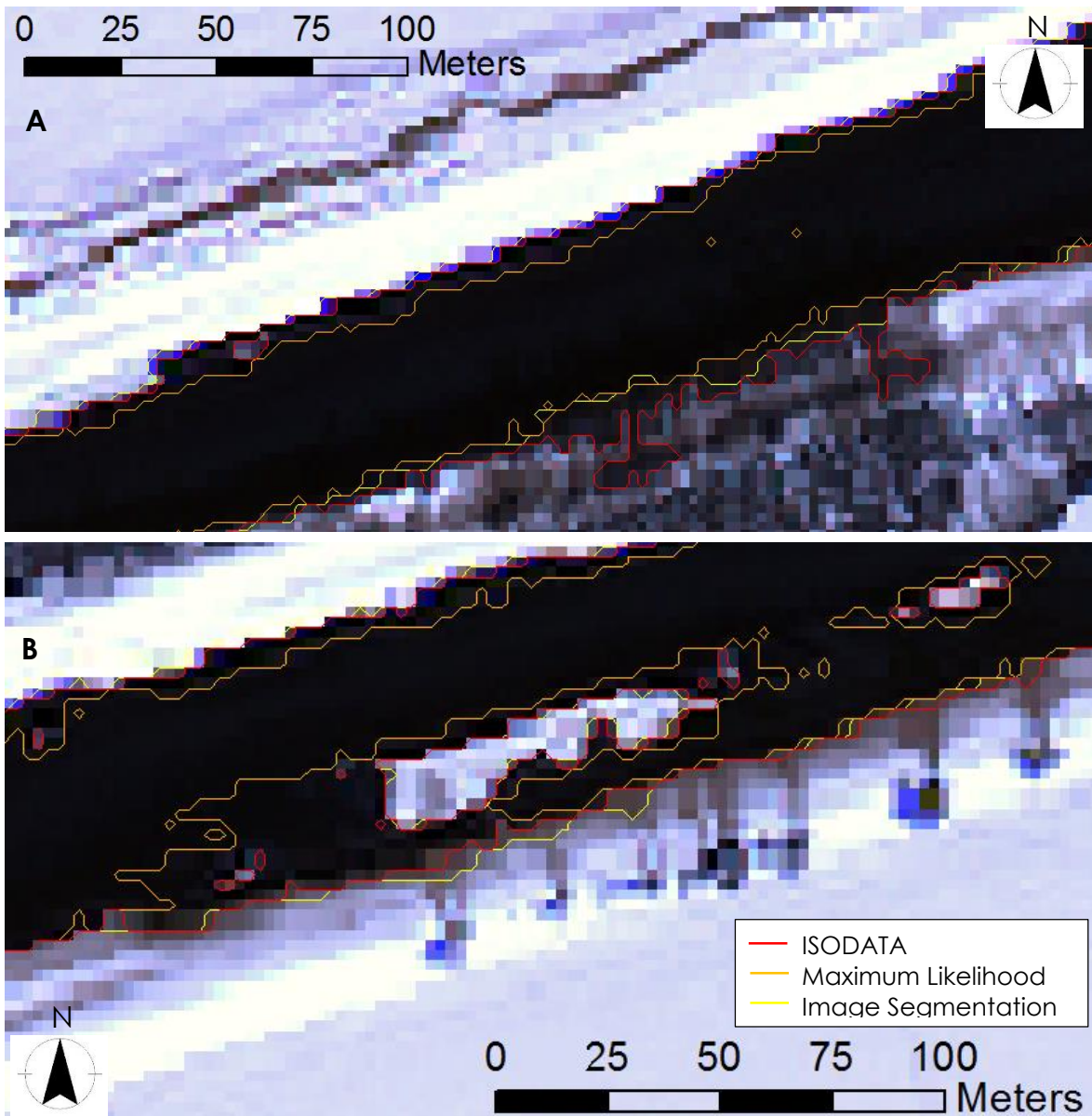


Figure 26: Result of the river classification in the WorView-2 winter scene at river Gail

For comparison purposes the same is done in the test site at the river Drau. Again, the winter scene of WorldView-2 is used for visual evaluation. Figure 27 visualizes two impressions of the result. While ISODATA in both images includes other land cover types, Image Segmentation algorithm adds alluvial forest to the river class in image B as well. Overall, the Maximum Likelihood algorithm again proves to be the most accurate one in detecting river shapes in winter situations but has some issues in not classifying shallower banks as river. Especially in image B Image Segmentation algorithm works inaccurately by including alluvial forest to the river shape.

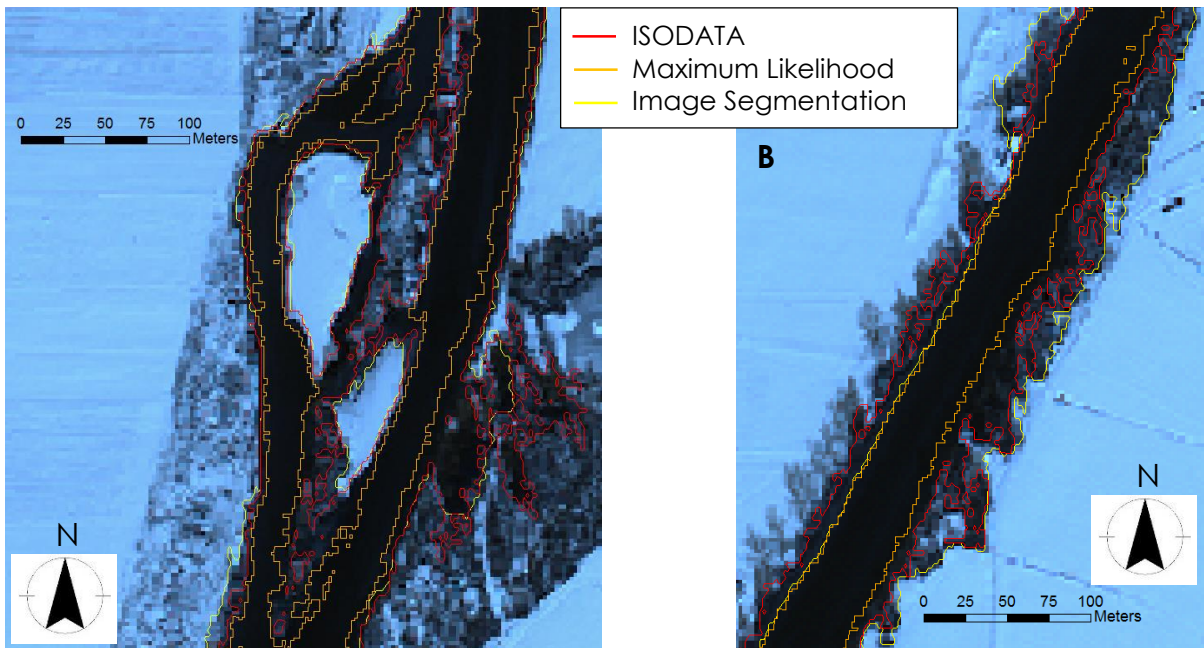


Figure 27: Result of the river classification in the WorlView-2 winter scene at river Drau

To conclude, the shape of the river can be extracted well in winter because the riverbanks are not hidden by overlapping tree crowns. The Maximum Likelihood algorithm delivers the overall best result, but often does not include shallower areas to the river class and instead concentrates more on the deeper water body. ISODATA and Image Segmentation classifier sometimes add objects of other classes to the river class because of their spectral and spatial similarity and therewith become inaccurate.

6.4.2. RPAS DATA

Caused by the missing certification of the RPAS in the project site at the river Drau, only recordings of the Gail are available and processed during this master's project. The RPAS-derived data caused a lot of problems during processing because of the very high resolution and thus high data size. As a consequence the classification techniques that require intensive post processing could not be applied. This means the unsupervised classification techniques fail for the RPAS-derived data as they result in clusters and require conversion from raster to vector to be assigned to target classes. For these reasons only the supervised Maximum Likelihood algorithm is applied to the RPAS-derived RGB, NIR and DSM data in different combinations as described in chapter 5.5. Figure 28 shows the result of the Maximum Likelihood classification for the RPAS-derived images in different combinations. The appropriate accuracy values can be found in Table 18.

Table 18: Classification accuracy of the RPAS-derived images at the river Gail (number of classes)

	Overall Accuracy	Kappa Coefficient
RGB	41.18 % (23)	0.3978 (23)
RGB + NIR	43.77 % (23)	0.4122 (23)
RGB + DSM	42.81 % (23)	0.4063 (23)
RGB + NIR + DSM	43.62 % (23)	0.4107 (23)

Image band combinations:

A: RGB

B: RGB + NIR

C: RGB + DSM

D: RGB + NIR + DSM



	Unclassified		bare soil
	reed bed		sowed meadow
	building		grain
	river		corn
	gravel/sand bank		gray alder
	oxbow		purple moor/tall oat grass
	path		tor grass/red fescue
	creek		white willow
	water lily		gray alder/ash
	pond		hay
	reed/willow bush		agriculture
	tall oat grass		street

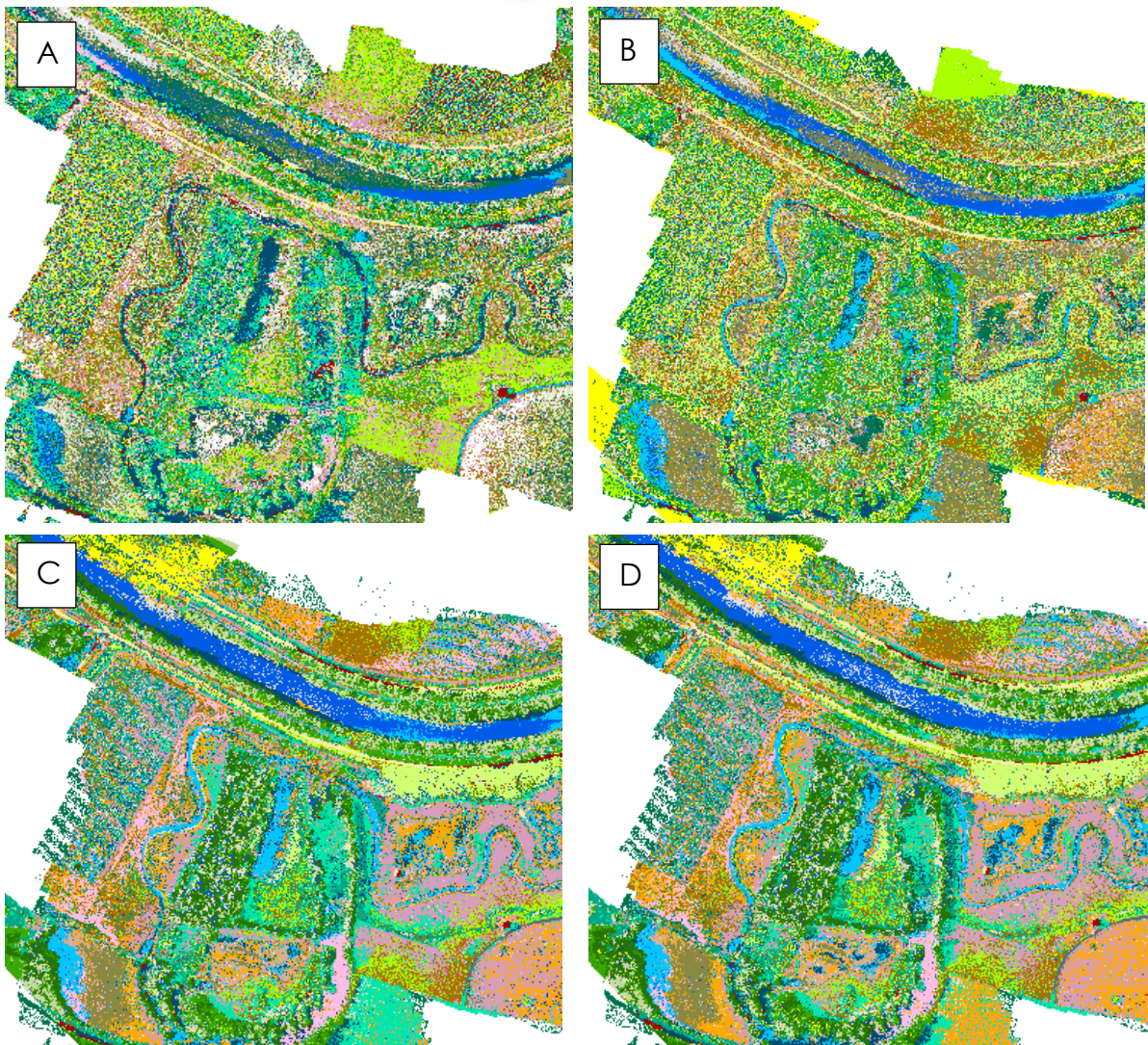


Figure 28: Maximum Likelihood classification results RPAS-derived data

6.4.3. COMPARISON

As can be seen in Table 18, classification accuracy for the RPAS-derived imagery is much lower than the accuracy of the multispectral satellite data. Although it could be argued that the RGB data include less bands than the multispectral satellite images, RGB + NIR contain the same number of bands and the combination with DSM even more. At first glance the classification results of the satellite images look much more accurate than the results of the RPAS-derived data. But in this case the values for overall accuracy and Kappa coefficient mislead. The reason for the lower values lies in the evaluation method as described in chapter 7.1. The punctual accuracy assessment method requires reference data in at least the same spatial resolution as the data to be assessed. In the present project the resolution of the reference data is lower than the original RPAS-derived imagery and therefore, the usually applied assessment method is not applicable. For the evaluation of the RPAS-derived images novel object-based accuracy assessment methods need to be developed to get meaningful accuracy values.

Table 19 displays another way of accuracy evaluation. Transformed divergence as described in chapter 5.4.3 is normally used to test separability of signatures for supervised classification. In computing statistical distance between the signatures its equations are very similar to Maximum Likelihood classification and therefore are best suited to predict Maximum Likelihood classification results (Sahu, 2008). As can be seen for the RPAS classifications the values increase continuously from poor separability for RGB imagery over good separability for combined RGB and NIR bands culminating in perfect separability in adding the DSM to RGB or combined RGB and NIR data. In comparison the multispectral satellite data show a good separability while the pan-sharpened images even result in excellent separability as well.

Table 19: Transformed Divergence separability values for Maximum Likelihood signatures

		Best average	Best minimum
RPAS	RGB	1566.50	58.224
	RGB + NIR	1735.20	145.300
	RGB + DSM	1941.58	479.208
	RGB + NIR + DSM	1960.57	504.224
Satellite	Multispectral (RGB+NIR)	1837.64	246.264
	Pan sharpened	1904.13	72.212

According to the values of transformed divergence, especially the additional altitude information in the form of the DSM increases classification accuracy. Furthermore, multispectral satellite and a combination of RPAS-derived RGB and NIR classification result in very similar results in terms of classification accuracy, whereas the satellite data show slightly better results. Comparing multispectral and pan-sharpened satellite classification shows a slightly better separability for pan-sharpened classification concerning best average. However, the best minimum value is much lower than for the multispectral data which can be caused by a spatial outlier or indicate poorer separability. The good or even perfect class separability of the RPAS-derived image classifications could even be improved by increasing positional accuracy. To support the good trend of classification suitability, working on the location accuracy of RGB and NIR RPAS-derived images should be one of the following most important research interests.

6.5. CHANGE DETECTION RESULTS

The pixel-based subtractive change detection technique results in probability change maps that can be seen in Figure 29 and Figure 30. Through subtractive map algebra the difference between two images with different recording time is computed and expressed as probability of change. Figure 29 shows the probability of change between RPAS-derived RGB images from September 2014 and June 2015. While green indicates no or a low probability of change, red visualizes areas with high probability of change. As both data sets are acquired after restoration, newly build restored areas are present in both images. Nevertheless, high probability of change can be seen around the ponds which can be caused in change of shape and depth but also water level at recording time. Other areas of high probability change are the agricultural fields. Understandably, they have a high probability of change because farmers change crop regularly. The small stripe of high probability change in the river curve is caused by different light conditions. While the image of 2014 shows larger shaded areas the same areas are sunny in 2015. To exclude these kind of errors flights with the RPAS should always take place at sun peak. Most other zones of higher probability change are caused by growing vegetation or landing of segments at groynes which changed shape and size of gravel banks.

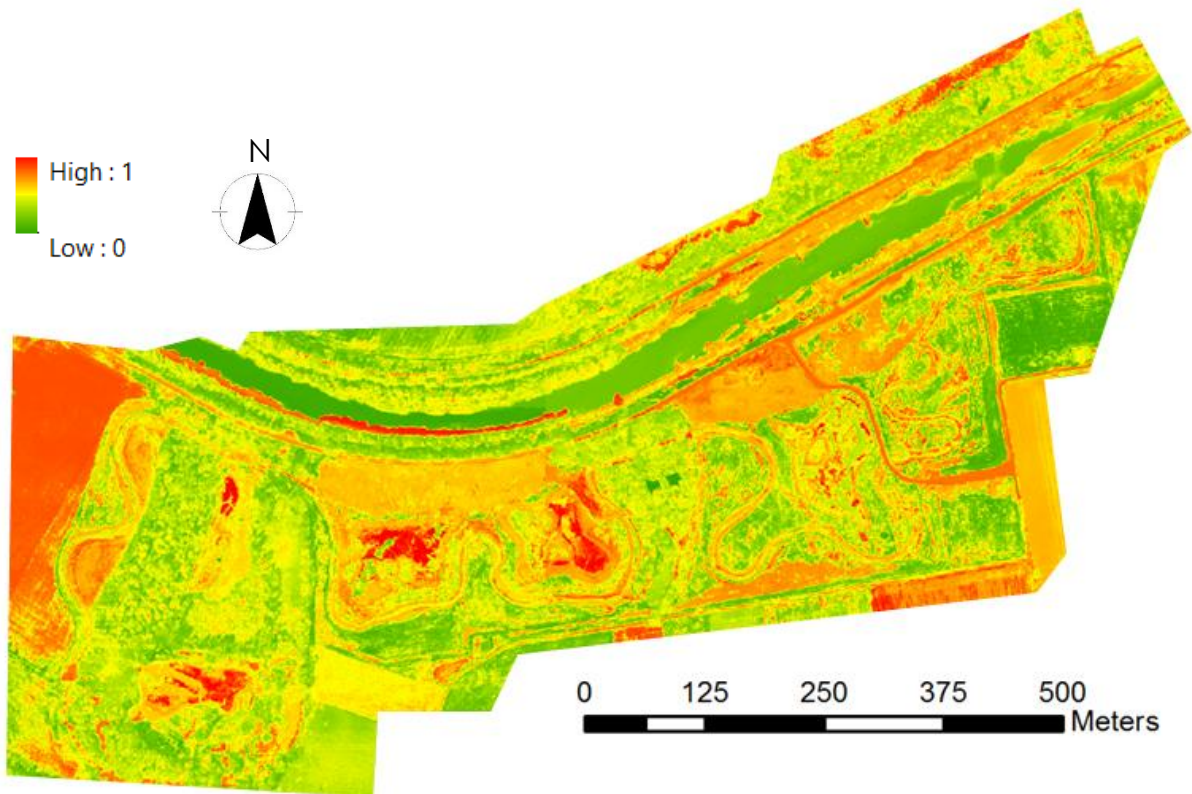


Figure 29: Probability of change between RPAS RGB images 2014 and 2015 at the river Gail

However, Figure 30 displays the probability of change between the pre and post restoration situation. The images are acquired by airplane by the Carinthian government in July 2010 and August 2013. All restoration actions are highlighted in red and therewith understandably show a high probability change as they only appear in the second image. All the newly formed ponds as well as the creek are highlighted in red as part of the restoration. The curved path in the right side of the image was created at the same time as the spruce forest surrounded by the lower left oxbow regions was deforested. The high probability change areas at forest borders and around power poles are errors caused by slight changes of recording angle and light conditions. Again, crop changes between both time stamps. In the river change can be observed where groynes were built and gravel or sand banks start building.

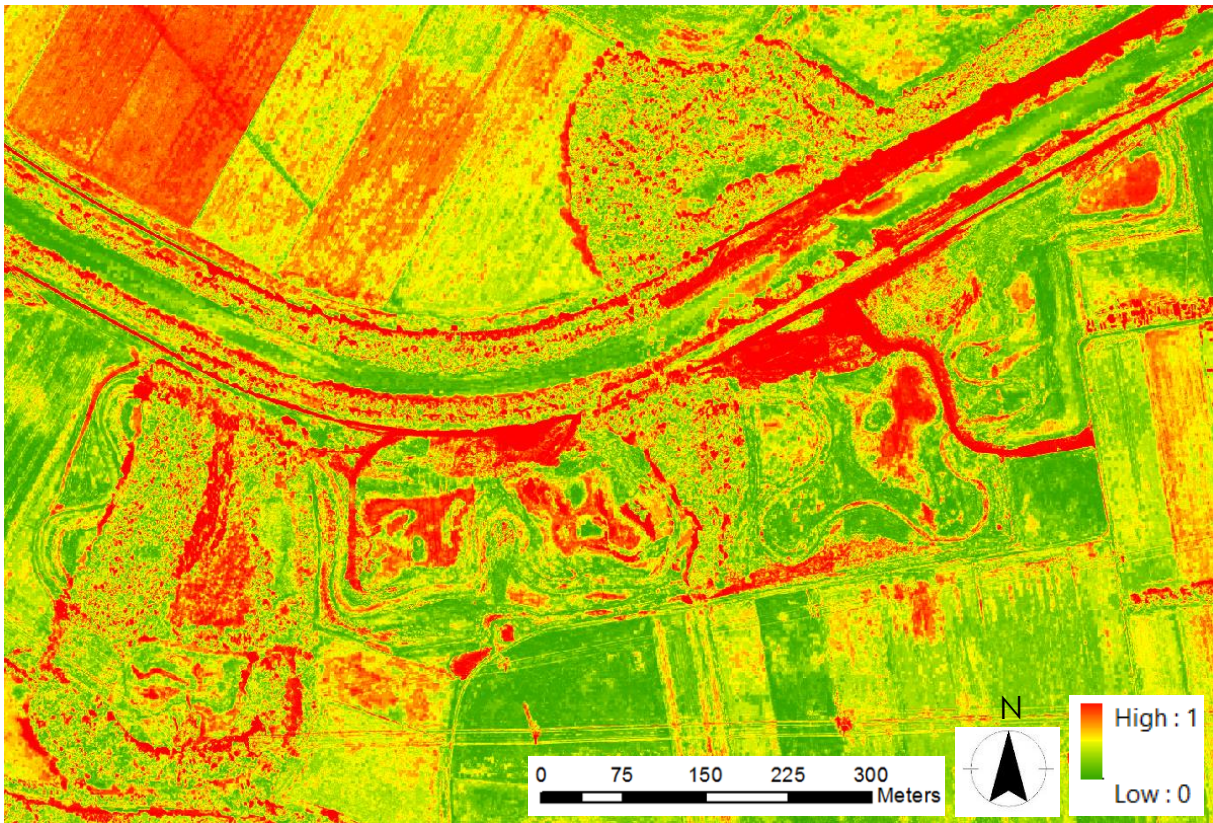


Figure 30: Probability of change between RGB ortho-photos from 2010 and 2013 at the river Gail

Secondly, post classification change detection is applied to the same data sets. Using Maximum Likelihood classifier for the RPAS images 18 classes are extracted while Image Segmentation algorithm results in 24 classes for the airplane-derived ortho-photos. The parameters for the ortho-photos are specified as follows: image 2010: Pixel:Segment Ratio: 100,000 (boundaries: 100-200,000), Relative Weights: spectral: 0.8, texture: 0.2, size: 0.2, shape: 0.2, Size Limits: Minimum: 100, Maximum: 10,000,000,000; image 2013: Pixel:Segment Ratio: 30,000 (boundaries: 100-60,000), Relative Weights: spectral: 0.8, texture: 0.2, size: 0.2, shape: 0.2, Size Limits: Minimum: 100, Maximum: 10,000,000,000. The areas of each class at each time stamp are calculated and compared to see in which class and how much change occurred. The results can be seen in Table 20 and Table 21.

Negative values in the columns difference and percentage change indicate loss of class areas while positive values show new regions of the appropriate class. As can be seen in Table 20 there are much less pixels classified as creek in 2015 than in 2014. This can be caused by different water levels as the scene from 2014 has been collected in autumn while the 2015 scene has been collected in summer. For evaluation of the restoration's success especially the water-related classes are of interest. Except the class creek, whose decrease might be caused by a classification or condition error, all other water-related

classes show an area gain to a certain percentage. The oxbow class increases by 27.29 % of area while pond, river and water lily even show a gain of 43.76 %, 45.32 % and 46.97 %, respectively. Additionally new gravel or sand banks are built with a percentage of 47.92 % during this year. Altogether after the post classification change detection result the restoration has been accepted successfully.

Table 20: Post classification change detection result RPAS-derived ortho-photos

Class	Area 2014 [m²]	Area 2015 [m²]	Difference [m²]	Percentage Change [%]
bare soil	626194.6	1471348.71	845154.11	57,44
building	319719.4	339401.91	19682.51	5,80
creek	651747.65	315472.35	-336275.3	-106,59
gravel/sand bank	579416.75	1112610.03	533193.28	47,92
gray alder	427864.45	1507098.93	1079234.48	71,61
gray alder/ash	120468.1	945156.9	824688.8	87,25
oxbow	320057.1	440191.95	120134.85	27,29
path	289297.6	469794.75	180497.15	38,42
pond	777294.3	1381985.67	604691.37	43,76
purple moor/tall oat	1905918.05	1433234.28	-472683.77	-32,98
reed bed	334706.7	1005987.78	671281.08	66,73
reed/willow bush	133390.95	806135.19	672744.24	83,45
river	642294.25	1174641.3	532347.05	45,32
sowed meadow	1085086.9	1230095.73	145008.83	11,79
tall oat grass	432407.95	814830.27	382422.32	46,93
tor grass/red fescue	797763.15	1997012.76	1199249.61	60,05
water lily	463034.05	873128.58	410094.53	46,97
white willow	1095947.85	573392.04	-522555.81	-91,13

The second post classification change detection is performed between the ortho-photos with pre and post restoration time stamp. Due to the nature of Image Segmentation classifier and the object size the creek was not recognized and therefore is not included in the results. But as can be seen in Table 21 the restoration helped to slow down the discharge in establishing gravel or sand banks with 92.66 % and gave the river more space as the area increased by 20.58 %. Additionally 83.02 % new ponds formed and build standing water habitats. The area of water lily slightly decreased by 8.65 % which again can be caused by classification inaccuracy or the nature of water lilies and different recording times as water lilies do not appear throughout the whole year. As another water-related class the oxbows areas increased significantly with 283.23 %. This statistical outlier shows a trend of increased oxbow areas but simultaneously constitutes the presumption that the high

value is either positively supported by classification inaccuracy or other conditions like covering tree canopies.

But again the comparison of pre and post restoration images supports the result of the RPAS-derived change detection that the restoration has been successfully accepted. While pixel-based change detection only helped in seeing where the changes occurred and how much changed in which area, the post classification change detection even could be used to evaluate the restoration and prove its success.

Table 21: Post classification change detection result airplane-derived ortho-photos

Class	Area 2010 [m²]	Area 2013 [m²]	Difference [m²]	Percentage Change [%]
bare soil	1146805.76	1106543.44	-40262.32	-3,64
agriculture 1	1871739.29	1765567.67	-106171.62	-6,01
agriculture 2	206576.185	259218.92	52642.735	20,31
agriculture 3	965782.35	762550.685	-203231.665	-26,65
alder/willow shrub	17461.19	30545.065	13083.875	42,83
building	170587.185	190272.24	19685.055	10,35
gravel/sand bank	486.35	6629.115	6142.765	92,66
gray alder/ash	976836.15	805049.155	-171786.995	-21,34
gray elder	56208.94	48775.325	-7433.615	-15,24
infrastructure	0	317.815	317.815	100,00
oxbow	5651.9	21659.775	16007.875	283,23
path	177050.93	181495.1	4444.17	2,45
pond/standing water	6040.99	35582.91	29541.92	83,02
reed bed	32120.595	20354.005	-11766.59	-57,81
reed/willow bush	86289.505	63087.445	-23202.06	-36,78
river	269119.05	338843.26	69724.21	20,58
single tree	1276.92	3660.92	2384	65,12
sowing meadow	3520354.32	3730392.96	210038.64	5,63
spruce forest	277283.115	376956.875	99673.76	26,44
tall oat/moor grass	194844.09	167169.19	-27674.9	-16,56
tor grass/fescue	134964.685	119295.185	-15669.5	-13,14
water lily	8005.6	7368.555	-637.045	-8,65
white clover	237390.44	284434.345	47043.905	16,54
white willow	182415.49	201960.595	19545.105	9,68

7. EVALUATION

To make statements about the accuracy and informational content of classification results, spatial base data is used for comparison. This data has been acquired based on field sampling and image interpretation as further explained in chapter 4.5. For accuracy assessment the most commonly used method of generating random points and check their agreement between classified and reference data is applied. As classification accuracy measure overall accuracy and Kappa coefficient are calculated. But besides, also informational content of the different classification results is analyzed and described. Finally, an error analysis is performed to highlight classes that are likely to be confused.

7.1. ACCURACY ASSESSMENT

With the advent of remote sensors with increasing resolution the necessity of performing an accuracy assessment has become an integral part. To evaluate the accuracy of the classes found by the different classification algorithms used in this project an accuracy assessment is performed. Therefore, a defined number of points is equally randomly distributed over the project area which means that for each class the same amount of random points is generated. The class of each point in the classified image is then compared to the appropriate class in the reference data set. The output of the accuracy assessment is a confusion matrix, stating the overall accuracy and the Kappa coefficient. The amount of assessment points per class is suggested by Congalton (1991) and Congalton and Green (1999) as follows: as a minimum 50 points per classes should be generated. If the classification results in a large number of classes or the area is particularly large, the number of assessment points should be increased to 75 or 100 samples per class.

As descriptive and analytical statistical technique the confusion or error matrix is widely used. Comparing each class to every other not only a measurement of the overall classification accuracy but also the information which classes are likely to become confused is stated. The overall accuracy is calculated by dividing the total correct by the total amount of pixels in the confusion matrix. Traditionally the accuracy for each class is derived by dividing the number of correctly classified pixels by the total amount of pixels of this class in the reference data. This accuracy measure indicates the probability of a reference

pixel being correctly classified and is also known as producer's accuracy or omission error. On the other hand the user's accuracy or commission error can be derived in dividing the number of correctly classified pixels in a class by the total amount of pixels classified in this class. However, this measure indicates the probability of a classified pixel in the image really presenting the class on the ground (Congalton, 1991).

Table 22 displays a randomly generated confusion matrix including 11 ISODATA classes resulting from GeoEye-1 classification. Besides the confrontation of classified and reference data, the column totals as well as the row totals and the sum of diagonals are calculated.

Table 22: Example of a confusion matrix evaluating the accuracy of eleven example classes

	spruce forest	river	alluvial forest	gravel/sand bank	agriculture 1	white clover	reed bed	agricultural field	sowing meadow	agriculture 2	path	row total
spruce forest	19	3	3	0	3	0	0	0	0	0	0	28
river	0	47	0	1	0	0	0	0	0	0	0	48
alluvial forest	52	15	23	2	4	2	3	1	2	2	2	108
gravel/sand bank	0	0	0	0	0	0	0	0	0	0	0	0
agriculture 1	2	0	18	1	62	5	5	0	13	3	0	109
white clover	0	0	0	0	0	8	11	1	0	0	1	21
reed bed	0	2	1	1	0	0	0	0	0	1	0	5
agricultural field	0	1	0	1	1	5	3	61	0	11	13	96
sowing meadow	2	0	26	3	5	51	46	5	57	26	6	227
agriculture 2	0	0	1	47	0	4	6	5	1	25	28	117
path	0	7	3	19	0	0	1	2	2	7	25	66
classified												
column total	75	75	75	75	75	75	75	75	75	75	75	327
overall accuracy	39,64%											

The Kappa analysis is a multivariate technique and a measure of agreement or accuracy between the remote sensing-derived image and the reference data (Jensen, 2005). While the overall accuracy measure only includes the major diagonal of the error matrix, the kappa coefficient indirectly also takes the omission and commission errors into account (Congalton, 1991). Kappa values of >0.80 represent high accuracy between the classification map and the ground reference data. Values between 0.40 and 0.80 represent moderate and values <0.40 poor agreement (Landis and Koch, 1977). To calculate the Kappa coefficient at first the expected accuracy needs to be computed. The expected accuracy can be derived by computing the sum of all column totals multiplied by the appropriate row total and divided by the total number of samples. Finally, the Kappa coefficient is calculated by subtracting the expected accuracy from the overall accuracy and dividing the result by 1 – the expected accuracy.

Table 23 shows the calculation of overall accuracy and Kappa coefficient per class for the same 11 example classes as shown in Table 22. As can be seen producer's and user's accuracy values often differ a lot and the analyst need to be aware of the differences for clear interpretation. But besides, the calculation for every single class provides the opportunity to differentiate between classes of high and those of low classification accuracy.

Table 23: Overall accuracy values for the 11 ISODATA classes of the example in Table 22

	reference totals	classified totals	number correct	producer's accuracy	user's accuracy	expected accuracy
spruce forest	75	28	19	25,33%	67,86%	2,545455
river	75	48	47	62,67%	97,92%	4,363636
alluvial forest	75	108	23	30,67%	21,30%	9,818182
gravel/sand bank	75	0	0	0,00%	0,00%	0
agriculture 1	75	109	62	82,67%	56,88%	9,909091
white clover	75	21	8	10,67%	38,10%	1,909091
reed bed	75	5	0	0,00%	0,00%	0,454545
agricultural field	75	96	61	81,33%	63,54%	8,727273
sowing meadow	75	227	57	76,00%	25,11%	20,63636
agriculture 2	75	117	25	33,33%	21,37%	10,63636
path	75	66	25	33,33%	37,88%	6
expected accuracy	9,09%					
Kappa	33,60%					

Although the Kappa coefficient is widely accepted as accuracy measure in remote sensing applications, it also has its opponents. Pontius and Millones (2011) remark in their paper "Death to Kappa" that Kappa is inaccurate and misleading and should not be used for accuracy assessment. They justify their conclusions in criticizing that Kappa compares observed accuracy to an accuracy expected due to randomness and prove that randomness is an irrelevant and misleading baseline. Therefore, Kappa coefficient as one measure of accuracy has to be handled with care and the analyst should always keep its issues in mind.

7.2. QUANTITATIVE ASSESSMENT

As mentioned in chapter 5.7 the classification results are not only evaluated based on their classification accuracy but also on their informational content concerning:

1. Accuracy of classification after the Habitats Directive
2. Accuracy of classification in accordance to the more detailed internal habitat type classification
3. Accuracy of classification of single vegetation species
4. Accuracy of classification of single vegetation varieties
5. Accuracy of classification of soil types

In terms of informational content the Image Segmentation algorithm delivers the best results, as it finds segments in the image which are then assigned to the appropriate class. With this classifier it was possible to determine the classes as mentioned in the Habitats Directive with an accuracy of 81.60 %. The more detailed internal habitats classification could be achieved with 77.18 % accuracy. However, the Image Segmentation classifier made it possible to neither identify single vegetation species nor varieties nor make statements about different soil types. On the other hand, ISODATA provides the least accurate results concerning informational content. Based on its nature, only fewer classes can be found because often clusters appear in multiple classes at once. For that reason, clusters can only be merged to broader classes. Therefore, it was not possible to identify all present classes as defined in the Habitats Directive or the internal classification. Finally, Maximum Likelihood algorithm offers the possibility to find all available classes according to the Habitats Directive. The difficulty is to find the balance between accuracy and informational content. Defining a signature for each and every class and therewith getting high informational content usually leads to a lower accuracy. With the help of the transformed divergence measure classes can be merged to increase the separability, but simultaneously informational content gets lost. Thus, the classes according to the habitats directive were found with an accuracy of 35.60 % and the more detailed internal classes with 33.30 % accuracy. But in the RPAS-derived data it was possible to differentiate vegetation species with the help of Maximum Likelihood classifier. But because of the high resolution issue as already mentioned, no meaningful accuracy

value could be derived. Statements about vegetation varieties or soil types could not be made with Maximum Likelihood classifier.

To conclude, in terms of accuracy Image Segmentation is the most accurate classifier used, but regarding quantity Maximum Likelihood can be used to identify three of the five defined categories. ISODATA is the most inaccurate classifier regarding both, qualitative and quantitative content.

7.3. ERROR ANALYSIS

Because of their spectral similarity, there are some classes that are most likely to be confused during the classification process. For the GeoEye-1 satellite imagery ISODATA classifies in 69.3 % of cases pixels that are belonging to the alluvial forest class as spruce forest. Furthermore, sowed meadow is classified as white clover in 68 % of cases and the class agriculture 2 is classified as gravel/sand bank with 62.7 %. However, Image Segmentation has a higher overall accuracy and therefore fewer classes are confused with a high percentage. Thus, pixels belonging to the class gray alder/ash are classified as reed bed with 60 % and 40 % of the pixels belonging to the class agriculture 1 are classified as gray alder/ash. Also very few high percentage confusions between classes are found in the results of Maximum Likelihood algorithm with 15 resulting classes. A third of the pixels of the river class are classified as natural eutrophic lakes and 14 % of the purple moor/tall oat grass pixels are classified as bare soil and white clover/ryegrass respectively.

8. DISCUSSION

Closing the circle, this chapter finally addresses the responses to the research questions formulated in the introductory chapters. Especially in the first part the research questions are treated intensively. In the subchapter Conclusion all findings are summarized to highlight the benefits of this master's project. Finally, the chapter closes with an outlook into future work and possible follow-up projects.

The key research question of this work asks for the suitability of the different remote sensors for monitoring riverine environments in terms of informational content and accuracy. The classification results have proven that both, the satellite as well as RPAS sensors, are usable for the assigned tasks according to riverine environmental monitoring. Concerning informational content even all of the more detailed internal classes could be achieved with at least satisfactory accuracy. Through change detection analyses temporal changes could be mapped and evaluated. One problem that still persists, lies with the ability to technically process and interpret the ultra-high resolution RPAS data. In this field of high resolution classification a research on efficient classification algorithms for VHR RPAS data should be conducted and suitable classifiers applied. Another possibility was to develop a novel algorithm specifically adopted to the present problem. Furthermore, accuracy assessment should be reconsidered concentrating on an object-based approach. Altogether the research question about the suitability of the different sensors for environmental monitoring has been successfully answered.

A sub-question asks for the scale to what it is possible to differentiate between vegetation. As shown through classification, plant communities as mentioned in the Habitats Directive are identified with high accuracy. Whereas for satellite images these plant communities are the highest level of differentiation reachable, RPAS-derived data can also be used to differentiate between tree groups and to a lower degree, tree species. Be it through visual image interpretation or through classification via Maximum Likelihood classifier, certain tree species are clearly discernible. This research question was satisfactorily addressed as well.

None of the systems fulfils all environmental monitoring tasks as mentioned in the EU directives. While statements about the health states of the habitats and animal mapping are lacking according to the Habitats and Birds Directive, it is the water quality that cannot be determined to fulfil the Water Framework

Directive. However, some statements about geomorphologic changes could be made in observing the gravel or sand banks and tracking the river course. In addition, the water quantity could be captured to a certain degree. Therewith, the question about the statements that can be made about water quality and quantity of the monitored rivers could be partially answered.

Although it has many advantages and the results of the RPAS are of higher resolution, the monitoring tasks according to the EU directives that could be fulfilled, could all be satisfied by the VHR satellite systems. This means that the resolution of VHR satellites is high enough to fulfil monitoring tasks. It is to be expected that the hyperspectral camera brings about a rebound and improves the RPAS-related results significantly through higher spectral resolution. But so far the spatial resolution of currently operating earth-observation satellites can be seen as high enough to partly fulfil monitoring tasks according to EU directives. Only health states of vegetation and water quality could not be monitored.

The RPAS has been proven to reliably fulfil environmental monitoring tasks and the appropriate research question was successfully answered. However, there is still a problem with the positional accuracy that by now already has partly been fixed. The advantage of the RPAS compared to satellites is besides the adoptable temporal and spatial resolution, the opportunity in changing spectral resolution. A hyperspectral camera could be from specific use for monitoring the health states of the habitats as well as detecting pioneer species and invasive neophytes and monitor their spread.

The expected results of this research have been defined in chapter 1.4 as follows:

1. Overall quality and suitability assessment of a small RPAS-based multi-sensor platform for high-resolution spatiotemporal monitoring of dynamic river environments in the context of vegetation and geomorphology
2. Evaluation of classification results for vegetation and geomorphic landforms
3. Comparison of the different remote sensing systems
4. A large quantity of environmental data sets generated by multiple missions during the project period

Result number 1 has been reached in classifying RPAS-derived data and conducting a change analysis between two temporally different recordings. Advantages as well as issues have been detected that can be used for further development of the platform. While the RPAS is attractive for its adjustability of spatial, temporal and even spectral resolution, geometric inaccuracy and issues in processing data in such an ultra-high resolution still need to be solved. The classification results of the different remote sensors have been evaluated and discussed in chapter 6.4. In addition, a detailed comparison between the different results took place. Therewith, the expected results 2 and 3 could be fulfilled successfully. Finally, due to the nature of the RPAS, a large quantity of environmental data sets have been generated during multiple missions. Additionally reference data in single tree resolution have been collected in the field for evaluation purpose of the visual image interpretation experiment. To conclude, all four expected results have been successfully reached during this master's project.

8.1. CONCLUSION

The suitability and accuracy of VHR satellite and even higher resolution RPAS images have been evaluated for the purpose of riverine environmental monitoring. A comparison of different unsupervised and supervised classification methods have been performed after geometrically and radiometrically correcting the imagery. The dependency of location accuracy and the spatial resolution of data used for ortho-rectification could be verified in preprocessing satellite data using DEMs in different resolutions. The accuracy assessment of the satellite images has proven that the FLS-based Image Segmentation algorithm delivers the best results in terms of accuracy and quantitative content, followed by Maximum Likelihood and ISODATA. Because of the ultra-high resolution and intensive post-classification requirements by unsupervised techniques, only Maximum Likelihood classifier could be applied on the RPAS data. Problems in the accuracy assessment of RPAS classification results caused by lower resolution of the reference data have shown that the development of new object-based techniques for accuracy assessment of ultra-high resolution data is crucially needed. A change detection analysis between two timestamps of the aerial images taken before and after restoration could highlight the regions of change during restoration and verify the success of restoration actions. Analyzing the change between RPAS

images with a temporal interval of one year has shown that the study area is still changing in essence. Although positional accuracy of the RPAS imagery could be improved through geo-referencing, an acceptable inaccuracy of less than pixel resolution could not be achieved. By now location accuracy of the RPAS system has already been improved and a strategy was developed to ensure high location accuracy and handle small deviations from the planned trajectory caused by local wind situations.

8.2. OUTLOOK

Besides environmental monitoring there is a large variety of other application areas imaginable for the RPAS. Particularly in these times of climate change, wars, poverty and suppression where each day more and more refugees reach European land, the RPAS could be used in crisis management. Supporting charity organizations in fast mapping of the situation or searching for completely overcrowded refugee boats in the Mediterranean Sea close to European borders are only two conceivable scenarios. Furthermore, natural disasters are another application area for the RPAS to quickly map the situation after e.g. an earth-quake or a fire and ensure to introduce the right type of help at the right place. In Austria the RPAS could be of particular interest for forestry. As different species are clearly discernible at least with aid of an interpretation key, RPAS-derived images could be used for forest inventory. In addition with the hyperspectral camera the system could even allow a better planning of actions to increase forest health and reduce pest infestation. This small selection of possible other application areas for the fixed-wing RPAS should give a cause for thought and highlight the diversity of this ultra-high resolution system.

In a further step a hyperspectral camera will be mounted on the RPAS platform to test if the higher spectral resolution increases classification accuracy as well as informational content. Because of the larger amount of spectral bands the hyperspectral camera is expected to improve the classification results significantly. Besides quantitatively assessing riverine habitats, hyperspectral data might also provide the possibility to qualitatively monitor present vegetation and river geomorphology.

The present data did not afford an opportunity to make statements about existence and spread of inverse neophytes. In this field the application of the hyperspectral camera could be worthwhile. Another research project should

concentrate on this sector to find ways classifying inverse species. In a first try a hand spectrometer could be used to select spectral signatures of neophytes and analyze their separability. If separability values are low, spatio-temporal analyses through the seasons could help identifying inverse species based on their spectral behavior throughout the year.

To counteract the, compared to resolution, low spatial agreement between RPAS images derived in different flights a new model for geo-referencing should be developed. As there is no possibility to load the RPAS with the RGB and NIR camera simultaneously, all images need to be geometrically corrected. Optimally the preprocessing step should take place before all single images are mosaicked together to reduce regional location inaccuracy. By the end of this thesis, location accuracy could already and will further be improved to ensure high spatial agreement between different images.

Additionally the WorldView-2 winter scenes could be used in combination with a hydraulic model of the rivers to evaluate their usage for detection of the river bed shapes and water quantity. Another interesting research question could be to try to classify trees in the winter scenes. Because of missing leaves other methods than spectral characteristics need to be developed to differentiate between deciduous species.

REFERENCES

- Ahmad, A. (2013). Mapping of a River using Close Range Photogrammetry Technique and Unmanned Aerial Vehicle System. In: 8th International Symposium on digital Earth, Aug 26-29, 2013, Sarawak.
- Albertz, J. (2007). Introduction to Remote Sensing. Principles of Interpreting Aerial and Satellite Images. 3rd edition, Scientific Literature Society, Darmstadt.
- Arnoldius. (2012). Birch Forest as Pioneer Species on the Stockpile of the former Mine 'Constantind der Große' in Herme [online]. Available from: http://upload.wikimedia.org/wikipedia/commons/d/d6/Herne_Halde_Constantin_birches.jpg [accessed at April 16, 2015].
- Ashraf, M. A., Maah, M. J., & Yusoff, I. (2011). Introduction to Remote Sensing of Biomass. Biomass and Remote Sensing of Biomass, Dr. Islam Atazadeh (Ed.), InTech, Rijeka.
- Ashraf, S., Brabyn, L., & Hicks, B. (2013). Introducing Contrast and Luminance Normalisation to improve the Quality of Subtractive Resolution Merge Technique. International Journal of Image and Data Fusion, Volume 4, Issue 3, pp. 230-251.
- Atzberger, C., & Schlerf, M. (2002). Automatic Stem Density Estimation in Coniferous Forests from High Spatial Resolution Orthophotos. Photogrammetry Remote Sensing Geoinformation 3/2002, pp. 171-180.
- Augsburger-Allgemeine. (2013). 800 Years old Bavaria Beech broken in Storm [online]. Augsburger Allgemeine Zeitung, available from: <http://bilder.augsburger-allgemeine.de/img/incoming/origs27257677/1612234845-w1280-h500.jpg> [accessed at April 16, 2015].
- Austrian-Federal-Environment-Agency. (2015). The "Aliens" have arrived! - Neobiota in Austria [online]. Available from:

<http://www.umweltbundesamt.at/aliens/> [accessed at February 2, 2015].

Bellingham, K. (2007). The Stevens Hydra Probe Inorganic Soil Calibrations [online]. Stevens Water Monitoring Systems, Inc., Portland, Available from:

http://www.stevenswater.com/catalog/products/soil_sensors/datasheet/The%20Stevens%20Hydra%20Probe%20Inorganic%20Soil%20Calibrations.pdf [accessed at August 25, 2015].

BMLFUW. (2010). River Gail - alive and secure (again). Press Release Project LIFE+ Gail, Provincial Government of Carinthia - Water Management, Klagenfurt.

BMLFUW. (2015a). LIFE+ Gail [online]. Available from: <http://www.life-gail.at/?tpl=text&id=72> [accessed 7 January 2015].

BMLFUW. (2015b). LIFE Upper Drau II [online]. Available from: http://www.life-drau.at/?tpl=text&id=16&menu=3&lng=&sub_id=3 [accessed at 7 January 2015].

BMLFUW. (2015c). Upper Drau River II [online]. Available from: http://www.life-drau.at/?tpl=text&id=16&menu=3&lng=&sub_id=3 [accessed at 10 January 2015].

BMLFUW. (2015c). Water in Austria [online]. Available from: <http://www.bmlfuw.gv.at/wasser/wasser-oesterreich.html> [accessed at April 20, 2015].

Boser, B. E., Guyon, I. M., & Vapnik, V. N. (1992). A Training Algorithm for Optimal Margin Classifiers. 5th Annual Workshop on Computational Learning Theory, ACM Press, Pittsburgh.

Bovolo, F., Bruzzone, L., & Marchesi, S. (2009). Analysis and Adaptive Estimation of the Registration Noise Distribution in Multitemporal VHR Images. IEEE Transactions on Geoscience and Remote Sensing, Vol. 47, No. 8, pp. 2658 -2671.

- Campbell, J. B. (2002). *Introduction to Remote Sensing*. 3rd Edition, Taylor & Francis, London, New York.
- Carbonneau, P., Piégay, H., Lejot, J., Dunford, R., & Michel, K. (2012). *Hyperspatial Imagery in Riverine Environments. Fluvial Remote Sensing for Science and Management*. John Wiley & Sons, Ltd., Hoboken.
- C-Astral. (2015). Technical Specifications BRAMOR rTK [online]. Available from: <http://www.c-astral.com/en/products/bramor-rtk#specs> [accessed at February 12, 2015].
- Chang, C.-I. (2013). *Hyperspectral Data Processing*. John Wiley & Sons Inc., Hoboken.
- Ciesla, W. M., & Hoppus, M. L. (1990). Identification of Port Oxford Cedar and Associated Species on Large Scale Color and CIR Aerial Photos. *Color Aerial Photography and Videography in the Plant Sciences and Related Fields: Proceedings for the Twelfth Biennial Workshop, Sparks, Nevada, May 23-29, 1989*.
- Congalton, R. G. (1991). Remote Sensing of Environment. *A Review of Assessing the Accuracy of Classifications of Remotely Sensed Data*. Volume 37, pp. 35–46.
- Congalton, R. G. (1999). *Assessing the Accuracy of Remotely Sensed Data: Principles and Practices*. Boca Raton, FL: Lewis Publishers.
- Congalton, R. G., & Green, K. (2009). *Assessing the Accuracy of Remotely Sensed Data: Principles and Practices*. Second Edition, CRC Press, Taylor & Francis Group, Boca Raton.
- Copernicus. (2015). Corine Land Cover [online]. Available from: <http://land.copernicus.eu/pan-european/corine-land-cover> [accessed at January 4, 2015].
- Cyberphysics. (2013). The Electromagnetic Spectrum [online]. <http://www.cyberphysics.co.uk/topics/radioact/Radio/EMSpectrumcolor.jpg> [accessed 12 January 2015].

- Dai, X., & Khorram, S. (1998). The Effects of Image Misregistration on the Accuracy of Remotely Sensed Change Detection. *IEEE Transactions on Geoscience and Remote Sensing*, Vol. 36, No. 5, pp. 1566-1577 .
- DAISIE. (2015). Delivering Alien Invasive Species Inventories for Europe [online]. Available from: <http://www.europe-aliens.org/default.do> [accessed at April 16, 2015].
- DigitalGlobe. (2013a). Standard Imagery [online]. Available from: https://www.digitalglobe.com/sites/default/files/StandardImagery_DS_10-14_forWeb.pdf [accessed at April 4, 2015].
- DigitalGlobe. (2013b). WorldView-2 - Data Sheet [online]. Available from: https://www.digitalglobe.com/sites/default/files/DG_WorldView2_DS_PROD.pdf [accessed at February 4, 2015].
- DigitalGlobe. (2015a). GeoEye-1 Data Sheet [online]. Available from: https://www.digitalglobe.com/sites/default/files/DG_GeoEye1.pdf [accessed at April 16, 2015].
- DigitalGlobe. (2015b). QuickBird Data Sheet [online]. Available from: <https://www.digitalglobe.com/sites/default/files/QuickBird-DS-QB-Prod.pdf> [accessed at April 16, 2015].
- Droj, G. (2007). The Applicability of Fuzzy Theory in Remote Sensing Image Classification. *Studia Universitatis Babeş-Bolyai, Informatica LII(1)* .
- Dufour, S., Bernez, I., Betbeder, J., Corgne, S., Hubert-Moy, L., Nabucet, J., Rapinel, S., Sawtschuk, J., Trollé, C. (2013). Monitoring Restored Riparian Vegetation: How can Recent Developments in Remote Sensing Sciences help? *Knowledge and Management of Aquatic Ecosystems*, Issue 410, Art. No. 10.
- EC. (2012). Commission Staff Working Document. *Towards a European strategy for the development of civil applications of Remotely Piloted Aircraft Systems (RPAS)*. Council of the European Union, Brussels.
- EC. (2015). Copernicus [online]. Available from: <http://www.copernicus.eu> [accessed at January 4, 2015].

- Ehlers, M., Greiwe, A., & Tomowski, D. (2006). On Segment based Image Fusion. 1st International Conference on Object-based Image Analysis, July 4-5, 2006, Salzburg University.
- Ellenberg, H., & Leuschner, C. (2010). Vegetation Ecology of Central Europe. 6th edition, Eugen Ulmer Publishing, Stuttgart.
- Elsharkawy, A., Elhabiby, M., & El-Sheimy, N. (2012). Quality Control on the Radiometric Calibration of the WorldView-2 Data. Global Geospatial Conference 2012, May 14-17, 2012, Québec City.
- Eltohamy, F., & Hamza, E. H. (2009). Effect of Ground Control Points and Distribution on Geometric Correction Accuracy of Remote Sensing Satellite Images. 13th International Conference on Aerospace Sciences & Aviation Technology, May 26-28, 2009, Military Technical College, Cairo.
- Engleder, T. (2004). Aerial Image Interpretation and Remote Sensing. University of Vienna, teaching material.
- ERDAS. (2009). Wavelet Resolution Merge. Erdas Inc., Norcross.
- Essl, F., & Rabitsch, W. (2002). Neobiota in Austria. Austrian Federal Environment Agency, Vienna.
- EU, B. D. (2009). DIRECTIVE 2009/147/EC of 30 November 2009 on the conservation of wild birds. Available from: <http://eur-lex.europa.eu/legal-content/EN/TXT/PDF/?uri=CELEX:32009L0147&from=EN> [accessed at August 25, 2015].
- EU, H. D. (1992). COUNCIL DIRECTIVE 92/43/EEC of 21 May 1992 on the conservation of natural habitats and of wild fauna and flora. Available from: <http://eur-lex.europa.eu/legal-content/EN/TXT/PDF/?uri=CELEX:31992L0043&from=EN> [accessed at August 25, 2015].
- EU, S. F. (2003). COUNCIL REGULATION (EC) No 1782/2003 of 29 September 2003 establishing common rules for direct support schemes under the

common agricultural policy and establishing certain support schemes for farmers. Available from: <http://eur-lex.europa.eu/legal-content/EN/TXT/PDF/?uri=CELEX:32003R1782&from=EN> [accessed at August 25, 2015].

EU, W. F. (2000). DIRECTIVE 2000/60/EC OF THE EUROPEAN PARLIAMENT AND OF THE COUNCIL of 23 October 2000 establishing a framework for community action in the field of water policy. Available from: http://eur-lex.europa.eu/resource.html?uri=cellar:5c835afb-2ec6-4577-bdf8-756d3d694eeb.0004.02/DOC_1&format=PDF [accessed at August 25, 2015].

European-Environment-Agency. (2012). Natura 2000 - Database of the European Environment Agency.

Exelis-Visual-Information-Solutions. (2015). ENVI Merge Algorithms Background [online]. Available from: <http://www.exelisvis.com/docs/BackgroundMergeAlgorithms.html>.

Federal-Environmental-Agency. (2014). CORINE Landcover Austria. Austrian Environment Agency, Vienna.

Federal-Environmental-Agency. (2015). NATURA 2000 sites [online]. Available from: <http://www.umweltbundesamt.at/umweltsituation/naturschutz/sg/n2000/> [accessed at January 18, 2015].

Filippi, A., & Archibald, R. (2009). Support Vector Machine-Based Endmember Extraction. *IEEE Transactions on Geoscience and Remote Sensing* 47(3): 771-791. doi:10.1109/TGRS.2008.2004708.

Fonstad, M. (2012). Hyperspectral Imagery in Fluvial Environments. *Fluvial Remote Sensing For Science and Mangement*. John Wiley & Sons, Ltd., Hoboken .

Frick, A. (2006). Contributions to Highest Resolution Satellite Remote Sensing for Habitats Monitoring. Thesis (PhD), Technical University Berlin.

- Gangkofner, U., & Holcomb, D. (2008). HP Resolution Merge. *ERDAS Imagine Help*. Leica Geosystems, Geospatial Imaging.
- German-Federal-Office-for-Nature-Conservation. (2015). Neobiota [online]. Available from: <http://www.neobiota.de/12601.html> [accessed at 2 February, 2015].
- Glanzbig, M. (2006). Carinthia General Map [online]. created using data from KAGIS, demis.nl and others, available from: https://upload.wikimedia.org/wikipedia/commons/c/c1/Map_at_carinthia_topo_hillshading.png [accessed at August 25, 2015].
- Goforth, M. A. (1998). Multispectral Image Sharpening with Multiresolution Analysis and the MTF. *Proc. SPIE, Algorithms for Multispectral and Hyperspectral Imagery IV*, Vol. 3372, pp. 123-131.
- Güneralp, İ., Filippi, A., & Hales, B. (2013). River flow boundary delineation from digital aerial photography and ancillary images using Support Vector Machines. *GIScience & Remote Sensing* 50(1): 1-25. doi:10.1080/15481603.2013.778560.
- Hagen, T. (1950). *Scientific Interpretation of Aerial Images*. Geographica Helvetica.
- Hexagon-Geospatial. (2015a). *ERDAS IMAGINE Help [online]*. Available from: <https://hexagongeospatial.fluidtopics.net/de/book#!book;uri=fb4350968f8f8b57984ae66bba04c48d;breadcrumb=be4e36518f3b39883b1633b55928207b-3a7b601b8baca6d02928f8df6c2af082-51e404353439d738f9141ccaa0662057> [accessed at August 5, 2015].
- Hexagon-Geospatial. (2015b). *Evaluating Signatures [online]*. Available from: https://wiki.hexagongeospatial.com/index.php?title=Evaluating_Signatures [accessed at August 5, 2015].
- Hoja, D., Scheider, M., Müller, R., Lehner, M., & Reinartz, P. (2008). Comparison of Orthorectification Methods suitable for rapid Mapping using direct Georeferencing and RPC for Optical Satellite Data. *International Archives of the Photogrammetry, Remote Sensing and Spatial Information Sciences* 37, pp. 1617-1624.

- Intergraph. (2013a). ERDAS Field Guide. Intergraph Corporation, Huntsville.
- Intergraph. (2013b). ERDAS IMAGINE 2014 Release Notes. Version 14.00.0000.
- Intermountain-Region. (2015). Herbarium Network [online]. Available from: <http://intermountainbiota.org/portal/imagelib/index.php> [accessed at April 16, 2015].
- Jensen, A. M., Hardy, T., McKee, M., & YanQuan, C. (2011). Using a Multispectral Autonomous Unmanned Aerial Remote Sensing Platform (AggieAir) for Riparian and Wetlands Applications. Geoscience and Remote Sensing Symposium (IGARSS), 2011 IEEE International .
- Jensen, J. R. (2005). Introductory Digital Image Processing. Pearson Prentice Hall, New York.
- KAGIS. (2015). Ortho-photos from Carinthia Atlas [online]. Available from: <http://gis.ktn.gv.at/atlas/> [accessed at January 10, 2015].
- Kollasch, R. P. (2005). Increasing the Detail of Land Use Classification: the Iowa 2002 Land Cover product. Proceedings of Global Priorities in Land Remote Sensing. Pecora 16 Symposium, October 23-27, 2005, Sioux Falls, South Dakota, USA.
- Landis, J., & Koch, G. (1977). The Measurement of Observer Agreement for Categorical Data. International Biometric Society, Biometrics, Volume 33, No 1, pp. 159-174 .
- Lane, E. W. (1954). The Importance of Fluvial Morphology in Hydraulic Engineering. US. Department of the Interior Bureau of Reclamation, Denver.
- Langanke, T. (2013). GIO land (GMES/Copernicus initial operations land) High Resolution Layers. European Environment Agency, version 7 of 2013-10-1.
- Lefsky, M. A., Cohen, W. B., Parker, G. G., & Harding, D. J. (2002). Lidar Remote Sensing for Ecosystem Studies. BioScience Vol. 52 No. 1, pp. 19-30.
- Leica. (2006). ERDAS IMAGINE Tour Guides. Leica Geosystems Geospatial Imaging, Norcross.

- Leitsch. (2012). *Biology of Trees. Legal Principles and Visual Tree Assessment - Modul I.*
- Linder, W. (2005). *Digital Photogrammetry on the PC. Habilitation treatise,* Heinrich Heine University Düsseldorf.
- LISA. (2015). *Land Information System Austria* [online]. Available from: <http://www.landinformationsystem.at/en-us/lisa/overview.aspx> [accessed 8 January 2015].
- LÖFFLER, E., HONECKER, U., & STABEL, E. (2005). *Geography and Remote Sensing.* Brothers Borntraeger Publishing, 3. edition, Berlin, Stuttgart.
- Lucas, R., Blonda, P., Bunting, P., Jones, G., Inglada, J., Arias, M., Kosmidou, V., Petrou, Z. I., Manakos, I., Adamo, M., Charnock, R., Tarantino, C., Múcher, C. A., Jongman, R. H. G., Kramer, H., Arvor, D., Honrado, J. P., Mairota, P. (2014). The Earth Observation Data for Habitat Monitoring (EODHaM) System. *International Journal of Applied Earth Observation and Geoinformation* Vol. 37, pp. 17–28.
- Magnes, M. (2012). *Problem Neophytes.* Austrian Horticultural Society, Vienna.
- Mäkeläinen, A., Saari, H., Hippel, I., Sarkeala, J., & Soukkamäki, J. (2013). 2D Hyperspectral Frame Imager Camera Data in Photogrammetric Mosaicking. *International Archives of the Photogrammetry, Remote Sensing and Spatial Information Sciences, Volume XL-1/W2, UAV-g2013,* 4 – 6 September 2013, Rostock.
- Mansberger, G., & Eisl, M. (2009). *Earth Observation with VHR Satellites – Status and Outlook. AGIT 2009: Extended Abstract Reviewed Papers.* AGIT Conference, July 8-10, 2009, Salzburg, pp. 25-30.
- Matusch, T. (2009). *Multi temporal Analysis of Land Cover in the Biosphere Reservat Schorfheide-Chorin and its Surrounding through Remote Sensing and Social Research . Thesis (Dipl.-Geogr.).* Ernst-Moritz-Arndt University Greifswald.

- Mishra, R. K., & Zhang, Y. (2013). A Comparison of Commercial Pan-Sharpener Techniques for HR Satellite Imagery. ESRI International User Conference 2013.
- Murai, S. (1993). Remote Sensing Note. Japan Association on Remote Sensing, Tokyo.
- NOBANIS. (2015). European Network of Invasive Alien Species [online]. *Factsheets on Invasive Alien Species*. Available from: <http://www.nobanis.org/Factsheets.asp> [accessed at April 16, 2015].
- Oester, B. (2003). Introduction to Remote Sensing. Forest Inventory II Lecture Notes, Research Institute WSL, Birmensdorf.
- Padwick, C., Deskevich, M., Pacifici, F., & Smallwood, S. (2010). WorldView-2 Pan Sharpening. American Society for Photogrammetry and Remote Sensing, Annual Conference April 26-30, 2010, San Diego.
- Palmer, M., Bernhardt, E., Allan, J., Lake, P., Alexander, G., Brooks, S., Carr, J., Clayton, S., Dahm, N., Follstad Shah, J., Galat, D., Loss, S., Goodwin, P., Hart, D., Hassett, B., Jenkinson, R., Kondolf, G., Lave, R., Meyer, J., O'Donnell, T., Pagano, L., Sudduth, E. (2005). Standards for Ecologically Successful River Restoration. *Journal of Applied Ecology* 2005, 42, pp. 208–217.
- Pontius, R. G., & Millones, M. (2011). Death to Kappa: Birth of Quantity Disagreement and Allocation Disagreement for Accuracy Assessment. *International Journal of Remote Sensing*, Taylor and Francis, London.
- Rango, A., Laliberte, A., Herrick, J. E., Winters, C., Havstad, K., Steele, C., & Browning, D. (2009). Unmanned Aerial Vehicle-based Remote Sensing for Rangeland Assessment, Monitoring and Management. *Journal of Applied Remote Sensing*, Vol. 3, pp. 033542.
- Rikola. (2015). The first Generation of 2D Hyperspectral Camera is Airborne [online]. Available from: <http://www.rikola.fi/hyperspectralcamera.pdf>.

- Roth-Kleyer, S. (2009). Soils, Earths and Substrates for Landscape Architecture. *Lecture Notes for the Course Vegetation Technology*. University of Applied Sciences RheinMain, Geisenheim.
- Roth-Kleyer, S. (2011). Biological Engineering. *Lecture Notes of the Course Biological Engineering for Landscape Architecture*. University of Applied Sciences RheinMain, Geisenheim.
- Sahu, K. C. (2008). Textbook of Remote Sensing and Geographical Information Systems. Atlantic Publishers and Distributers LTD, New Delhi.
- Salamí, E., Barrado, C., & Pastor, E. (2014). UAV Flight Experiments Applied to the Remote Sensing of Vegetated Areas. *Remote Sensing*, 6, 2014, pp. 11051-11081.
- Satellite-Imaging-Corporation. (2015). Satellite Sensors [online]. Available from: <http://www.satimagingcorp.com/satellite-sensors/> [accessed at April 16, 2015].
- Scheidegger, C., Werth, S., Gostner, W., Schleiss, A., & Peter, A. (2012). Support of Dynamics in Revitalization. Leaflet Collection Hydraulic Engineering and Ecology, Swiss Federal Office for Environment (BAFU), Leaflet Number 1, Bern.
- Shaoqing, Z., & Lu, X. (2008). The Comparative Study of three Methods of Remote Sensing Image Change Detection. *The International Archives of the Photogrammetry, Remote Sensing and Spatial Information Sciences*, Volume XXXVII, Part B7, Beijing.
- Shigo, A. L., & Marx, H. G. (1977). Compartmentalization of Decay in Trees. Forest Service U.S. Department of Agriculture, Washington.
- Siddiqui, Y. (2003). The modified IHS Method for Fusing Satellite Imagery. American Society for Photogrammetry & Remote Sensing, Annual Conference May 5-9, 2003, Anchorage.
- Slama, C. C. (1980). Manual of photogrammetry (4. edition). American Society of Photogrammetry, Falls Church.

- Sohl, T. L. (1999). Change analysis in the United Arab Emirates: an Investigation of Techniques. *Photogrammetric Engineering and Remote Sensing* 65 (4), pp. 475-484.
- Stiftung-Hessischer-Jaegerhof. (2015). bioversum Kranichstein [online]. *Neophytes Gallery*. Available from: <http://www.bioversum-kranichstein.de/aktuelles/neophyten-galerie/> [accessed at April 16, 2015].
- Thenkabaill, P., Lyon, J., & Huete, A. (2012). *Hyperspectral Remote Sensing of Vegetation*. CRC Press Taylor & Francis Group, London.
- Tuck, M. (2010). *Gestalt Principles Applied in Design* [online]. Available from: http://sixrevisions.com/web_design/gestalt-principles-applied-in-design/ (accessed at April 28, 2015).
- USGS. (2015). Landsat 1 History [online]. Available from: http://landsat.usgs.gov/about_landsat1.php [Accessed at January 12, 2015].
- Vapnik, V. N. (1995). *The Nature of Statistical Learning Theory*. Springer Verlag, New York.
- Vapnik, V. N. (1999). An Overview of Statistical Learning Theory. *IEEE Transactions on Neural Networks*, Volume 10, No. 5, pp. 988-999.
- Zaman, B., Jensen, A. M., & McKee, M. (2011). Use of High-Resolution Multispectral Imagery Aquired with an Autonomous Unmanned Aerial Vehicle to Quantify the Spread of an Invasive Wetlands Species. *Geoscience and Remote Sensing Symposium (IGARSS), 2011 IEEE International* .

ANNEX A

NATURAL HABITAT TYPES OF COMMUNITY INTEREST WHOSE CONSERVATION REQUIRES THE DESIGNATION OF SPECIAL AREAS OF CONSERVATION (Habitats Directive)

Interpretation

Guidance on the interpretation of habitat types is given in the 'Interpretation Manual of European Union Habitats' as approved by the committee set up in Article 20 ('Habitats Committee') and published by the European Commission. The code corresponds to the NATURA 2000 code.

The sign '*' indicates priority habitat types.

1. COASTAL AND HALOPHYTIC HABITATS

11. Open sea and tidal areas

1110 Sandbanks which are slightly covered by sea water all the time

1120 * *Posidonia* beds (*Posidonion oceanicae*)

1130 Estuaries

1140 Mudflats and sandflats not covered by seawater at low tide

1150 *Coastal lagoons

1160 Large shallow inlets and bays

1170 Reefs

1180 Submarine structures made by leaking gases

12. Sea cliffs and shingle or stony beaches

1210 Annual vegetation of drift lines

1220 Perennial vegetation of stony banks

1230 Vegetated sea cliffs of the Atlantic and Baltic Coasts

1240 Vegetated sea cliffs of the Mediterranean coasts with endemic *Limonium* spp.

1250 Vegetated sea cliffs with endemic flora of the Macaronesian coasts

13. Atlantic and continental salt marshes and salt meadows

1310 *Salicornia* and other annuals colonizing mud and sand

1320 *Spartina* swards (*Spartinion maritimae*)

1330 Atlantic salt meadows (*Glauco-Puccinellietalia maritimae*)

1340 * Inland salt meadows

14. Mediterranean and thermo-Atlantic salt marshes and salt meadows

1410 Mediterranean salt meadows (*Juncetalia maritimi*)

1420 Mediterranean and thermo-Atlantic halophilous scrubs (*Sarcocornetea fruticosi*)

1430 Halo-nitrophilous scrubs (*Pegano-Salsoletea*)

15. Salt and gypsum inland steppes

1510 * Mediterranean salt steppes (*Limonietalia*)

1520 * Iberian gypsum vegetation (*Gypsophiletalia*)

1530 * Pannonic salt steppes and salt marshes

16. Boreal Baltic archipelago, coastal and landupheaval areas

1610 Baltic esker islands with sandy, rocky and shingle beach vegetation and sublittoral vegetation

1620 Boreal Baltic islets and small islands

1630 * Boreal Baltic coastal meadows

1640 Boreal Baltic sandy beaches with perennial vegetation

1650 Boreal Baltic narrow inlets

2. COASTAL SAND DUNES AND INLAND DUNES

21. Sea dunes of the Atlantic, North Sea and Baltic coasts

2110 Embryonic shifting dunes

2120 Shifting dunes along the shoreline with *Ammophila arenaria* ('white dunes')

2130 * Fixed coastal dunes with herbaceous vegetation ('grey dunes')

2140 * Decalcified fixed dunes with *Empetrum nigrum*

2150 * Atlantic decalcified fixed dunes (*Calluno-Ulicetea*)

2160 Dunes with *Hippophaë rhamnoides*

2170 Dunes with *Salix repens* ssp. *argentea* (*Salicion arenariae*)

2180 Wooded dunes of the Atlantic, Continental and Boreal region

2190 Humid dune slacks

21A0 Machairs (* in Ireland)

22. Sea dunes of the Mediterranean coast

2210 *Crucianellion maritimae* fixed beach dunes

2220 Dunes with *Euphorbia terracina*

2230 *Malcolmietalia* dune grasslands

2240 *Brachypodietalia* dune grasslands with annuals

2250 * Coastal dunes with *Juniperus* spp.

2260 *Cisto-Lavenduletalia* dune sclerophyllous scrubs

2270 * Wooded dunes with *Pinus pinea* and/or *Pinus pinaster*

23. Inland dunes, old and decalcified

2310 Dry sand heaths with *Calluna* and *Genista*

2320 Dry sand heaths with *Calluna* and *Empetrum nigrum*

2330 Inland dunes with open *Corynephorus* and *Agrostis* grasslands

2340 * Pannonic inland dunes

3. FRESHWATER HABITATS

31. Standing water

3110 Oligotrophic waters containing very few minerals of sandy plains (*Littorelletalia uniflorae*)

3120 Oligotrophic waters containing very few minerals generally on sandy soils of the West Mediterranean, with *Isoetes* spp.

3130 Oligotrophic to mesotrophic standing waters with vegetation of the *Littorelletea uniflorae* and/or of the *Isoëto-Nanojuncetea*

3140 Hard oligo-mesotrophic waters with benthic vegetation of *Chara* spp.

3150 Natural eutrophic lakes with *Magnopotamion* or *Hydrocharition*- type vegetation

3160 Natural dystrophic lakes and ponds

3170 * Mediterranean temporary ponds

3180 * Turloughs

32. Running water - sections of water courses with natural or semi-natural dynamics (minor, average and major beds) where the water quality shows no significant deterioration

3210 Fennoscandian natural rivers

3220 Alpine rivers and the herbaceous vegetation along their banks

3230 Alpine rivers and their ligneous vegetation with *Myricaria germanica*

3240 Alpine rivers and their ligneous vegetation with *Salix elaeagnos*

3250 Constantly flowing Mediterranean rivers with *Glaucium flavum*

3260 Water courses of plain to montane levels with the *Ranunculion fluitantis* and *Callitricho-Batrachion* vegetation

3270 Rivers with muddy banks with *Chenopodion rubri* p.p. and *Bidention* p.p. vegetation

3280 Constantly flowing Mediterranean rivers with *Paspalo-Agrostidion* species and hanging curtains of *Salix* and *Populus alba*

3290 Intermittently flowing Mediterranean rivers of the *Paspalo-Agrostidion*

4. TEMPERATE HEATH AND SCRUB

4010 Northern Atlantic wet heaths with *Erica tetralix*

4020 * Temperate Atlantic wet heaths with *Erica ciliaris* and *Erica tetralix*

4030 European dry heaths

4040 * Dry Atlantic coastal heaths with *Erica vagans*

4050 * Endemic macaronesian heaths

4060 Alpine and Boreal heaths

4070 * Bushes with *Pinus mugo* and *Rhododendron hirsutum* (*Mugo Rhododendretum hirsuti*)

4080 Sub-Arctic *Salix* spp. scrub

4090 Endemic oro-Mediterranean heaths with gorse

5. SCLEROPHYLLOUS SCRUB (MATORRAL)

51. Sub-Mediterranean and temperate scrub

5110 Stable xerothermophilous formations with *Buxus sempervirens* on rock slopes (*Berberidion* p.p.)

5120 Mountain *Cytisus purgans* formations

5130 *Juniperus communis* formations on heaths or calcareous grasslands

5140 * *Cistus palhinhae* formations on maritime wet heaths

52. Mediterranean arborescent matorral

5210 Arborescent matorral with *Juniperus* spp.

5220 * Arborescent matorral with *Zyziphus*

5230 * Arborescent matorral with *Laurus nobilis*

53. Thermo-Mediterranean and pre-steppe brush

5310 *Laurus nobilis* thickets

5320 Low formations of *Euphorbia* close to cliffs

5330 Thermo-Mediterranean and pre-desert scrub

54. Phrygana

5410 West Mediterranean cliff-top phryganas (*Astragalo-Plantaginietum subulatae*)

5420 *Sarcopoterium spinosum* phryganas

5430 Endemic phryganas of the *Euphorbio-Verbascion*

6. NATURAL AND SEMI-NATURAL GRASSLAND FORMATIONS

61. Natural grasslands

6110 * Rupicolous calcareous orbisophilic grasslands of the *Alyso-Sedion albi*

6120 * Xeric sand calcareous grasslands

6130 Calaminarian grasslands of the *Violetalia calaminariae*

6140 Siliceous Pyrenean *Festuca eskia* grasslands

6150 Siliceous alpine and boreal grasslands

6160 Oro-Iberian *Festuca indigesta* grasslands

6170 Alpine and subalpine calcareous grasslands

6180 Macaronesian mesophile grasslands

62. Semi-natural dry grasslands and scrubland facies

6210 Semi-natural dry grasslands and scrubland facies on calcareous substrates (*Festuco Brometalia*) (* important orchid sites)

6220 * Pseudo-steppe with grasses and annuals of the *Thero-Brachypodietea*

6230 * Species-rich *Nardus* grasslands, on silicious substrates in mountain areas (and submountain areas in Continental Europe)

6240 * Sub-Pannonic steppic grasslands

6250 * Pannonic loess steppic grasslands

6260 * Pannonic sand steppes

6270 * Fennoscandian lowland species-rich dry to mesic grasslands

6280 * Nordic alvar and precambrian calcareous flatrocks

63. Sclerophyllous grazed forests (dehesas)

6310 Dehesas with evergreen *Quercus* spp.

64. Semi-natural tall-herb humid meadows

6410 *Molinia* meadows on calcareous, peaty or clayey-silt-laden soils (*Molinion caeruleae*)

6420 Mediterranean tall humid grasslands of the *Molinio-Holoschoenion*

6430 Hydrophilous tall herb fringe communities of plains and of the montane to alpine levels

- 6440 Alluvial meadows of river valleys of the *Cnidion dubii*
6450 Northern boreal alluvial meadows
65. Mesophile grasslands
6510 Lowland hay meadows (*Alopecurus pratensis*, *Sanguisorba officinalis*)
6520 Mountain hay meadows
6530 * Fennoscandian wooded meadows

7. RAISED BOGS AND MIRES AND FENS

71. Sphagnum acid bogs

- 7110 * Active raised bogs
7120 Degraded raised bogs still capable of natural regeneration
7130 Blanket bogs (* if active bog)
7140 Transition mires and quaking bogs
7150 Depressions on peat substrates of the *Rhynchosporion*
7160 Fennoscandian mineral-rich springs and springfens

72. Calcareous fens

- 7210 * Calcareous fens with *Cladium mariscus* and species of the *Caricion davallianae*
7220 * Petrifying springs with tufa formation (*Cratoneurion*)
7230 Alkaline fens
7240 * Alpine pioneer formations of the *Caricion bicoloris-atrofuscae*

73. Boreal mires

- 7310 * Aapa mires
7320 * Palsa mires

8. ROCKY HABITATS AND CAVES

81. Scree

- 8110 Siliceous scree of the montane to snow levels (*Androsacetalia alpinae* and *Galeopsietalia ladani*)
8120 Calcareous and calcshist screes of the montane to alpine levels (*Thlaspietea rotundifolii*)
8130 Western Mediterranean and thermophilous scree
8140 Eastern Mediterranean screes
8150 Medio-European upland siliceous screes

8160 * Medio-European calcareous scree of hill and montane levels

82. Rocky slopes with chasmophytic vegetation

8210 Calcareous rocky slopes with chasmophytic vegetation

8220 Siliceous rocky slopes with chasmophytic vegetation

8230 Siliceous rock with pioneer vegetation of the *Sedo-Scleranthion* or of the *Sedo albi-Veronicion dillenii*

8240 * Limestone pavements

83. Other rocky habitats

8310 Caves not open to the public

8320 Fields of lava and natural excavations

8330 Submerged or partially submerged sea caves

8340 Permanent glaciers

9. FORESTS

(Sub)natural woodland vegetation comprising native species forming forests of tall trees, with typical undergrowth, and meeting the following criteria: rare or residual, and/or hosting species of Community interest

90. Forests of Boreal Europe

9010 * Western Taïga

9020 * Fennoscandian hemiboreal natural old broad-leaved deciduous forests (*Quercus*, *Tilia*, *Acer*, *Fraxinus* or *Ulmus*) rich in epiphytes

9030 * Natural forests of primary succession stages of landupheaval coast

9040 Nordic subalpine/subarctic forests with *Betula pubescens* ssp. *czerepanovii*

9050 Fennoscandian herb-rich forests with *Picea abies*

9060 Coniferous forests on, or connected to, glaciofluvial eskers

9070 Fennoscandian wooded pastures

9080 * Fennoscandian deciduous swamp woods

91. Forests of Temperate Europe

9110 *Luzulo-Fagetum* beech forests

9120 Atlantic acidophilous beech forests with *Ilex* and sometimes also *Taxus* in the shrublayer (*Quercion robori-petraeae* or *Ilici-Fagenion*)

9130 *Asperulo-Fagetum* beech forests

9140 Medio-European subalpine beech woods with *Acer* and *Rumex arifolius*
 9150 Medio-European limestone beech forests of the *Cephalanthero-Fagion*
 9160 Sub-Atlantic and medio-European oak or oak-hornbeam forests of the
Carpinion betuli
 9170 *Galio-Carpinetum* oak-hornbeam forests
 9180 * *Tilio-Acerion* forests of slopes, screes and ravines
 9190 Old acidophilous oak woods with *Quercus robur* on sandy plains
 91A0 Old sessile oak woods with *Ilex* and *Blechnum* in the British Isles
 91B0 Thermophilous *Fraxinus angustifolia* woods
 91C0 * Caledonian forest
 91D0 * Bog woodland
 91E0 * Alluvial forests with *Alnus glutinosa* and *Fraxinus excelsior* (*Alno-Padion*,
Alnion incanae, *Salicion albae*)
 91F0 Riparian mixed forests of *Quercus robur*, *Ulmus laevis* and *Ulmus minor*,
Fraxinus excelsior or *Fraxinus angustifolia*, along the great rivers (*Ulmenion*
minoris)
 91G0 * Pannonic woods with *Quercus petraea* and *Carpinus betulus*
 91H0 * Pannonian woods with *Quercus pubescens*
 91I0 * Euro-Siberian steppic woods with *Quercus* spp.
 91J0 * *Taxus baccata* woods of the British Isles

92. Mediterranean deciduous forests

9210 * Apennine beech forests with *Taxus* and *Ilex*
 9220 * Apennine beech forests with *Abies alba* and beech forests with *Abies*
nebrodensis
 9230 Galicio-Portuguese oak woods with *Quercus robur* and *Quercus*
pyrenaica
 9240 *Quercus faginea* and *Quercus canariensis* Iberian woods
 9250 *Quercus trojana* woods
 9260 *Castanea sativa* woods
 9270 Hellenic beech forests with *Abies borisii-regis*
 9280 *Quercus frainetto* woods
 9290 *Cupressus* forests (*Acero-Cupression*)
 92A0 *Salix alba* and *Populus alba* galleries
 92B0 Riparian formations on intermittent Mediterranean water courses with
Rhododendron ponticum, *Salix* and others
 92C0 *Platanus orientalis* and *Liquidambar orientalis* woods (*Platanion orientalis*)

92D0 Southern riparian galleries and thickets (*Nerio-Tamaricetea* and *Securinegion tinctoriae*)

93. Mediterranean sclerophyllous forests

9310 Aegean *Quercus brachyphylla* woods

9320 *Olea* and *Ceratonia* forests

9330 *Quercus suber* forests

9340 *Quercus ilex* and *Quercus rotundifolia* forests

9350 *Quercus macrolepis* forests

9360 * Macaronesian laurel forests (*Laurus*, *Ocotea*)

9370 * Palm groves of *Phoenix*

9380 Forests of *Ilex aquifolium*

94. Temperate mountainous coniferous forests

9410 Acidophilous *Picea* forests of the montane to alpine levels (*Vaccinio-Piceetea*)

9420 Alpine *Larix decidua* and/or *Pinus cembra* forests

9430 Subalpine and montane *Pinus uncinata* forests (* if on gypsum or limestone)

95. Mediterranean and Macaronesian mountainous coniferous forests

9510 * Southern Apennine *Abies alba* forests

9520 *Abies pinsapo* forests

9530 * (Sub-) Mediterranean pine forests with endemic black pines

9540 Mediterranean pine forests with endemic Mesogean pines

9550 Canarian endemic pine forests

9560 * Endemic forests with *Juniperus* spp.

9570 **Tetraclinis articulata* forests

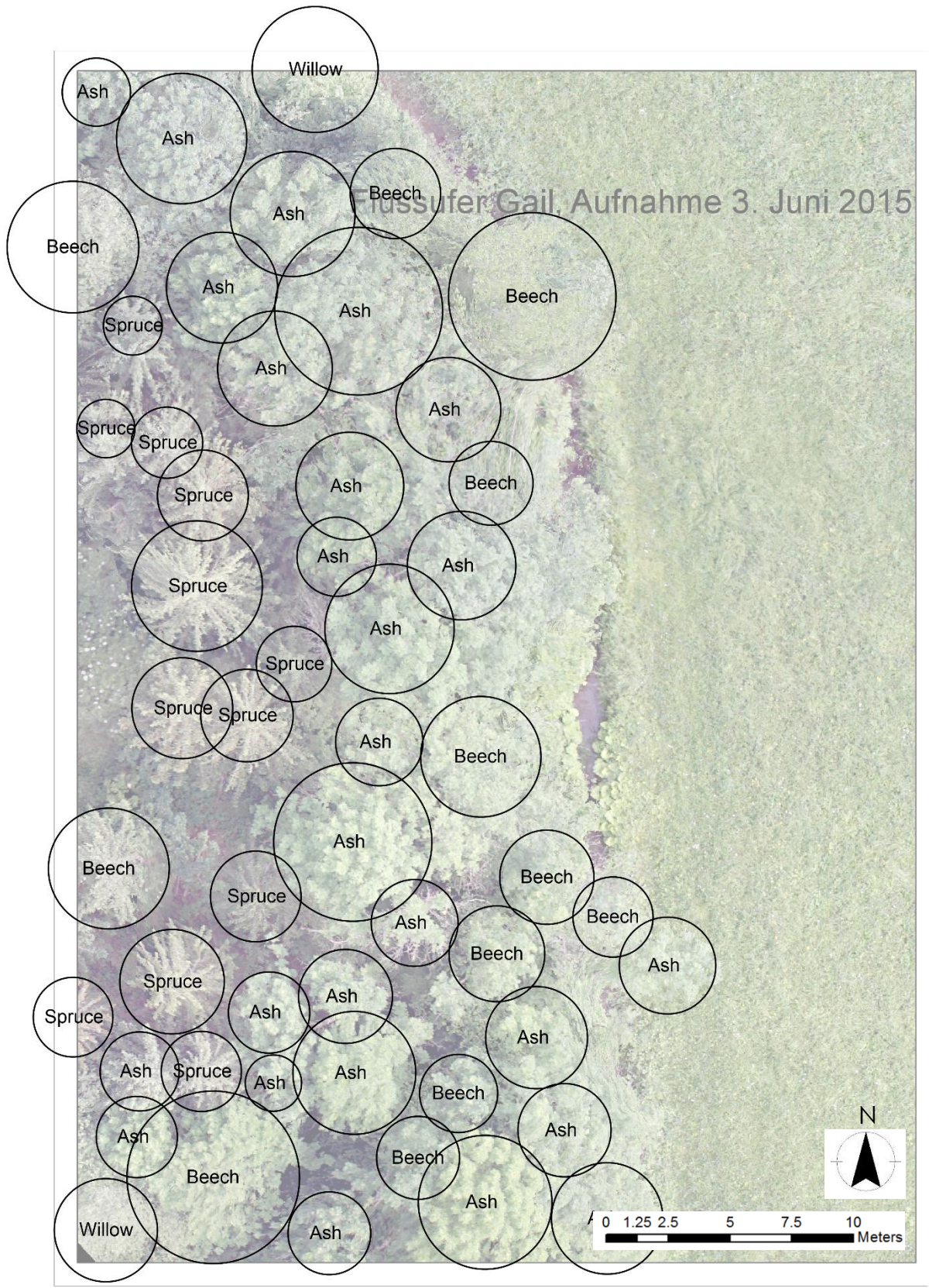
9580 * Mediterranean *Taxus baccata* woods

ANNEX B

Results visual image interpretation



Scaled aerial image derived by RPAS of a sample area in study site Gail, edited by expert 1



Reference data for sample site of expert 1



Result of expert 1 of the above shown sample area in study site Gail ("Nadelbaum" = coniferous tree, "Laubbaum" = deciduous tree)

Flussufer Gail

Bearbeiteter Maßstab: 1:118

Datum der Aufnahme: 3. Juni 2015

Ungefähr benötigte Zeit: 30 min

Anmerkungen:

Es gibt natürlich noch mehr Bäume auf dem Bild, aber eindeutige Einzelbäume konnte ich nicht herausondieren. Welche Arten es sind kann ich nur vermuten, weiß es aber nicht. Bei den Nadelbäumen tippe ich auf Lärchen, bei den meisten Laubbäumen auf Weiden. Falls das was bringt.

Analogous Translation:

Riverside Gail

Scale: 1:118

Recording Date: June 3rd, 2015

Time needed: ca. 30 min

Comments:

There are more trees in the image of course, but I could not clearly identify definite single trees. I can only assume their species, but I do not know. I think the coniferous trees are larches (*Larix*), most deciduous trees are willows (*Salix*). If this helps you.

Size Sample Area	1595.72 m ²
Total Number of Trees	52
Ash	26
Beech	12
Spruce	12
Willow	2
Coniferous	12
Deciduous	40
Estimated collection time	1.5 hours

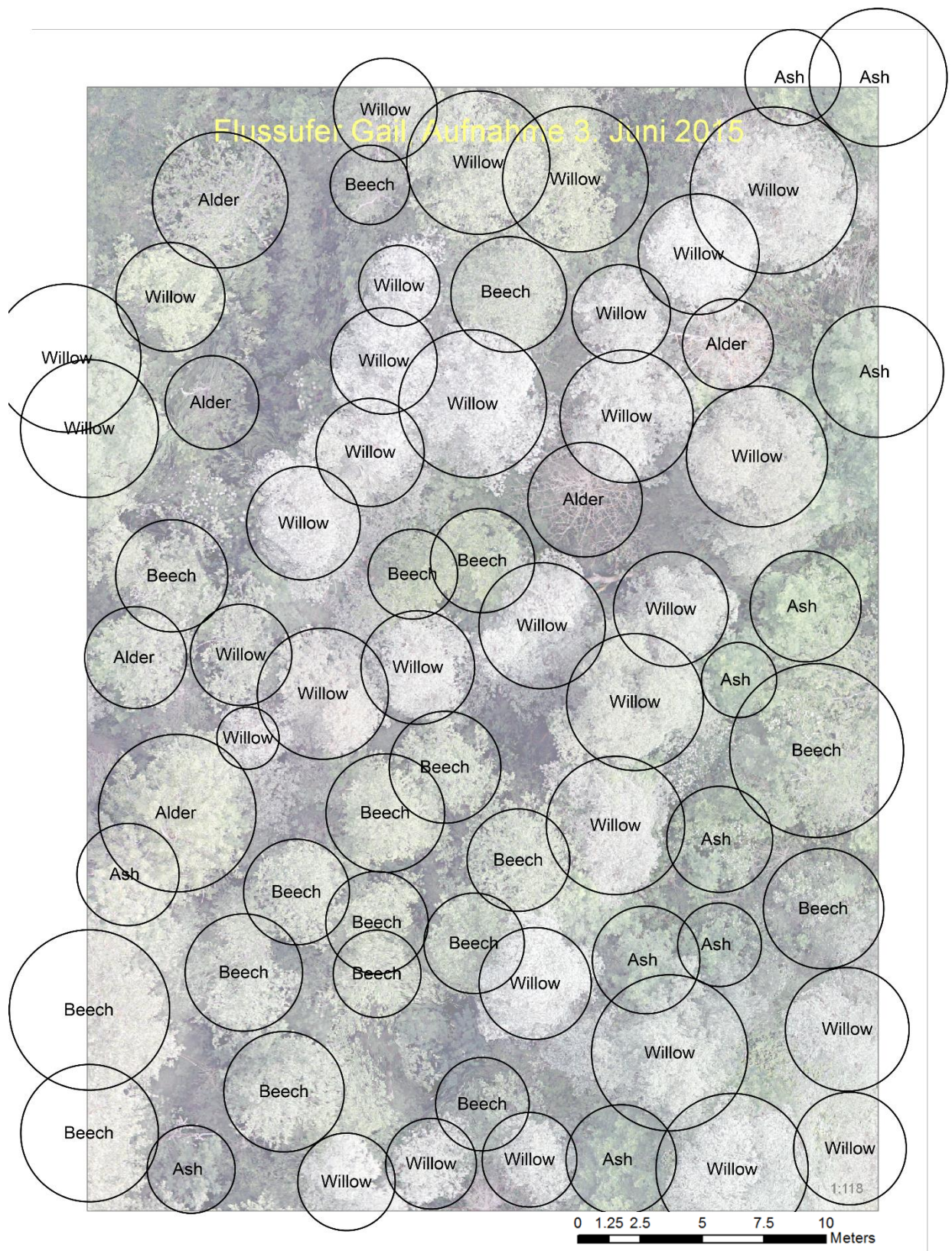
Summarized reference data sample site of expert 1

Size Sample Area	1595.72 m ²
Total Number of Trees	21
Coniferous	14
Deciduous	7
Estimated identification time	0.5 hours

Summarized interpretation results expert 1

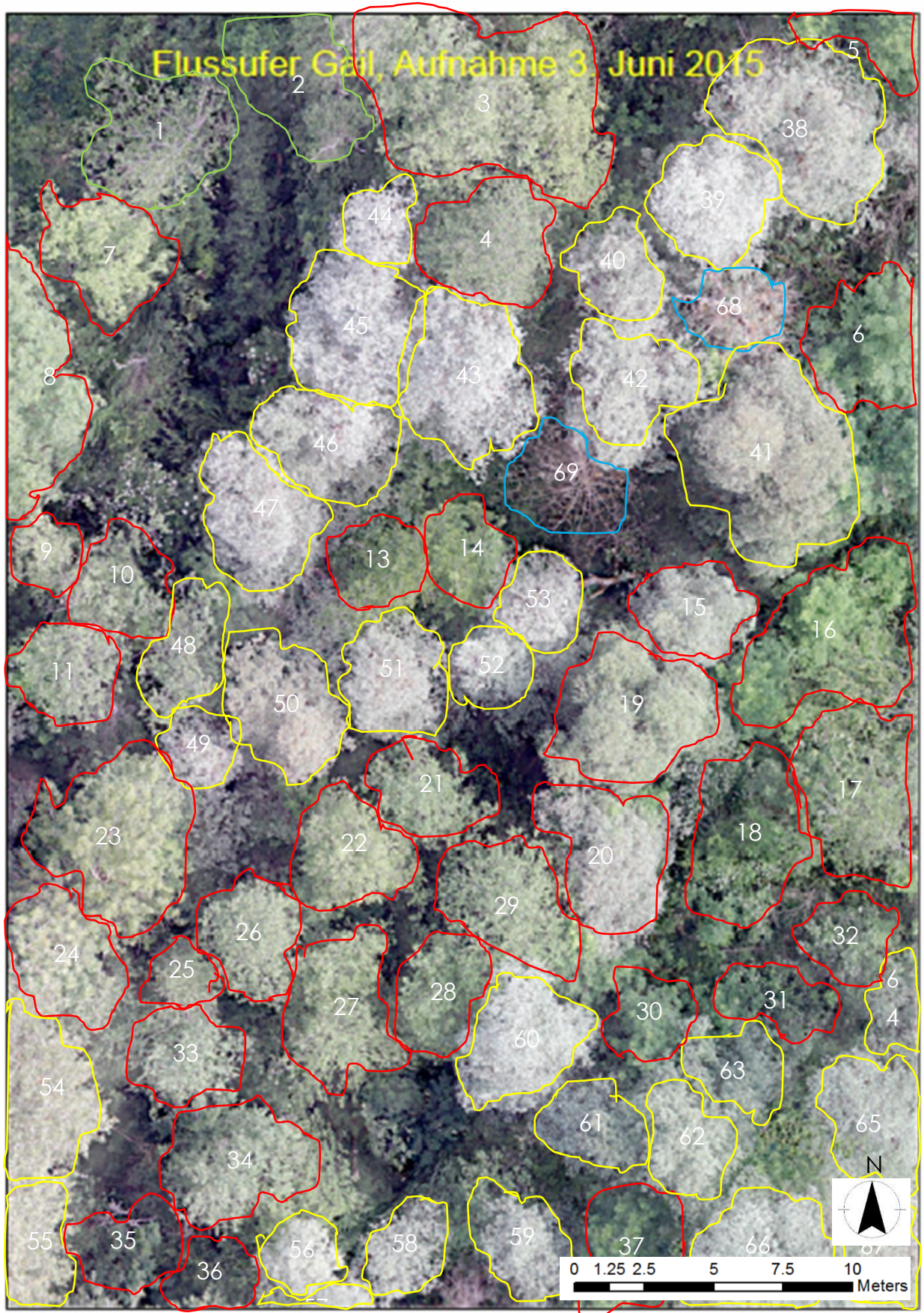


Scaled aerial image derived by RPAS of a sample area in study site Gail, edited by expert 2



Reference data for sample area of expert 2





Result of expert 2 of the above shown sample area in study site Gail

Maßstab 1:118
Datum der Aufnahme 03.06.2015 (am 05.07.2015 von mir bearbeitet)
Benötigte Zeit 1 Stunde

GRÜN #1+2 Laubbäume
ROT #3-37 hauptsächlich Weiden und Pappeln
GELB #38-67 Prunus, meist Vogelkirsche
BLAU #68+69 könnten Nadelbäume sein

Den verschwommenen Bereich konnte ich leider nicht identifizieren und habe ihn deshalb ausgelassen

Analogous Translation:

Scale: 1:118
Recording Date: June 3rd, 2015 (edited on July 7th)
Time needed: 1 hour

GREEN number 1+2 deciduous trees
RED number 3-37 primarily willows and poplars
YELLOW number 38-67 *Prunus*, primarily wild cherry
BLUE number 68+69 might be coniferous trees

Unfortunately, I was not able to identify the blurry part of the image and therefore skipped it.

Size Sample Area	1572.35 m ²
Total Number of Trees	68
Alder	6
Ash	11
Beech	19
Willow	32
Coniferous	0
Deciduous	68
Estimated collection time	2.0 hours

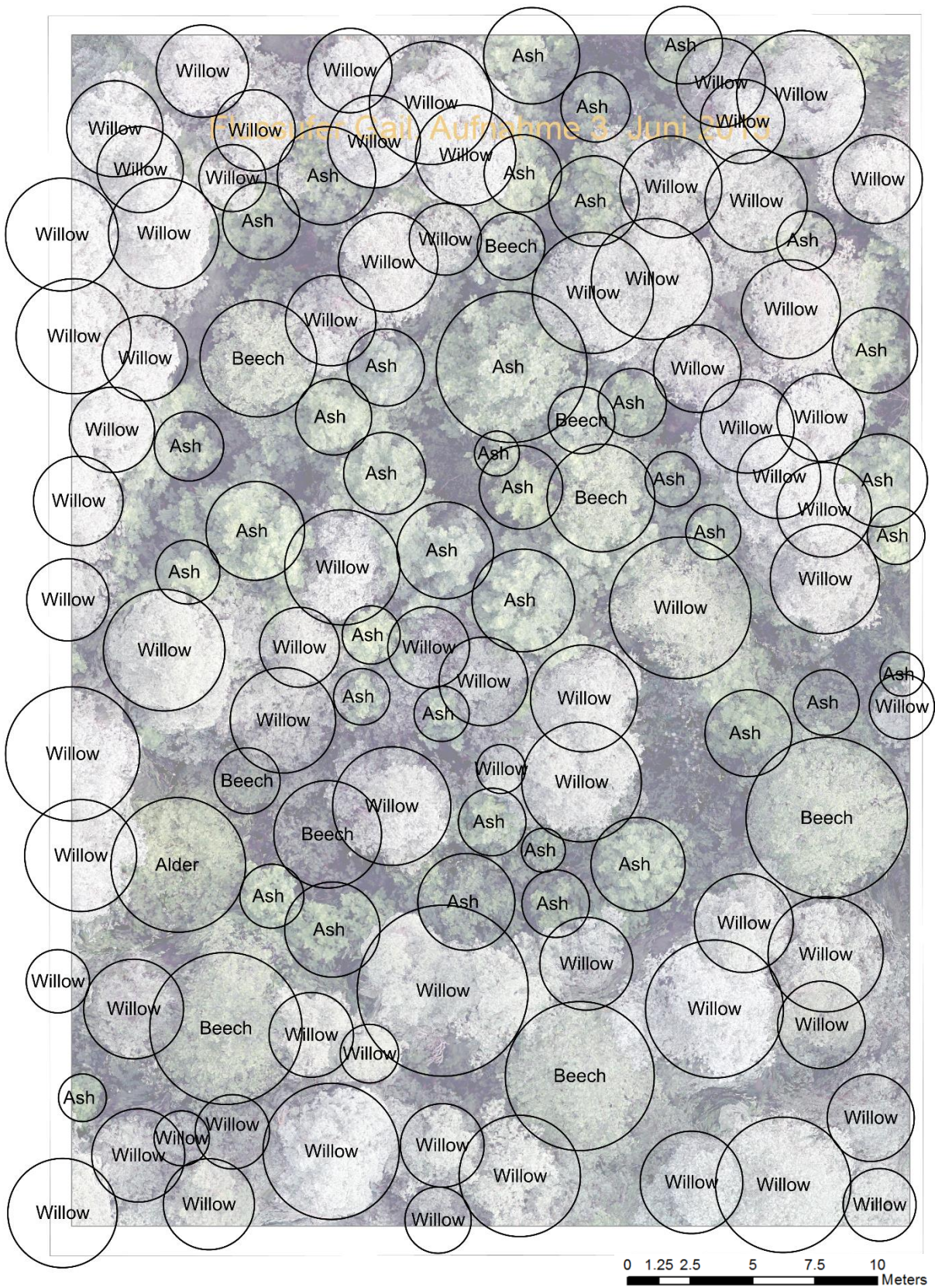
Summarized reference data sample site of expert 2

Size Sample Area	1572.35 m ²
Total Number of Trees	68
Other Coniferous Tree	2
Other Deciduous Tree	2
Wild Cherry	30
Willow	34
Coniferous	2
Deciduous	66
Estimated collection time	1.0 hour

Summarized interpretation results expert 2

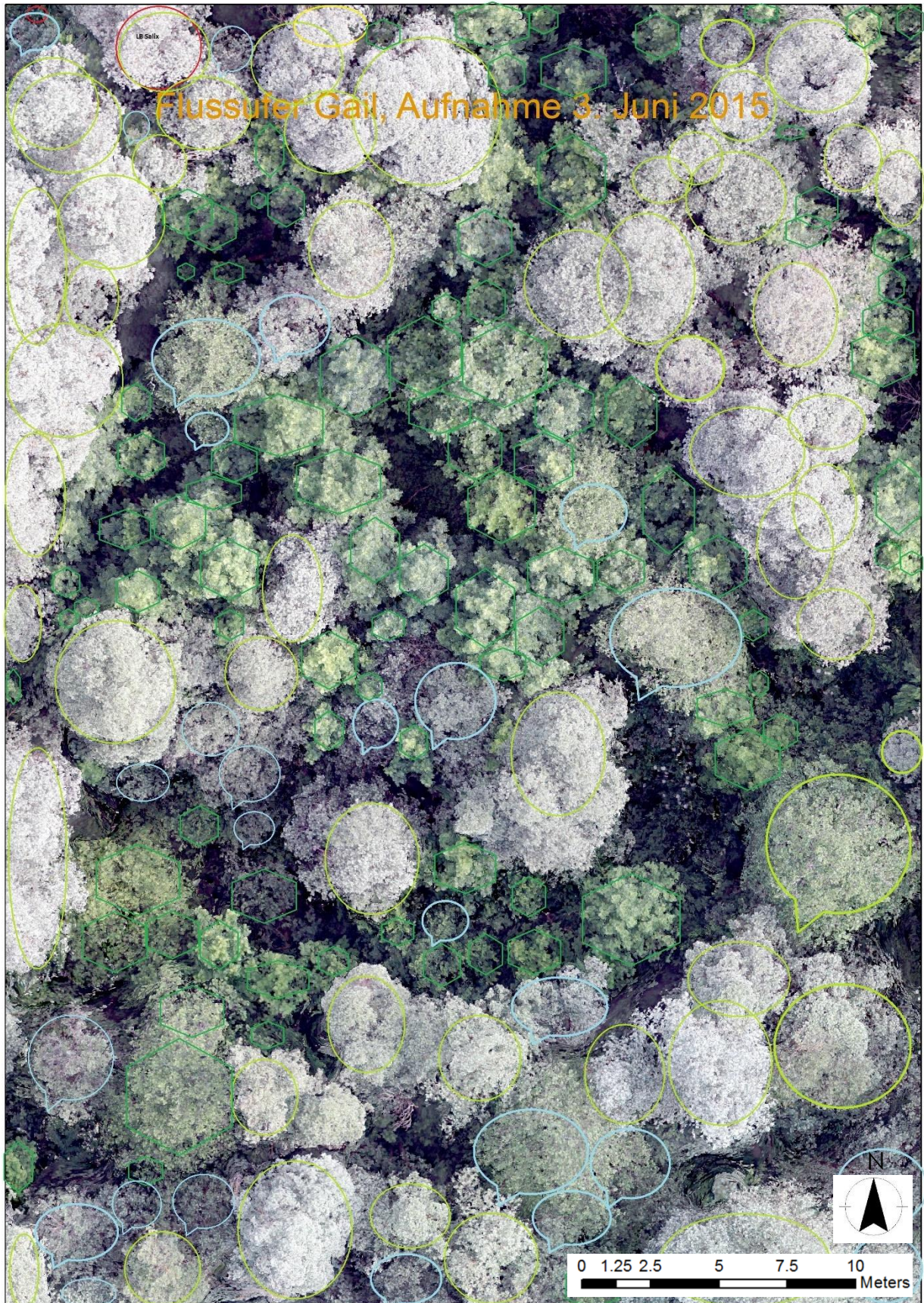


Scaled aerial image derived by RPAS of a sample area in study site Gail, edited by expert 3



Reference data for sample area of expert 3





Result of expert 3 of the above shown sample area in study site Gail

Ich habe folgendes gekennzeichnet: runder hellgrüner Ring sind für mich die Weiden, dunkelgrüner Wabenrand sind Nadelbäume, und die hellblauen Sprechblasen sind Laubbäume verschiedener Arten, dies wage ich mir nicht zu bestimmen. Ich habe noch nie eine Luftbildauswertung gemacht. Ich habe dies mit Paint bearbeitet, bitte ignoriere die oberen roten Ringe diese konnte ich nicht wieder entfernen.

Analogous Translation:

I marked the following: round, light-green circles are willows, dark-green hexagons are coniferous trees and the light-blue balloons are deciduous trees of different species which I do not dare to identify. I have never done an aerial image interpretation before.

I worked in Paint, please ignore the upper red circles, I was not able to remove them.

Size Sample Area	1598.04 m ²
Total Number of Trees	121
Alder	1
Ash	39
Beech	11
Willow	70
Coniferous	0
Deciduous	121
Estimated collection time	2.5 hours

Summarized reference data sample site of expert 3

Size Sample Area	1598.04 m ²
Total Number of Trees	166
Other Coniferous Tree	85
Other Deciduous Tree	27
Willow	54
Coniferous	85
Deciduous	81
Estimated collection time	Not specified

Summarized interpretation results expert 3

ANNEX C

Confusion Matrices of the Classification Processes

1. GeoEye-1 Image Segmentation
2. GeoEye-1 ISODATA
3. GeoEye-1 Maximum Likelihood

3. GeoEye-1 Maximum Likelihood

Classified Data	river	purple moor/fall oat grass	agriculture 2	building/infrastructure	gravel/sand bank	tall oat grass	natural eutrophic lakes	agriculture 3	agriculture 1	agriculture sowing meadow	bare soil	path	spruce forest	alluvial forests	white clover	Row Total
river	98	0	0	2	3	0	33	0	0	0	0	0	0	0	0	136
purple moor grass/fall oat grass	0	78	0	4	7	6	0	2	1	1	14	8	1	1	14	137
agriculture 2	0	0	88	1	2	0	0	0	0	5	0	0	2	8	1	108
building/infrastructure	0	1	0	53	9	0	0	0	0	0	3	0	0	0	0	66
gravel/sand bank	2	1	1	12	51	0	2	0	0	0	0	1	1	1	0	72
tall oat grass	0	5	1	0	1	82	0	2	0	4	3	1	1	6	9	115
natural eutrophic lakes	0	0	0	1	1	0	62	0	0	0	0	0	0	0	0	64
agriculture 3	0	0	0	0	0	0	0	88	1	0	0	1	0	0	0	90
agriculture 1	0	0	0	9	5	0	0	4	95	0	0	2	0	0	0	115
sowing meadow	0	2	1	1	2	5	0	0	0	86	0	0	0	0	0	107
field/bare soil	0	10	0	5	2	0	0	0	1	0	68	3	0	0	2	89
path	0	0	0	6	5	2	1	4	2	0	3	81	3	0	0	107
spruce forest	0	0	0	3	6	2	0	0	0	1	1	0	81	8	0	102
alluvial forests	0	1	9	2	8	2	2	0	0	3	5	1	11	67	1	112
white clover/ryegrass meadow	0	2	0	0	0	1	0	0	0	0	3	0	0	0	73	79
Column Total	100	100	100	100	100	100	100	100	100	100	100	100	100	100	100	1151

Class Name	Reference Totals	Classified Totals	Number Correct	Producers Accuracy	Users Accuracy
river	100	136	98	98.00%	72.06%
purple moor/fall oat grass	100	137	78	78.00%	56.93%
agriculture 2	100	108	88	88.00%	81.48%
building/infrastructure	100	66	53	53.00%	80.30%
gravel/sand bank	100	72	51	51.00%	70.83%
Seggen/Rasenssch	100	115	82	82.00%	71.30%
tall oat grass	100	64	62	62.00%	96.88%
natural eutrophic lakes	100	90	88	88.00%	97.78%
agriculture 1	100	115	95	95.00%	82.61%
sowing meadow	100	107	86	86.00%	80.37%
field/bare soil	100	89	68	68.00%	76.40%
path	100	107	81	81.00%	75.70%
spruce forest	100	102	81	81.00%	79.41%
alluvial forests	100	112	67	67.00%	59.82%
white clover	100	79	73	73.00%	92.41%
Totals	1500	1500	1151		

Overall Classification Accuracy = **76.73%**

Overall Kappa Statistics = **0.7507**